DESY–THESIS–1999–024
September 1999

Higher-Twist Contributions to Deep Inelastic Structure Functions at small x_{B}

Dissertation
zur Erlangung des Doktorgrades
des Fachbereichs Physik
der Universität Hamburg

vorgelegt von
Claas Bontus
aus Wipperfürth

Hamburg
1999

Gutachter der Dissertation:	Prof. Dr. J. Bartels Prof. Dr. W. Buchmüller
Gutachter der Disputation:	Prof. Dr. J. Bartels Prof. Dr. G. Kramer
Datum der Disputation:	10. September 1999
Dekan des Fachbereichs Physik und Vorsitzender des Promotionsausschusses:	Prof. Dr. F.-W. Büßer

Abstract

We analyse gluonic twist-four contributions to inclusive deep inelastic structure functions. For this, we estimate these contributions numerically in the first part. The results are based on the DLA contributions of gluon-operators which are expected to dominate at small x_{B}. We, first, summarize relations of the two-, three- and four-gluon amplitude and show how to extract the relevant twist-four parts. Moreover, we are using experimental data on diffractive final states in order to fix free parameters within the initial distribution of the four-gluon amplitude. Therefore, it is also necessary to study relations between diffractive and inclusive amplitudes. This relation can be established with help of the AGK rules. Finally, we present our numerical results for three different choices of the input distributions.
In the second part we consider gluonic higher-twist contributions from a more general point of view. Using a graphical method we can find expressions for gluonic twist-four contributions at leading order. For this we consider diagrams with up to four t-channel gluons. The used scheme is an extension of the methods developed by R.K. Ellis, W. Furmanski, R. Petronzio (EFP). Making systematic use of the axial gauge, Ward identities and symmetry relations, we can write the results as explicitly gauge invariant expressions. Moreover, we can perform the factorization of matrix-elements of gluon-operators and coefficient functions.

Zusammenfassung

Wir analysieren gluonische Twist-vier Beiträge zu inklusiven tief-inelastischen Strukturfunktionen. Dazu präsentieren wir im ersten Teil zunächst eine numerische Abschätzung. Die vorgestellten Ergebnisse basieren auf den DLA Näherungen der Beiträge von Gluon-Operatoren, da von diesen erwarten wird, dass sie im Bereich kleiner x_{B} dominieren. Zuerst fassen wir Relationen der Zwei-, Drei- und Vier-Gluon Amplituden zusammen und zeigen, wie aus diesen die Twist-vier Beiträge extrahiert werden können. Da wir experimentelle Daten über diffraktive Prozesse nutzen, um freie Parameter innerhalb der Anfangsverteilung der Vier-Gluon Amplitude festzulegen, untersuchen wir darüber hinaus Zusammenhänge zwischen diffraktiven und inklusiven Amplituden. Der gesuchte Zusammenhang kann dabei mit Hilfe der AGK-Regeln gefunden werden. Schließlich präsentieren wir unsere numerischen Ergebnisse für drei verschiedene Festlegungen der Anfangsverteilungen.
Im zweiten Teil untersuchen wir gluonische Higher-Twist Beiträge aus einem allgemeineren Blickwinkel. Mit Hilfe einer grafischen Methode leiten wir Relationen für gluonische Twist-vier Beiträge in führender Ordnung her. Dazu betrachten wir Diagramme mit bis zu vier t-Kanal Gluonen. Das hierbei verwendete Schema baut auf Methoden auf, die von R.K. Ellis, W. Furmanski, R. Petronzio (EFP) entwickelt wurden. Durch systematischen Gebrauch der axialen Eichung, von Ward-Identitäten und Symmetrie-Relationen können wir die Ergebnisse in einer explizit eichinvarianten Form schreiben. Darüber hinaus führen wir die Faktorisierung zwischen Matrix-Elementen von Gluon-Operatoren und Koeffizienten-Funktionen durch.

Contents

Introduction **5**

1 A Numerical Estimate of Gluonic Twist-Four Contributions to DIS Structure Functions **17**

1 Higher Twist at small x_{B} 18

1.1 The Two-Gluon Operator 19

1.2 The Four-Gluon Operator 22

1.3 Contributions with Three t-channel Gluons 31

1.4 Running α_{s} 31

2 Diffractive Dissociation 32

2.1 Diffractive $q\bar{q}$-Production 33

2.2 Diffractive Vector Meson Production 36

2.3 Diffractive $q\bar{q}g$-Production and Multi-Jet Processes 38

2.4 Connection with the Structure Functions $F_{\ell,t}$ and the AGK Cutting Rules . . 40

2.5 The Sign Structure 42

3 Numerical Results 44

3.1 General Procedure and Determination of Initial Parton Distributions 44

3.2 Constant Initial Parton Distributions 47

3.3 Increasing Initial Parton Distributions 52

4 Conclusions 55

2 Twist-Four Gluon-Operators **57**

5 EFP's Approach 58

6 Conventions 59

7 Factorization 60

8 Ward Identities 61

8.1 Generating Functional 62

8.2 Relations Between Two- and Three-Gluon Quark-Loops 63

8.3 Relations Between Three- and Four-Gluon Quark-Loops 64

9 Gluonic Operators 66

10 Dimensional Analysis 67

10.1 Two Gluons 68

10.2 Three Gluons 68

10.3 Four Gluons 69

11 Results of the Factorization Procedure 69

11.1 Two and Three Gluons 70

11.2 Four Gluons 71

11.3 Discussion of the Results 76

12 Conclusions 77

Summary **79**

A Some Useful Quantities for the Four-Gluon Amplitude **81**

B Numerical Inverse Mellin Transforms **85**

Bibliography **88**

Introduction

The strong interaction is responsible for the hadronic spectrum, i.e. the spectrum of mesons and baryons. Nowadays, it is widely believed that Quantum-Chromodynamics (QCD) it the correct theory for the strong interactions. Unfortunately QCD turns out to be a rather complicated theory seen from the mathematical point of view. A closed solution which yields exact results for the hadronic spectrum as well as for scattering amplitudes seems to be beyond reach. It is, therefore, necessary to develop approximation schemes which are suitable for computations of the quantities under consideration. These approximation schemes can coarsely be separated into two groups: perturbative and non-perturbative ones.

For the formulation of QCD a coupling constant has been introduced, which is usually termed α_{s}. As it turns out, after renormalization, the value of this coupling constant depends on a certain momentum scale, and α_{s} becomes smaller and smaller if this scale tends to infinity; a property of QCD which became known as *asymptotic freedom*. On the other hand, in the low energy limit α_{s} becomes arbitrarily large. Since perturbative methods try to expand physical quantities into powers of the coupling constant, these methods can only be applied for sufficiently large scales. The non-perturbative methods, on the other hand, are supposed to yield statements about physical quantities in the low energy limit. They are usually based on interactions between mesons and baryons as fundamental objects. One of the purposes of this thesis is a contribution to the examination of the transition between the perturbative and the non-perturbative regime. The applied methods belong, however, to the perturbative ones.

Deep Inelastic Scattering

One of the most interesting processes for the exploration of QCD is deep inelastic scattering (DIS). In DIS a lepton with momentum k scatters off a hadron with momentum p via exchange of a virtual photon with momentum q. For the description of deep inelastic processes it is useful to introduce, besides the photon virtuality $Q^2 = -q^2$ and the Bjorken scaling variable $x_{\mathrm{B}} = Q^2/2p \cdot q$, also the photon-proton center-of-mass energy $s = (p+q)^2$ and the quantity $y = p \cdot q / p \cdot k$. Now, the cross section for inclusive deep inelastic scattering can be written with the help of the structure functions

$F_2(x_\mathrm{B}, Q^2)$ and $F_\mathrm{L}(x_\mathrm{B}, Q^2)$:

$$\frac{\mathrm{d}^2\sigma}{\mathrm{d}x_\mathrm{B}\,\mathrm{d}Q^2} = \frac{2\pi\alpha_\mathrm{em}^2}{x_\mathrm{B}Q^4}\left\{\left[1+(1-y)^2\right]F_2(x_\mathrm{B},Q^2) - y^2 F_\mathrm{L}(x_\mathrm{B},Q^2)\right\}\,.$$

The currently available experimental data on F_2 covers a gratifying large regime for different values of x_B and Q^2.

Theoretical physics, now, faces the task to describe the structure functions quantitatively within the framework of QCD. Fortunately, the scale at which α_s has to be evaluated in this case is equal to Q^2. For sufficiently large Q^2, perturbation theory can, therefore, be applied. Since we are interested in inclusive quantities, we can make use of the optical theorem, which tells us that the inclusive cross section is proportional to the imaginary part of the forward Compton scattering amplitude of virtual photons. Now, it turns out that certain phase space integrations over the corresponding Feynman diagrams yield not only quantities which are proportional to certain powers of α_s but also to certain powers of $\ln(Q^2/Q_0^2)$, where Q_0^2 is some scale. If these logarithms are sufficiently large they can spoil the smallness of α_s. It is, therefore, necessary to resum these terms, i.e. to sum all quantities which are proportional to factors $(\alpha_\mathrm{s}\ln Q^2/Q_0^2)^n$ with arbitrary n. This corresponds to the summation of an infinite number of Feynman diagrams. Fortunately, this is feasible with the help of the DGLAP approach [1–3]. The DGLAP equations are integro-differential equations with a finite number of parameters, which can be computed with the help of perturbative methods. On the other hand these integro-differential equations need initial conditions as input. These initial conditions are considered as the non-perturbative input at some scale Q_0^2 and the DGLAP equations serve as evolution equations which yield values of the structure functions for $Q^2 > Q_0^2$. Since the input distributions at the scale Q_0^2 are of non-perturbative origin, one has to answer the question: "What is the smallest legitimate value for Q_0^2 before perturbation theory breaks down?". The results presented in this thesis also show which difficulties can arise if Q_0^2 is chosen too small.

Higher-Twist Contributions

One particular problem arises since, besides the fact that there are quantities proportional to factors like $\alpha_\mathrm{s}^m(\alpha_\mathrm{s}\ln Q^2/Q_0^2)^n$, there are also corrections proportional to certain powers of $1/Q^2$, viz. higher-twist terms. Although, for low values of Q^2, these higher-twist terms are likely to become important, they are neglected for descriptions of F_2 within the DGLAP formalism [4–6]. If we consider F_2 as a function of x_B for different values of Q^2, we know from experiment that F_2 becomes flatter with decreasing Q^2. Now, the question arises: What is the origin of this flattening? Can it be explained as an interplay of leading- and higher-twist? If this is the case, is there a region in which the higher-twist part can be treated perturbatively, so that we might get an insight into how the transition from the perturbative into the non-perturbative region takes place?

There are also some experimental results which support our effort to explore higher-twist contributions. First, experiments show that there is a sizeable amount of vector mesons produced diffractively from longitudinally polarized photons within the kinematical regime of HERA. This process has been shown to be computable perturbatively and it belongs definitely to higher-twist [7–10]. One, therefore, expects higher-twist contributions also to inclusive DIS structure functions in the same kinematical regime. We will show in this thesis that the situation is more subtle. There

are quantities with different signs which can result in cancellations. A naive estimate of higher-twist contributions to DIS structure functions based on diffractive vector meson production [11] is, therefore, not quite correct.

The second reason based on empirical data why we believe that higher-twist contributions to F_2 should be taken into consideration is given by a kind of evaluation of experimental data which became known as the *Caldwell plot* (fig. 1). For this plot the slope $\mathrm{d}F_2/\mathrm{d}\ln Q^2$ is computed and the experimental data shows that this slope has a *kink* which sets in at $10^{-4} < x_\mathrm{B} < 10^{-3}$ and $3\,\mathrm{GeV}^2 < Q^2 < 8\,\mathrm{GeV}^2$ [12]. A possible explanation for this *kink* might be the mentioned interplay of leading- and higher-twist contributions.

History

Most results on higher-twist contributions to inclusive DIS structure functions have been published in the early 1980s. For example, S. Gottlieb [13] classified all twist-four operators and computed some of their anomalous dimensions. He discusses in some detail the operator mixing problem and the implications on experimental data. M. Okawa [14] computed the anomalous dimensions of twist-four four-quark operators and of flavor octet, three-body operators. Exploiting the spinor calculus and some Ward identities, Okawa could resolve the mixing problem and find some closed expressions. S.P. Luttrell et.al. [15] calculated the Wilson coefficient functions of the four-quark operators. The set of twist-four operators introduced by Gottlieb [13] is overdetermined, since one can find relations between certain operators by use of the equations of motion. It is, therefore, necessary to introduce some basis [16]. R.L. Jaffe and M. Soldate [17,18] have chosen a special basis which they call *canonical*. This basis consists of operators which fulfil the following three demands: they are (1) totally symmetrical, (2) traceless (in all index pairs), and (3) have no contracted derivatives. Using this basis Jaffe and Soldate could compute the operators' tree-level coefficient functions.

The approaches mentioned so far are all based on the operator product expansion (OPE). The OPE makes use of the fact that the hadronic tensor $W^{\alpha\beta}$ factorizes into two parts, viz. coefficient functions C_i and parton correlation functions f_i:

$$W^{\alpha\beta} = \sum_{\substack{\tau=2 \\ \tau \text{ even}}} \left(\frac{\Lambda^2}{Q^2}\right)^{\frac{\tau-2}{2}} \sum_i \int \mathrm{d}\{x\}\, C_{i,\tau}^{\alpha\beta}(\{x\}) f_{i,\tau}(\{x\})\,,$$

where τ corresponds to the twist of the quantities and we have dropped details like the dependence on logarithms of Q^2. While the coefficient functions C_i can be computed perturbatively, the correlation functions f_i contain some non-perturbative input. Using the renormalization group equations the connection between the OPE and the DGLAP approach can be established. Usually the correlation functions f_i are expressed as matrix elements of certain operators between proton states. For this, one starts with a classification of all possible operators by their twist τ. In this context the twist of an operator is defined as its mass dimension minus its spin. Using general arguments, one can show that the contributions due to certain operators are at least suppressed by a factor $(1/Q^2)^{(\tau-2)/2}$. Throughout this thesis, we do not define the twist of the quantities under consideration in this sense, but by the power of $(1/Q^2)$-factors with which they are suppressed. This will prove to be convenient, since we can apply dimensional considerations.

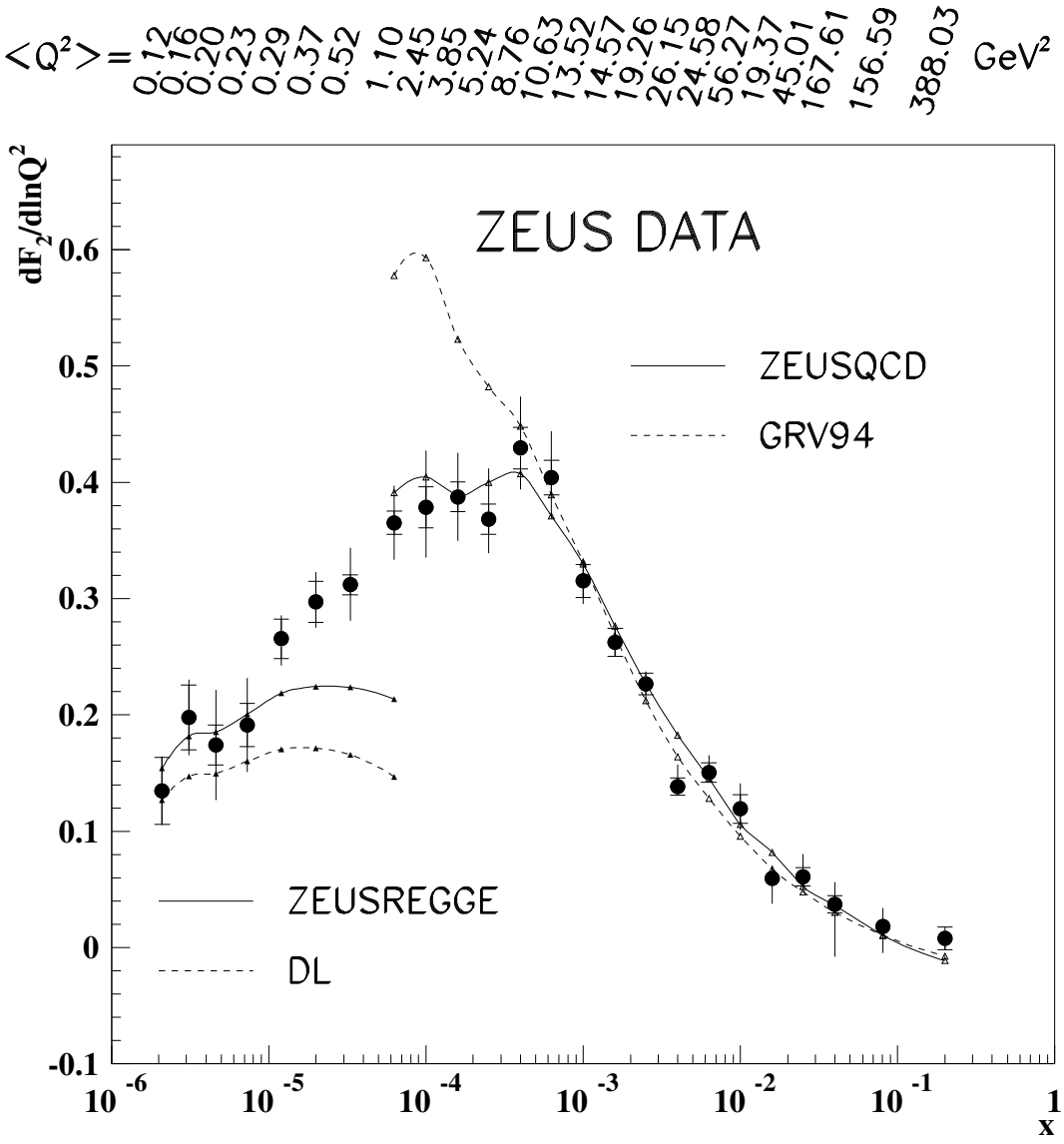

FIG. 1: ZEUS data on $\mathrm{d}F_2/\mathrm{d}\ln Q^2$ as a function of x. Taken from [12].

In contrast to these rather formal methods, R.K. Ellis, W. Furmanski, R. Petronzio (EFP) [19] have introduced a graphical method which is useful for the determination of $1/Q^2$-corrections in the Born approximation. For this the authors consider all tree-level diagrams in which up to four t-channel partons couple to the proton. EFP make use of the axial gauge and with the help of a dimensional argument they can show that their analysis is consistent in so far as diagrams with more than four t-channel partons would lead to contributions which belong at least to twist-six. Moreover, using special techniques in order to classify the spinor, color and momentum structure and by usage of equations of motion they can write the expressions for the contributing quantities in a very compact form. For this EFP show that the *canonical* basis introduced by Jaffe and Soldate [17] is not the one which gives the most intuitive results. Instead they choose a basis which they call *transverse*.

EFP's results have been used as the basis for many other studies. For example, introducing a quantity named *special propagator*, J. Qiu [20] could reproduce the results published in [19] in a very elegant way. Qiu's method is based on the space-time picture of twist-four short-distance contributions. It enables the author to separate the different twist short-distance contributions from a given Feynman diagram. A.P. Bukhvostov et.al. [21] have classified a special class of composite local operators. They call these operators *quasi-partonic* (QPO), formulate the evolution equations for these operators and compute the integral kernels for all possible $2 \to 2$ transitions in the one-loop approximation. The set of QPO is not complete. For a consistent treatment of higher-twist one has to incorporate also non-QPO, although the authors of ref. [21] show that the class of QPO is closed under renormalization.

Small x_{B} Physics

After these digressions on general methods of QCD and on higher-twist, let us, now, turn to physics in the regime of small x_{B}. In pre-QCD times physicists have developed Regge theory in order to be able to describe the strong interactions. For this they tried to extract as much as possible by studying the consequences of a reasonable set of postulates about the S-matrix. This proved to be useful especially in the so called Regge region in which the center-of-mass energy is much larger than the momentum transfer, $s \gg |t|$, also known as the high-energy limit [22]. One of the major theoretical challenges, today, is the description of Regge theory within the framework of QCD. For DIS the high-energy limit corresponds to the small x_{B} limit. Using general arguments, one can show that, in the limit $s \to \infty$, exchange particles with the largest spin will lead to the strongest rise of the cross sections. Therefore, the gluon plays a special rôle at small x_{B}.

As we have discussed above, loop-integrations within Feynman diagrams over certain regions of the phase space lead to terms proportional to logarithms of Q^2. Now, it turns out that integrations over other regions of the phase space also lead to logarithms in x_{B}. If we are interested in certain quantities at small x_{B} it is, therefore, necessary to resum in $\ln x_{\mathrm{B}}$. This resummation has been performed by Ya.Ya. Balitskii, V.S. Fadin, E.A. Kuraev and L.N. Lipatov [23] and yielded the celebrated BFKL equation. As it turns out, the solution of the leading-order (LO) BFKL equation will eventually violate the so-called Froissart-Martin bound. The Froissart-Martin bound [24, 25] has been derived using unitarity and the partial wave expansion. It states that, as $s \to \infty$, total hadronic cross sections must satisfy the inequality [22]

$$\sigma_{\mathrm{tot}} < A \ln^2 s$$

where A is some constant which is expected to be $\mathcal{O}(60\,\mathrm{mb})$. A violation of the Froissart-Martin bound corresponds, therefore, to a violation of unitarity. In order to examine how to overcome the problem of violation of unitarity, the next-to-leading order (NLO) corrections to the BFKL equation have recently been published [26].

Multi-Gluon Amplitudes

The computations of the NLO BFKL equation turned out to be a complicated and long lasting effort and the estimated time for the computation of even the NNLO corrections is far beyond the average lifetime of graduate students. It would, therefore, be appreciated if one could, at least, restore unitarity with the help of easier approximations. J. Bartels [27] argued that one should sum diagrams with n reggeized t-channel gluons in order to take, in each order of perturbation theory, just those contributions into account which are necessary to restore unitarity. The first approach in this direction has been performed by L.V. Gribov, E.M. Levin and M.G. Ryskin [28]. They considered freely evolving parton cascades, which merge at a triple ladder vertex (fan diagrams). A systematic program towards the calculation of higher-order corrections based on multi-gluon amplitudes has been started in [27, 29, 30]. For this, one considers amplitudes which are computed with the help of the so called high-energy (small-x_B) approximation and which have a certain number of reggeized t-channel gluons. In this scheme the LO BFKL amplitude corresponds to the first approximation, i.e. the two-gluon amplitude. Results for the three- and four-gluon amplitudes have been obtained by J. Bartels [29] and J. Bartels and M. Wüsthoff [30].

As it turns out the three-gluon amplitude can be written completely as a sum of expressions for the two-gluon (BFKL) amplitude with adequate evaluation of momenta. This phenomenon has been termed reggeization, as well, since it generalizes the reggeization of the gluon. The situation for the four-gluon amplitude is more complicated. It splits up into a reggeizing part which can, again, be written as a sum of expressions for the two-gluon amplitude and a part which is *irreducible* with respect of reggeization. It is especially this *irreducible* part which is of particular interest, since it is expected to give the largest contributions of the mentioned amplitudes at small x_B. Unfortunately, the integral equation for this *irreducible* part could, up to today, not be solved. Although this equation has been examined intensively – this led to the prove of the conformal invariance of its solution in configuration space among other interesting properties of the four-gluon amplitude [31–37] – there exists only an approximation, which is based on the double-logarithmic approximation (DLA) [29, 38]. Within the DLA one takes only terms which are proportional to $(\alpha_\mathrm{s} \ln Q^2/Q_0^2 \ln x_\mathrm{B})^n$ into account, i.e. logarithms in Q^2 and x_B to the same power. The expressions for the multi-gluon amplitudes contain terms proportional to certain powers of logarithms in x_B. These terms depend also on Q^2 and contain factors like $(1/Q^2)^\tau$, i.e. they sum over contributions of *all* twist.

Let us just briefly comment on amplitudes with more than four t-channel gluons. It is immediately clear that the time for the computation of these amplitudes increases with the number of gluons. If one could show that all amplitudes with a certain number of reggeized t-channel gluons can be constructed with the help of just a few basic quantities, the computation time could distinctly be lowered. Using the known results on the two-, three- and four-gluon amplitudes one gets the idea that such a general analysis could be feasible in terms of an effective $2+1$-dimensional conformal field theory [31–37]. In order to study this possibility and to get more insight into the structure

of multi-gluon amplitudes, C. Ewerz [39] recently published his results on the five- and six-gluon amplitudes.

Higher-Twist at Small x_B and Low Q^2

For the description of DIS structure functions in the small x_B, low Q^2 region, one has to handle both, large logarithms in x_B and higher-twist contributions. An analysis of the structure functions in the mentioned region, therefore, necessitates the treatment of gluonic higher-twist contributions.

Considering the twist-four part of the *irreducible* part of the four-gluon amplitude, it turns out that this contribution rises stronger with decreasing x_B than leading-twist. Moreover, its $1/Q^2$-suppression gets weakened due to evolution which is stronger than in the leading-twist case. For sufficiently small x_B, this amplitude will, therefore, become stronger than leading-twist. In this thesis, we will try to estimate the twist-four contributions at small x_B numerically. We will argue, that, besides the consideration of the *irreducible* part of the four-gluon amplitude, it is also necessary to take twist-four contributions of the two- and three-gluon amplitudes, as well as of the *reggeizing* part of the four-gluon amplitude into account. Since each of the mentioned amplitudes needs some initial distribution as input, one ends up with a large number of free parameters. Within a consistent treatment of twist-four contributions at small x_B a naive fit to experimental data seems, therefore, to be at least difficult. With the help of measured cross sections on exclusive processes which are known to belong to higher-twist it should be possible to reduce the number of free parameters. The most promising process in this sense is the DIS diffractive production of vector mesons.

Diffractive Scattering

As mentioned above, experiments show that there is a sizeable amount of diffractively produced vector mesons within the kinematical regime of HERA. Since this process, at least for the scattering of longitudinal photons, is a higher-twist process and we are using the measured cross section in order to fix a free parameter in our numerical analysis, we shortly discuss it here, as well. Seen from the angle of the proton rest frame, the virtual photon splits into a $q\bar{q}$-pair, which interacts via colorless exchange with the proton before it results in the vector meson. As we have discussed above, gluons are expected to be the dominating exchange particles at small x_B. The colorless exchange can, therefore, most likely be described via exchange of (at least) two t-channel gluons, i.e. via the gluon structure function [40]. For the vector meson, one can introduce a projector which transfers the $q\bar{q}$-pair into the final state particle [10]. Squaring the amplitude one ends up with diagrams with four t-channel gluons (two ladders). If we are not interested in any particular vector meson in the final state, we can sum over all vector mesons. Now, one can apply a duality argument [55] and show that this (summed) cross section is equal to open $q\bar{q}$-production with M^2 and p_t^2 integrated over, where M^2 is the invariant mass squared of the $q\bar{q}$-pair and $\boldsymbol{p}_t$ is the transverse component of its momentum. An expression for this (integrated) diffractive cross section has been given in ref. [30]. Diffractive $q\bar{q}$-production is expected to be the dominating contribution to the diffractive cross section for low values of M^2 (compared to Q^2). For larger values of M^2 it is argued that one should also consider amplitudes with gluons in the final state. The cross section for (integrated) diffractive $q\bar{q}g$-production has also been given in [30]. As it turns out, it can be written with the help of an effective vertex which consists of terms that enter also into the *irreducible* part of the four-gluon amplitude.

Knowing this, we have reached an important point in our discussion, viz. the question of how diffractive processes contribute to the inclusive cross section. The four t-channel gluons of the four-gluon amplitude have to be in the color singlet, but if we pick out just one pair of these four gluons this pair can be in any color state. On the other hand, each pair of gluons on the l.h.s. and on the r.h.s. of the diffractive amplitudes has to be in the color singlet. It is, therefore, immediately clear that the four-gluon amplitude cannot be consider as just a sum of diffractive amplitudes with arbitrarily many gluons in the final state. Instead, the diffractive amplitudes enter completely into the four-gluon amplitude, but they are just one part of contributions. Moreover, the determination of how a specific diffractive amplitude enters into the four-gluon amplitude turns out to be rather difficult. Although the amplitude for diffractive $q\bar{q}$-production enters completely into the *reggeizing* part, such an assignment cannot be made for diffractive $q\bar{q}g$-production. The latter contributes to both, the *reggeizing* and the *irreducible* part of the four-gluon amplitude.

Relations Between Diffractive and Inclusive Amplitudes and the AGK Cutting Rules

Both, the diffractive and the inclusive amplitudes couple to the proton. This coupling corresponds to the input of non-perturbative initial distributions. If one takes all enumerated gluonic twist-four contributions into account, one ends up with a large set of free parameters for these initial distributions. Using a relation between the twist-four contributions to diffractive $q\bar{q}$-production and the four-gluon amplitude, it is possible to minimize this set of free parameters with the help of experimental data on diffractive vector meson production. For this one makes use of the duality argument, outlined above. The desired relation can be found if one compares the diagrams which enter into the diffractive amplitudes with those which enter into the inclusive ones and by application of the Abramovsky, Gribov, Kancheli (AGK) cutting rules [42]. The AGK rules have originally been introduced in order to study cuts of unenhanced reggeon diagrams and of the triple pomeron vertex. They can be applied to QCD [43]. Within our analysis we are using them in order to get the correct signs and the correct factors of the twist-four contributions to the diffractive cross sections and the contribution of the four-gluon amplitude.

For the application of the AGK rules it is necessary to distinguish carefully between even and odd signature contributions and between diagonal and non-diagonal terms. This results in a relation which does not correspond to the naive expectation in which one would set the initial distribution that enters into the diffractive amplitudes equal to minus one times the color singlet projection of the initial distribution that enters into the four-gluon amplitude. In particular, the initial distributions can consist of symmetrical and anti-symmetrical parts. Using such a general ansatz, the resulting relation between diffractive and inclusive amplitudes contains still an undetermined parameter, since the ratio of the symmetrical and the anti-symmetrical parts is a priori not fixed. As it turns out, the *irreducible* part of the four-gluon amplitude couples only to the symmetrical initial distribution, while the *reggeizing* part couples to both, the symmetrical and the anti-symmetrical one. Different choices for this ratio have, therefore, a large effect on the numerical results. With the help of a toy model one can, at least, estimate this ratio.

Relations Between the DGLAP Approach and the High-Energy Approximation

After we have been discussing the DGLAP approach and the high-energy approximation in some detail, it is, now, time to discuss the *overlap* of the two approaches. As mentioned before, this

thesis deals with higher-twist contributions to inclusive DIS structure functions at small x_{B}. We have also argued that at small x_{B} the gluon should be the dominating exchange particle. Seen from the point of view of the OPE, one would, therefore, start with a consideration of higher-twist gluon operators. These operators could, for example, be classified in terms of the *canonical* basis of Jaffe and Soldate [17], mentioned above. For twist-four there are two kinds of gluon operators, viz. two-gluon operators[1]

$$\mathrm{tr}\, F^{\mu_1\alpha}\mathrm{D}^{\mu_2}\ldots\mathrm{D}^{\mu_{n-1}}F^{\mu_n}{}_{\alpha}\, g_{\mu_i\,\mu_j} \;+\; \text{perm.}$$

and four-gluon operators

$$\begin{aligned}
&\mathrm{tr}\, F^{\mu_1\alpha}\ldots F^{\mu_i}{}_{\alpha}\ldots F^{\mu_j\beta}\ldots F^{\mu_n}{}_{\beta}\\
&\mathrm{tr}\, F^{\mu_1\alpha}\ldots F^{\mu_i\beta}\ldots F^{\mu_j}{}_{\alpha}\ldots F^{\mu_n}{}_{\beta}\\
&\mathrm{tr}\, F^{\mu_1\alpha}\ldots F^{\mu_i\beta}\ldots F^{\mu_j}{}_{\beta}\ldots F^{\mu_n}{}_{\alpha},
\end{aligned}$$

where the traces have to be applied to color indices. A systematic analysis of the contributions of these operators to inclusive DIS does not yet exist. Such an approach necessitates the computation of the corresponding coefficient functions and the anomalous dimensions. Especially the latter task will provide some difficulties, since the operators mix under renormalization. In this thesis we perform a first step into the direction of taking the complete set of gluonic twist-four operators into account. For this we do not start with a certain class of operators. Instead we have extended the method of EFP [19] in order to perform the factorization of gluonic twist-four operators and their coefficient functions and to write the resulting expressions in an explicitly gauge invariant form.

On the other hand, as we have mentioned above, the amplitudes obtained within the high-energy approximation contain also corrections which are proportional to higher powers of $1/Q^2$. If these higher-twist parts can be separated, a first analysis of higher-twist at small x_{B} should also be possible. Such a separation is feasible within the DLA. For the DLA one takes only contributions into account in which the logarithms in Q^2 and in x_{B} enter with the same power. It, therefore, corresponds to the overlap region of the DGLAP and the high-energy approximation approaches. Moreover, the integral equation for the *irreducible* part of the four-gluon amplitude can be solved within the DLA. For a first analysis of twist-four contributions one should, for consistency reasons, take contributions of DLA expressions of the two-, three- and four-gluon amplitudes into account. An analysis of this kind has the advantage that it also covers the overlap with the (not available) twist-four corrections to the DGLAP equation. Unfortunately, a quantitative fit of DIS structure functions based on leading-twist DLA results is not very reliable, since the DLA is a rather bad approximation. A quantitative twist-four analysis based on the DLA is, therefore, also likely to be inaccurate. On the other hand, if one consistently takes DLA expressions for the leading- and sub-leading twist contributions and considers only the ratio of both, one can hope that, at least, part of the inaccuracy cancels.

EFP's Approach

Besides a numerical analysis we have also extended the method developed by EFP [19] to the gluonic case. Let us, therefore, shortly outline this method here. Starting with diagrams with

[1] The factor $g_{\mu_i\,\mu_j}$ decreases the spin of the operator while its dimension remains unchanged. It, therefore, increases the twist of the operator.

up to four t-channel partons, EFP have performed the factorization of twist-four quark coefficient functions and quark-operators in the Born approximation. For this the authors are working in the axial gauge. Treating the expressions for the coefficient functions separately from the remaining parts of the diagrams, and analysing the color-, Lorentz- and momentum-structure, they could write the resulting expressions in an explicitly gauge invariant form. Moreover, using equations of motion and introducing the *transverse* basis EFP could reduce the number of entering quantities to a minimal set.

For the extension of EFP's method to the gluonic case one has to start with diagrams which involve up to four t-channel gluons. Since the photon couples only to electrically charged particles, these diagrams have a quark-loop at the top and the scheme, now, consists of treating the expressions for these quark-loops separately from the remaining parts of the diagrams. Expanding the quark-loop expressions about the longitudinal components of the gluon-momenta they depend on and making use of Ward identities for the derivatives occurring in these expansions, the factorization can be performed. The axial gauge proves to be convenient for several reasons. First, gluonic A_a^μ-operators within matrix-elements between proton states can easily be replaced by $F_a^{\mu\nu}$-operators in order to get explicitly gauge invariant expressions. Secondly, diagrams with more than four t-channel gluons will lead to contributions of, at least, twist-six. In this thesis we are not computing explicit expressions for the quark-loops. Instead we are making use of general properties concerning the color-, Lorentz- and momentum-structure. Moreover, we have to explore symmetry relations of the four-gluon quark-loop expression. These symmetry relations will also lead to restrictions on the color tensor with which the four-gluon operator is multiplied.

Outline

This thesis consists of two major parts. In the first part we describe numerical results obtained with the help of the DLA expressions for the twist-four parts of multi-gluon amplitudes. For this, we, first, give the expressions for the two-, three- and four-gluon amplitudes in section 1. As discussed above, the initial distribution that enters into the four-gluon amplitude can be related to the initial distribution that enters into diffractive $q\bar{q}$-production. We, therefore review results on diffractive cross sections in section 2, where we also repeat the duality argument which relates diffractive vector meson production with a sum over all vector mesons to integrated $q\bar{q}$-production. The AGK rules are discussed in section 2.4.

In section 3 we present our numerical results. For this we study different scenarios with different assumptions on the initial conditions. We consider contributions of longitudinally and transversely polarized photons separately and show how the four twist-four contributions under consideration – contributions of the two-, three- and four-gluon amplitude – sum up to a total twist-four contribution. One of the main results of our analysis is the observation that the different twist-four contributions enter with different signs and this leads to cancellations. Within the two scenarios in which we have chosen constant initial distributions, the transverse photon gives the main twist-four contributions. The sum over these is negative and ranges between fifteen and hundred per cent (depending on the choice of parameters) of the transverse leading-twist contribution at $Q^2 = 1\,\mathrm{GeV}^2$.

While the first part of this thesis is devoted to a numerical estimation of twist-four contributions based on the DLA of high-energy approximation results, the second part considers gluonic higher-

twist contributions from a more theoretical point of view. Using a graphical method, we have extended the procedure developed by EFP [19] in order to factorize gluonic twist-four operators and the corresponding coefficient functions. For this we summarize the results obtained by EFP in section 5, clarify our conventions in section 6 and outline the used scheme in section 7. We are working in the axial gauge and consider diagrams with up to four t-channel gluons. In section 8 we derive some Ward identities for the derivatives occurring in the expansions of the quark-loop expressions in these diagrams. For this we make use of the path-integral formulation of QCD, since the diagrammatical derivation of these Ward identities is rather tedious and leads to less general results.

In section 9 we show how A_a^μ-operators occurring in matrix elements between proton states can be exchanged by $F_a^{\mu\nu}$-operators in order to get expressions which are explicitly gauge invariant. In section 10 we are using a dimensional argument in order to show that our analysis is consistent in the same sense as the analysis of EFP, i.e. diagrams with more than four t-channel gluons lead to contributions of, at least, twist-six. Moreover, the quantities under consideration initially contain also leading-twist parts and parts which belong to twist larger than four. With the help of the dimensional analysis in section 10 we also find a way of projecting out the twist-four parts. For this first analysis we do not take evolution into account and we do not compute explicit expressions for the quark-loops. Instead we make use of some general properties concerning the color-, Lorentz- and momentum structure of these quark-loops.

In section 11 we give the results of our analysis. The gluonic twist-four contributions are written as explicitly gauge invariant expressions. They are factorized into the coefficient functions and matrix-elements of gluon-operators between proton states. While these results can easily be derived in the cases in which two or three t-channel gluons are exchanged (section 11.1), the situation is more peculiar in the case of four gluons. For four gluons we give, first, the formulae on which the derivation is based in subsection 11.2.1 and explore the symmetry relations of the four-gluon quark-loop in subsection 11.2.2. Using these, the explicitly gauge invariant expressions are derived in subsection 11.2.3. Moreover, in subsection 11.2.4 we consider the color tensor within the four-gluon operator expression. We show that terms within this color tensor survive only if they fulfil certain symmetry relations. In section 11.3 we discuss the obtained results in some detail and in section 12 we describe the steps which have to be completed before our results can be used in a phenomenological analysis.

In appendix A we list some basic formulae which are useful within expressions of the four-gluon amplitude. In particular, we list color tensors, which can serve as a basis for the expansion of the color structure of a four-gluon (color singlet) state. Moreover, we give matrices for the transformation between different basisses. Finally, we give an analytic expression for a quantity which enters into the four-gluon amplitude and can be obtained by inversion of a specified 9×9 matrix. In appendix B we outline a numerical formalism which we have developed in order to perform numerical inverse Mellin transforms efficiently.

Part 1

A Numerical Estimate of Gluonic Twist-Four Contributions to DIS Structure Functions

As mentioned in the introduction, we have performed a numerical analysis based on the twist-four contributions of amplitudes with two, three and four t-channel gluons. The analysis is based on the DLA results of these amplitudes, which are believed to correspond to the DLA contributions of the twist-four two- and four-gluon operators in the limit $x_{\mathrm{B}} \to 0$, $Q^2 \to \infty$.

A numerical analysis of twist-four corrections to, say, F_2 follows the same sequence of steps as the usual twist-two strategy: for an input scale Q_0^2 one has to choose an initial distribution (with a certain number of free parameters), and by application of evolution equations one gets values of the structure functions for $Q^2 > Q_0^2$. Since the number of twist-four operators that mix under renormalization will, in general, be larger than in the twist-two case, the number of free parameters in such an analysis will be large, and a reliable combined analysis of twist-two and twist-four terms looks extremely difficult. It might, therefore, be helpful to include information on specific final states, which are known to belong to higher-twist. The most promising candidates are diffractive final states, in particular the diffractive production of vector mesons from longitudinal photons: this process has been shown to be calculable within perturbative QCD [7–10]. It belongs to higher-twist, and the measured cross section is substantial (about 20 % of the total diffractive cross section). Another candidate for a determination of higher-twist contributions are diffractive final states with hard jets.

In this first part of the thesis, we present the results of a numerical estimation of gluonic twist-four corrections at small x_{B} and low Q^2, making use of the currently available elements of the twist-four evolution equations. In our scheme we first have to review the existing small x_{B} calculations of gluonic scattering amplitudes, and extract the relevant parts of the Q^2 evolution. The currently existing calculations do not allow to go beyond DLA. Generally, we are dealing with gluonic amplitudes which couple to the photon through a fermion-loop. First, we find that, for a systematic analysis of twist-four, we have to consider both the transverse and the longitudinal polarization of the photon. The reason for this is the fact that the transverse twist-four expression for the fermion-loop has no factor $\ln Q^2$, whereas the longitudinal one does. This is quite opposite to the leading-twist case where the transverse expression has the logarithm, and the longitudinal one does

not. Unfortunately, in DLA this result forces us to compare contributions of different order in α_s: in order to make a legitimate comparison between the twist-four transverse and longitudinal contributions, we should know the longitudinal one up to the (in the sense of DLA) next-to-leading terms. A second general result of our investigation is the sign structure of the different higher-twist terms. Both for the longitudinal and for the transverse twist-four contributions we shall argue that there are four different parts that have to be taken into account, and they enter with alternating signs. The total twist-four contribution, therefore, depends crucially on the magnitude of each individual term, i.e. the size of the initial condition. As one of our results we find that, although strong cancellations occur, the total twist-four contribution enters with a significant amount. For the scenarios in which we have chosen constant initial distributions, the total twist-four contribution enters with a negative sign and it is the transverse photon which leads to the main contribution.

Besides a numerical evaluation of twist-four contributions we have also defined a practical procedure useful for the determination of how the different contributions enter into the structure functions. We propose to use experimental data on DIS diffractive final states. It is, therefore, necessary to first investigate the rôle of higher-twist in diffractive dissociation and to analyse the connection with the inclusive structure functions. In section 2 we, therefore, review diffractive dissociation, with particular emphasis on higher-twist. For the determination of free parameters in our numerical analysis we will make use only of longitudinal vector production; in order to understand the origin of the different signs, however, we have to analyse also other diffractive final states. Contact with the corrections to the structure functions is made through the AGK cutting rules [42]. We found that, in contrast to the naive expectation, we cannot simply use the diffractive cross section to estimate the higher-twist corrections to F_2. There still remain some uncertainties which we, presently, cannot eliminate. Our central result on the AGK rules is contained in eqn. (2.21).

For the numerical results, which we present in section 3, we have to distinguish carefully between the different contributions. In particular, we write

$$F_i(x,Q^2) = F_i^{\tau=2} + \Delta F_i\,, \qquad i = t, \ell$$

for the inclusive DIS structure functions. In this equation, the twist-four corrections ΔF_i (both for $i = t$ and $i = \ell$), by themselves, consists of four pieces (cf. (1.46)). As noted before, we can work only in DLA which puts severe limitations on the accuracy of our results. Despite our idea of using experimental information on diffractive final states, there is still freedom in choosing initial conditions for the different twist-four operators. Our conclusions, therefore, can be only very tentative.

1 Higher Twist at small x_B

We begin with a brief summary of the present theoretical status of the evolution of higher-twist gluon-operators. As mentioned already in the introduction, using general dimensional arguments [13] one ends up with two classes of gluonic operators. First, there are the four-gluon operators:

$$\begin{aligned} &\mathrm{tr}\, F^{\mu_1\alpha} \ldots F^{\mu_i}{}_{\alpha} \ldots F^{\mu_j\beta} \ldots F^{\mu_n}{}_{\beta} \\ &\mathrm{tr}\, F^{\mu_1\alpha} \ldots F^{\mu_i\beta} \ldots F^{\mu_j}{}_{\alpha} \ldots F^{\mu_n}{}_{\beta} \\ &\mathrm{tr}\, F^{\mu_1\alpha} \ldots F^{\mu_i\beta} \ldots F^{\mu_j}{}_{\beta} \ldots F^{\mu_n}{}_{\alpha} \end{aligned} \tag{1.1}$$

(here $1 < i, j < n$, and the dots denote products of covariant derivatives). Bukhvostov et.al. [21] called these operators "quasipartonic", and they gave a general discussion of the operator's evolution. In particular, it has been shown that at leading order only two-body interaction kernels are needed. These are the non-forward generalizations of the Altarelli-Parisi splitting functions. In ref. [29] a discussion of the small $x_{\rm B}$ evolution equations of the four-gluon amplitude in DLA is given. As we will discuss in more detail below, a particular part of the four-gluon amplitude, viz. the part which is *irreducible* with respect of reggeization, is believed to be related to the four-gluon operator (1.1). Besides the quasipartonic operators (1.1), there exists another gluonic twist-four operator which is related to the BFKL equation [41]:

$$\mathrm{tr}\, F^{\mu_1\alpha} D^{\mu_2} \ldots D^{\mu_{n-1}} F^{\mu_n}{}_{\alpha} g_{\mu_i\,\mu_j} \;+\; \text{Perm}\,. \tag{1.2}$$

Using the BFKL equation one can deduce the anomalous dimension of this operator in DLA. The recently derived [26] second order corrections to the BFKL kernel allow to go beyond DLA. In general, the twist-four operators (1.1) and (1.2) should mix, i.e. there should be off-diagonal elements in the anomalous dimension matrix. These off-diagonal elements are known in DLA-accuracy [29], cf. the discussion in the sequel of eqn. (1.39).

In the discussion below we shall see that at small $x_{\rm B}$ the four-gluon operators (1.1) are the ones which are most interesting: they result in contributions which rise stronger at small $x_{\rm B}$ than the contributions of the leading-twist gluon operator. Although the four-gluon operator contributions are suppressed by one factor $\alpha_{\rm s}$ and despite of the $1/Q^2$ suppression, they will eventually catch up with leading-twist contributions at sufficiently small $x_{\rm B}$ due to this stronger rise. The $\alpha_{\rm s}$-suppression of (1.1) will, however, force us to consider higher order corrections to (1.2).

In the following we shall list the presently available results for the contributions of operators (1.1) and (1.2). As mentioned before, we will relate these contributions to two-, three-, and four-gluon amplitudes in the double logarithmic approximation.

1.1 The Two-Gluon Operator

As we have said before, the DLA expression for the anomalous dimension of the twist-four two-gluon operator can be obtained from the BFKL equation. Let $D_2^i(x, Q_0^2/Q^2)$ $(i = t, \ell)$ denote the imaginary part of the scattering amplitude of the photon (virtuality Q^2) off the gluon (virtuality Q_0^2). It is convenient to write this amplitude as a double Mellin-transform

$$D_2^i(x, Q_0^2/Q^2) = \int \frac{\mathrm{d}\omega}{2\pi\mathrm{i}}\, x^{-\omega} \int\limits_{-1/2-\mathrm{i}\infty}^{-1/2+\mathrm{i}\infty} \frac{\mathrm{d}\nu}{2\pi\mathrm{i}} \left(\frac{Q_0^2}{Q^2}\right)^{-\nu} D_2^i(\omega,\nu)\,. \tag{1.3}$$

In the BFKL approximation, the amplitude $D_2^i(\omega,\nu)$ can be written as

$$D_2^i(\omega,\nu) = D_{2,0}^i(\nu) \frac{1}{\omega - \chi(\nu)}\,, \tag{1.4}$$

where $D_{2,0}^i$ denotes the quark-loop at the upper end of the gluon ladder (fig. 1.1a), and the BFKL characteristic function has the form

$$\chi(\nu) = \frac{N_{\rm c}\alpha_{\rm s}}{\pi}\left[2\psi(1) - \psi(\nu+1) - \psi(-\nu)\right]\,. \tag{1.5}$$

It has poles at integer values of ν, and the anomalous dimensions of the leading-twist two-gluon operator and the twist-four two-gluon operator are obtained by solving the equation

$$0 = \omega - \chi(\nu) \tag{1.6}$$

near the poles at $\nu = -1$ and $\nu = -2$, resp.:

$$\gamma^{\tau=2}(\omega) = \frac{N_c}{\pi\omega}\alpha_s + \mathcal{O}\left(\left(\frac{\alpha_s}{\omega}\right)^4\right) \tag{1.7}$$

$$\gamma^{\tau=4}(\omega) = \frac{N_c}{\pi\omega}\alpha_s - 2\left(\frac{N_c\alpha_s}{\pi\omega}\right)^2 + \mathcal{O}\left(\left(\frac{\alpha_s}{\omega}\right)^3\right)\ldots \tag{1.8}$$

Using the recently published NLO calculations [26] it is possible to derive the singular part of the NLO corrections to the anomalous dimensions, i.e. corrections of the form $\alpha_s^2 \frac{\text{const}}{\omega}$.

The quark-loop expressions $D^i_{2,0}(\omega,\nu)$ correspond to the coefficient functions. We give the results for the transverse photon [30, 45]:

$$\frac{1}{\omega}D^t_{2,0}(\omega,\nu) = \frac{1}{\omega}\sum_f e_f^2 \frac{\sqrt{8}}{2\pi}\alpha_s \frac{\pi^2}{4}\frac{(\nu-1)(\nu+2)}{(\nu-\frac{1}{2})(\nu+\frac{1}{2})(\nu+\frac{3}{2})}\frac{\sin\left[\pi(\nu+\frac{1}{2})\right]}{\cos^2\left[\pi(\nu+\frac{1}{2})\right]} \tag{1.9}$$

and for the longitudinal one

$$\frac{1}{\omega}D^\ell_{2,0}(\omega,\nu) = \frac{1}{\omega}\sum_f e_f^2 \frac{\sqrt{8}}{2\pi}\alpha_s \frac{\pi^2}{4}\frac{\nu(\nu+1)}{(\nu-\frac{1}{2})(\nu+\frac{1}{2})(\nu+\frac{3}{2})}\frac{\sin\left[\pi(\nu+\frac{1}{2})\right]}{\cos^2\left[\pi(\nu+\frac{1}{2})\right]}\,. \tag{1.10}$$

By expanding eqns. (1.9) and (1.10) in Laurent-series,

$$D^{t,\ell}_{2,0}(\omega,\nu) = \sum_f e_f^2 \frac{\sqrt{8}}{2\pi}\alpha_s \sum_{n=-\infty}^{\infty}\left(\frac{b_n^{t,\ell}}{(\nu+n)^2} + \frac{a_n^{t,\ell,}}{\nu+n}\right)\,, \tag{1.11}$$

and considering the residues at negative integer values of ν we obtain the twist expansion as a series in powers of Q_0^2/Q^2. The coefficients a_n and b_n for leading- and next-to-leading twist are listed in table 1.1. Since the double poles with factors b_n correspond to logarithms of Q^2 while the simple poles with factors a_n correspond to constants, we recognize with the help of table 1.1 that, for leading-twist, the longitudinal contribution is sub-leading at large Q^2 (compared to the transverse cross section). For twist-four we have the opposite situation: the longitudinal contribution has the factor $\ln Q^2/Q_0^2$, whereas the transverse cross section is suppressed. Moreover, we note the sign structure of the coefficients in table 1.1: the longitudinal twist-four part contributes with a negative sign.

For our twist-four analysis we perform our computations in DLA and, therefore, consider only amplitudes proportional to b_2^ℓ and a_2^t for the longitudinal and transverse contributions, respectively. Taking into account the evolution in Q^2, we get a factor $\gamma_2/\omega(\nu+2)$ for each rung, where[1]

$$\gamma_2 \equiv \frac{N_c\alpha_s}{\pi}\,. \tag{1.12}$$

[1]Within our conventions the singular part of the gluon anomalous dimension is given by γ_2/ω and not by γ_2 itself.

n	a_n^ℓ	b_n^ℓ	a_n^t	b_n^t
1	$\frac{2}{3}$	0	$\frac{14}{9}$	$\frac{4}{3}$
2	$-\frac{94}{225}$	$-\frac{4}{15}$	$\frac{2}{5}$	0

TABLE 1.1: Twist-expansion coefficients of $D_{2,0}$ for leading- and next-to-leading twist.

Performing the ν-integration we end up with

$$D_2^t(\omega, Q_0^2/Q^2)^{\tau=4} = a_2^t \sum_f e_f^2 \frac{\sqrt{8}}{2\pi}\alpha_{\rm s} \left(\frac{Q_0^2}{Q^2}\right)^2 \frac{1}{\omega} \exp\left(\frac{\gamma_2}{\omega}\ln(Q^2/Q_0^2)\right), \qquad a_2^t = \frac{2}{5} \tag{1.13}$$

for the transverse amplitude, and

$$D_2^\ell(\omega, Q_0^2/Q^2)^{\tau=4} = b_2^\ell \sum_f e_f^2 \frac{\sqrt{8}}{2\pi}\frac{\alpha_{\rm s}}{\gamma_2} \left(\frac{Q_0^2}{Q^2}\right)^2 \left[\exp\left(\frac{\gamma_2}{\omega}\ln(Q^2/Q_0^2)\right) - 1\right], \qquad b_2^\ell = -\frac{4}{15} \tag{1.14}$$

for the longitudinal one. As stated before, the longitudinal amplitude has an extra factor $\ln Q^2/Q_0^2$, in comparison with the transverse case: in the DLA approximation, therefore, we have to be careful when comparing the transverse amplitude with the longitudinal one. However, the extra logarithm only emphasises the dominance of the longitudinal amplitude at large Q^2. In the low Q^2 region, there is no reason why the (twist-four) part of the transverse cross section should be smaller than the longitudinal one. We will, therefore, be slightly inconsistent with the counting of 'leading' and 'sub-leading'.

Finally, we note the connection between the amplitudes $D_2^{t,\ell}$ and the twist-four corrections to the structure functions:

$$\Delta F_{t,\ell}^{(2)}(x,Q^2) \;=\; \frac{1}{4\sqrt{8}}\frac{Q^2}{Q_0^2}\int \frac{{\rm d}\omega}{2\pi{\rm i}}\, x^{-\omega} \int_{-1/2-{\rm i}\infty}^{-1/2+{\rm i}\infty} \frac{{\rm d}\nu}{2\pi{\rm i}} \left(\frac{Q_0^2}{Q^2}\right)^{-\nu} D_2^{t,\ell}(\omega,\nu)\varphi_2(\omega,\nu)^{\tau=4}, \tag{1.15}$$

where the superscript '2' refers to the '2-gluon' ladder. In the subsequent sections we will add further terms to ΔF_i. Within our representations the twist-four part is obtained by evaluating the residue at $\nu = -2$ ($\nu = -1$ corresponds to the leading-twist term). $\varphi_2(\omega,\nu)$ denotes the initial condition: in the context of the BFKL equation (which is an evolution equation in $y = \ln 1/x_{\rm B}$) φ_2 would define, at fixed x_0, the distribution in Q^2. However, in our DLA approximation, where the BFKL equation coincides with the small $x_{\rm B}$ limit of the DGLAP evolution equation, φ_2 denotes, at fixed scale Q_0^2, the initial distribution in $x_{\rm B}$. In order to write down the most general case, we have, here, chosen a representation in which φ_2 depends upon both ν and ω. Thinking in terms of DGLAP, i.e. evolution in Q^2, φ_2 has to be considered as a function of ω, and the singularity structure at $\nu = -1$ and $\nu = -2$ defines the $x_{\rm B}$-shape of the leading- and next-to-leading twist initial distributions, resp. As usual, both, the leading-twist and the twist-four, input distributions have to be modelled and cannot be computed within pQCD. In the following, unless stated differently, we will use φ_2 to denote the leading-twist initial distribution.

Our discussion below will show that the situation with the two-gluon amplitude, in fact, is more complicated. In particular, we shall argue that the reggeization of the gluon provides extra contributions to the two-gluon operator. As we have mentioned before, we try to draw relations between

the contributions of twist-four operators and multi-gluon amplitudes. In the next subsection we will turn to a discussion of the four-gluon amplitude which contains a part which is expected to be related to the four-gluon operators (1.1). At lowest order in α_s, one has to consider diagrams in which four gluons are exchanged between the quark-loop and the target proton (fig. 1.2). These diagrams are suppressed by one factor α_s compared to the LO contributions of the two-gluon amplitude. When higher-order diagrams are included, it will turn out that, at small x_B, the sum of all these diagrams has to be split up into two separate classes. The first one is expected to correspond to the four-gluon operator (which, however, mixes with the two-gluon operator (1.2)). For this part, the α_s-suppression (relative to the twist-four two-gluon operator) is compensated by the stronger rise at small x_B. However, the second part is due to the reggeization of the gluon. Symbolically, this contribution has the same form of gluon ladders as the BFKL equation, except that at the lower end the reggeized gluon lines split up into two or more gluon propagators (fig. 1.4). Seen from the angle of the proton, the four emitted gluons turn immediately into a state of two reggeized gluons. This contribution, therefore, has the same Q^2 dependence as the BFKL amplitude. Since it is suppressed by one factor α_s, it can be considered as a NLO contribution of the two-gluon operator (1.2). On the other hand, it corresponds to the exchange of four t-channel gluons. We will show that it can be estimated using the measured diffractive cross section, and as it turns out this contribution is surprisingly large. After the discussion in the next subsection we, therefore, will, once more, return to a discussion of the two-gluon amplitude and add two more separate contributions.

Let us briefly summarize the main results of this subsection. Starting with the BFKL amplitude we have collected the known results on the twist-four two-gluon operator (1.2). Rather than writing the BFKL amplitude as an evolution equation we have used the closed expression in the (ω, ν)-representation. Presently, only expressions within the DLA are completely available. In order to go beyond the DLA it will be necessary to perform a more complete calculation. For the anomalous dimension in (1.8), the next-to-leading order term can be extracted from the recently published results on the second order BFKL kernel [26]. For the coefficient functions ((1.9), (1.10)) a NLO calculation has not yet been performed.

1.2 The Four-Gluon Operator

While the contributions of the two-gluon twist-four operator (1.2) in DLA could be derived with the help of the BFKL equation, the four-gluon operators (1.1) require a separate analysis. The simplest diagrams are shown in fig. 1.2. In the limit of small x_B, these diagrams (together with higher order corrections) have been investigated in [29, 30], and we simply summarize the results and draw the relation with the operators in eqns. (1.1) and (1.2).

In the investigation of [29,30], the starting point was the triple Regge limit of a six-point amplitude; from this an amplitude D_4 was defined which describes the coupling of four t-channel gluons to two virtual photons. We recall only those results which are relevant here. The four-gluon amplitude D_4 satisfies an integral equation which we illustrate with the help of fig. 1.3. As one main result of ref. [30], it was shown that D_4 should be written as a sum of two parts, the *reggeizing* terms D_4^R, which consist of terms proportional D_2 (eqn. (1.41) below), and terms which are *irreducible* with respect of reggeization D_4^I:

$$D_4 = D_4^R + D_4^I \,. \tag{1.16}$$

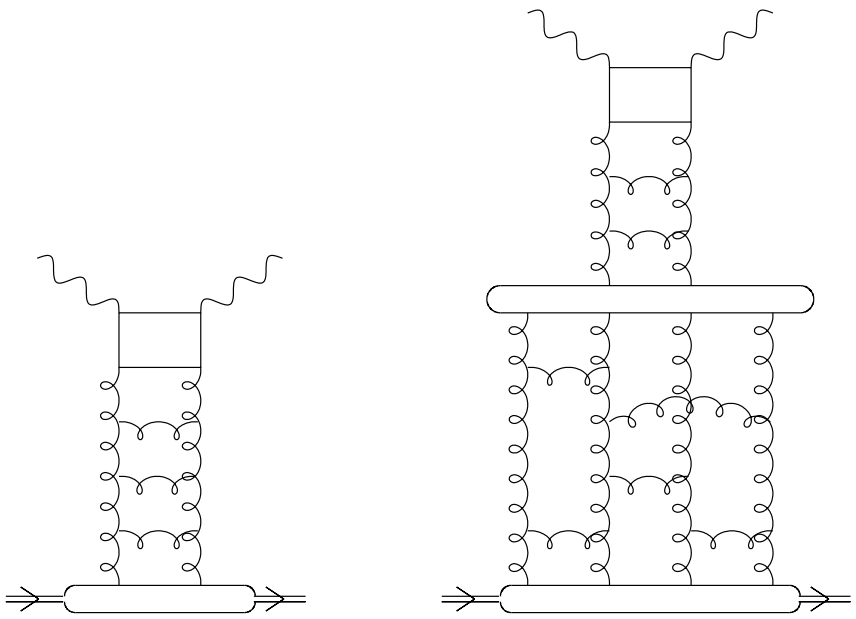

(a) (b)

FIG. 1.1: (a) The two-gluon amplitude and (b) D_4^{I}, the part of the four-gluon amplitude which is *irreducible* with respect of reggeization.

The two terms D_4^{R} and D_4^{I} have also different symmetry properties: whereas D_4^{I} is totally symmetrical under permutation of the outgoing gluons, D_4^{R} has mixed symmetry properties. We are, now, going to discuss these two contributions in some detail. In particular, the results will be interpreted in terms of the operators (1.1) and (1.2). In order to avoid a too complicated notation, we will from now on suppress the references to the photon polarization.

We choose our conventions such that the connection with the cross section $\sigma_{\gamma^* p}$ is as follows:

$$\sigma_{\gamma^* p} = -\frac{4\pi^2 \alpha_{\mathrm{em}}}{Q^2} \frac{1}{128\pi^2} \int \frac{\mathrm{d}\omega}{2\pi \mathrm{i}} \left(\frac{1}{x}\right)^{\omega} \int \frac{\mathrm{d}\nu}{2\pi \mathrm{i}} \left(\frac{Q_0^2}{Q^2}\right)^{-\nu-1} D_4^{abcd} \, \varphi_4^{abcd} \,. \tag{1.17}$$

In the following we will describe this formula in more detail. In particular, we will use the AGK rules [42] in order to justify the minus sign in front of (1.17).

We begin with the *irreducible* part. Since D_4^{R} has a particularly simple form (fig. 1.4 and eqn. (1.41) below), we simply subtract it on both sides of the equation in fig. 1.3 and make use of the integral equation for D_2. Regrouping the terms on the r.h.s. of fig. 1.3, one arrives at the following integral equation:

$$\omega D_4^{\mathrm{I};abcd}(\boldsymbol{k}_1, \boldsymbol{k}_2, \boldsymbol{k}_3, \boldsymbol{k}_4) = \Big[D_2 \otimes V^{abcd} + D_4^{\mathrm{I}} \otimes \sum (K_{2\to 2} + \alpha - 1) \Big] (\boldsymbol{k}_1, \boldsymbol{k}_2, \boldsymbol{k}_3, \boldsymbol{k}_4) \,. \tag{1.18}$$

Here $\boldsymbol{k}_1, \ldots, \boldsymbol{k}_4$ are the transverse components (in the Sudakov decomposition) of the momenta of the four gluons at the lower end in fig. 1.1b, and a, b, c, d are the corresponding color labels. $K_{2\to 2}$ and α are the common BFKL kernel and the gluon trajectory function, and the sum has to be taken

over all possible pairs of gluons. V represents the transition vertex from $2 \to 4$ gluons (fig. 1.1b),

$$\begin{aligned} V^{abcd} = \frac{g^2}{12\sqrt{2}}\Big\{ \quad & \delta^{ab}\delta^{cd}\,\big[G(\boldsymbol{k}_1,\boldsymbol{k}_3)+G(\boldsymbol{k}_2,\boldsymbol{k}_3)+G(\boldsymbol{k}_1,\boldsymbol{k}_4)+G(\boldsymbol{k}_2,\boldsymbol{k}_4) \\ & \quad -G(\boldsymbol{k}_1,\boldsymbol{k}_3+\boldsymbol{k}_4)-G(\boldsymbol{k}_2,\boldsymbol{k}_3+\boldsymbol{k}_4)-G(\boldsymbol{k}_3,\boldsymbol{k}_1+\boldsymbol{k}_2) \\ & \quad -G(\boldsymbol{k}_4,\boldsymbol{k}_1+\boldsymbol{k}_2)+G(\boldsymbol{k}_1+\boldsymbol{k}_2,\boldsymbol{k}_3+\boldsymbol{k}_4)\big] + \\ & +\delta^{ac}\delta^{bd}\big[G(\boldsymbol{k}_1,\boldsymbol{k}_2)+G(\boldsymbol{k}_2,\boldsymbol{k}_3)+G(\boldsymbol{k}_1,\boldsymbol{k}_4)+G(\boldsymbol{k}_3,\boldsymbol{k}_4) \\ & \quad -G(\boldsymbol{k}_1,\boldsymbol{k}_2+\boldsymbol{k}_4)-G(\boldsymbol{k}_3,\boldsymbol{k}_2+\boldsymbol{k}_4)-G(\boldsymbol{k}_2,\boldsymbol{k}_1+\boldsymbol{k}_3) \\ & \quad -G(\boldsymbol{k}_4,\boldsymbol{k}_1+\boldsymbol{k}_3)+G(\boldsymbol{k}_1+\boldsymbol{k}_3,\boldsymbol{k}_2+\boldsymbol{k}_4)\big] + \\ & +\delta^{ad}\delta^{bc}\big[G(\boldsymbol{k}_1,\boldsymbol{k}_3)+G(\boldsymbol{k}_3,\boldsymbol{k}_4)+G(\boldsymbol{k}_1,\boldsymbol{k}_2)+G(\boldsymbol{k}_2,\boldsymbol{k}_4) \\ & \quad -G(\boldsymbol{k}_1,\boldsymbol{k}_2+\boldsymbol{k}_3)-G(\boldsymbol{k}_4,\boldsymbol{k}_2+\boldsymbol{k}_3)-G(\boldsymbol{k}_3,\boldsymbol{k}_1+\boldsymbol{k}_4) \\ & \quad -G(\boldsymbol{k}_2,\boldsymbol{k}_1+\boldsymbol{k}_4)+G(\boldsymbol{k}_1+\boldsymbol{k}_4,\boldsymbol{k}_2+\boldsymbol{k}_3)\big]\Big\}\,. \end{aligned} \tag{1.19}$$

The convolution $D_2 \otimes G$ is given by the expression [30]

$$\begin{aligned} (D_2\otimes G)(\boldsymbol{a},\boldsymbol{b}) = 3g^2\int\frac{\mathrm{d}^2k}{(2\pi)^3}\Bigg\{ & \left[\frac{\boldsymbol{a}^2}{(\boldsymbol{k}-\boldsymbol{a})^2\boldsymbol{k}^2}+\frac{\boldsymbol{b}^2}{(\boldsymbol{k}+\boldsymbol{b})^2\boldsymbol{k}^2}-\frac{(\boldsymbol{a}+\boldsymbol{b})^2}{(\boldsymbol{k}-\boldsymbol{a})^2(\boldsymbol{k}+\boldsymbol{b})^2}\right]D_2(\boldsymbol{k}^2) \\ & -\frac{1}{(\boldsymbol{k}-\boldsymbol{a})^2}\left[\frac{\boldsymbol{a}^2}{(\boldsymbol{k}-\boldsymbol{a})^2+\boldsymbol{k}^2}-\frac{(\boldsymbol{a}+\boldsymbol{b})^2}{(\boldsymbol{k}-\boldsymbol{a})^2+(\boldsymbol{k}+\boldsymbol{b})^2}\right]D_2(\boldsymbol{a}^2) \\ & -\frac{1}{(\boldsymbol{k}+\boldsymbol{b})^2}\left[\frac{\boldsymbol{b}^2}{(\boldsymbol{k}+\boldsymbol{b})^2+\boldsymbol{k}^2}-\frac{(\boldsymbol{a}+\boldsymbol{b})^2}{(\boldsymbol{k}-\boldsymbol{a})^2+(\boldsymbol{k}+\boldsymbol{b})^2}\right]D_2(\boldsymbol{b}^2)\Bigg\}\,. \end{aligned} \tag{1.20}$$

For the twist analysis in DLA it is useful to perform a Mellin-transform in the following way (cf. eqn. (1.3)):

$$\big(D_2\otimes G\big)(\omega,\boldsymbol{a},\boldsymbol{b}) = \int\frac{\mathrm{d}\nu}{2\pi\mathrm{i}}\;D_2(\omega,\nu)\tilde{G}(\nu,\boldsymbol{a},\boldsymbol{b}) \tag{1.21}$$

with [30]

$$\begin{aligned} \tilde{G}(\nu,\boldsymbol{a},\boldsymbol{b}) = \frac{3g^2}{(2\pi)^2}\Theta\big(|\boldsymbol{a}|-|\boldsymbol{b}|\big)\Bigg\{ & \left[\ln\left(\frac{|\boldsymbol{a}|}{|\boldsymbol{b}|}\right)-\frac{1}{\nu}\right]\big(b^2\big)^{-\nu} \;+ \\ & +\sum_{n=1}^{\infty}\left(-\frac{|\boldsymbol{b}|}{|\boldsymbol{a}|}\right)^n\cos(n\theta)\Bigg[\left(\frac{1}{n+\nu}-\frac{1}{n}\right)\big(a^2\big)^{-\nu}+ \\ & +\left(\frac{1}{n-\nu}-\frac{1}{n}\right)\big(b^2\big)^{-\nu}\Bigg]\Bigg\}+\Big(|\boldsymbol{a}|\leftrightarrow|\boldsymbol{b}|\Big)\,, \end{aligned} \tag{1.22}$$

where θ represents the angle between $\boldsymbol{a}$ and $\boldsymbol{b}$. The leading-twist part in the DLA can be obtained by evaluating the residue at $\nu=-1$:

$$\tilde{G}(\nu,\boldsymbol{a},\boldsymbol{b})^{\tau=2} = -\frac{3g^2}{(2\pi)^2}\,\boldsymbol{a}\cdot\boldsymbol{b}\,\frac{\big(\max\big(a^2,b^2\big)\big)^{-\nu-1}}{\nu+1}\,, \tag{1.23}$$

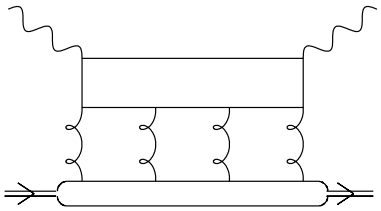

FIG. 1.2: The four-gluon amplitude at leading order. The fermion-loop symbolizes the sum over all Feynman-diagrams with all possible couplings of the four t-channel gluons.

whereas the twist-four contribution is related to the pole at $\nu = -2$:

$$\tilde{G}(\nu, \boldsymbol{a}, \boldsymbol{b})^{\tau=4} = \frac{3g^2}{(2\pi)^2} \left[2(\boldsymbol{a}\cdot\boldsymbol{b})^2 - a^2\, b^2\right] \frac{\left(\max\left(a^2, b^2\right)\right)^{-\nu-2}}{\nu+2}\,. \tag{1.24}$$

Inserting the twist-two result (1.23) in (1.19), we find that the sum of the various terms cancel. Returning to (1.18), this cancellation means that we are loosing one factor $\ln Q^2$, i.e. we have a non-leading correction to the DLA. For the twist-four result, on the other hand, we find a non-vanishing contribution. In (1.18) the twist-four part of the first term on the r.h.s. reads (we use DLA accuracy, and we assume, for simplicity, that all k_i^2 are of the same order, k^2):

$$\begin{aligned}\frac{1}{\omega} D_2^t \otimes V(\omega; \boldsymbol{k}_1, \boldsymbol{k}_2, \boldsymbol{k}_3, \boldsymbol{k}_4)^{\tau=4} = a_2^t \sum_f e_f^2 \frac{\sqrt{8}}{2\pi} 2\sqrt{2}\alpha_{\rm s}^3 \frac{Q^2}{Q_0^2} \int \frac{{\rm d}\tilde{\nu}}{2\pi{\rm i}} \left(\frac{1}{k^2}\right)^{\tilde{\nu}} \frac{1}{\omega\tilde{\nu}} \frac{1}{(\omega\tilde{\nu} - \gamma_2)} \times \\ \times \big\{(-\delta^{ab}\delta^{cd} + \delta^{ac}\delta^{bd} + \delta^{ad}\delta^{bc})\boldsymbol{k}_1\cdot\boldsymbol{k}_2\, \boldsymbol{k}_3\cdot\boldsymbol{k}_4 + \\ + (\delta^{ab}\delta^{cd} - \delta^{ac}\delta^{bd} + \delta^{ad}\delta^{bc})\boldsymbol{k}_1\cdot\boldsymbol{k}_3\, \boldsymbol{k}_2\cdot\boldsymbol{k}_4 + \\ + (\delta^{ab}\delta^{cd} + \delta^{ac}\delta^{bd} - \delta^{ad}\delta^{bc})\boldsymbol{k}_1\cdot\boldsymbol{k}_4\, \boldsymbol{k}_2\cdot\boldsymbol{k}_3\,\big\}\,.\end{aligned} \tag{1.25}$$

Here $\tilde{\nu} \equiv \nu + 2$, and all momenta are normalized by Q. The factors in the first line of eqn. (1.25) belong to expressions of the two-gluon amplitude and the quark-loop in DLA, while the lower three lines correspond to the transition $2 \to 4$ gluons. A similar result holds for the longitudinal structure function (with a_2^t replaced by b_2^ℓ, and an extra factor $1/\tilde{\nu}$ in the first line).

Making systematic use of the double logarithmic approximation, it is possible to find an explicit solution of eqn. (1.18). This can be done if we solve the integral equation by iteration: This yields the following structure for $D_4^{\rm I}$ (fig. 1.1b). There is a quark-loop $D_{2,0}$ and a BFKL ladder at the top. This BFKL ladder couples to the $2 \to 4$ transition vertex V which, by itself, couples to a system of four gluons. These four gluons interact pairwise in all possible ways. It is, now, convenient to use the method of Faddeev [46]. For this, we reorganize the sum over all pairwise gluon interactions and introduce auxiliary potentials $T_{(ij)(kl)}$ which describe pairs of two-gluon ladders for the gluon lines (ij) and (kl). The original sum over all pairwise interactions between the four gluon lines then translates into the iteration of these auxiliary potentials, allowing for all possible recombinations ("switches") $(ij)(kl) \to (ik)(jl)$ etc.

For each gluon ladder there are six irreducible color states ($8 \otimes 8 = 1 \oplus 8_{\rm A} \oplus 8_{\rm S} \oplus 10 \oplus \overline{10} \oplus 27$). However, if we add one additional rung right below of the vertex in eqn. (1.25), e.g. to gluons 1 and 2, the three terms in (1.25) become proportional to $\boldsymbol{k}_1\cdot\boldsymbol{k}_2 \boldsymbol{k}_3\cdot\boldsymbol{k}_4$ and the anti-symmetrical color

states cancel, so that only the symmetrical ones (1, 8_S, 27) survive. This remains true if one adds further rungs. As result, our four-gluon system can be written in terms of nine components: three color terms for each coupling scheme (12)(34), (13)(24) and (14)(23). Concentrating, now, on the twist-four point $\nu = -2$ and collecting the maximum number of logarithms, we find the following pattern. For each two-ladder state described by the auxiliary potential $T_{(ij)(kl)}$ we have a factor γ_i:

$$\gamma_i = \left(1 - \frac{4\sigma_i}{\omega\tilde{\nu}}\right)^{-\frac{1}{2}} - 1\,, \tag{1.26}$$

where $\pi\sigma_i/\alpha_s = \{3, 3/2, -1\}$ for the color states $i = \{1, 8_S, 27\}$, cf. (A.7). At each switch from the two-ladder state $(ij)(kl)$ to the configuration $(ik)(jl)$, we get a factor 1/2 due to the angular integration, and we have to insert a color recoupling matrix S. In our nine-component matrix notation, the Green's function Σ for the four-gluon system then becomes:

$$\Sigma = \sum_{n=0}^{\infty}\left(G\frac{1}{2}S\right)^n G = \left(G^{-1} - \frac{1}{2}S\right)^{-1}, \quad G = \begin{pmatrix}\gamma & 0 & 0\\ 0 & \gamma & 0\\ 0 & 0 & \gamma\end{pmatrix}, \quad S = \begin{pmatrix}0 & \Lambda & \Lambda\\ \Lambda & 0 & \Lambda\\ \Lambda & \Lambda & 0\end{pmatrix}, \tag{1.27}$$

where the sub-matrices γ and Λ have the following components:

$$\gamma = \begin{pmatrix}\left(1 - \frac{4\sigma_1}{\omega\tilde{\nu}}\right)^{-\frac{1}{2}} - 1 & 0 & 0\\ 0 & \left(1 - \frac{4\sigma_{8_S}}{\omega\tilde{\nu}}\right)^{-\frac{1}{2}} - 1 & 0\\ 0 & 0 & \left(1 - \frac{4\sigma_{27}}{\omega\tilde{\nu}}\right)^{-\frac{1}{2}} - 1\end{pmatrix} \qquad \Lambda = \begin{pmatrix}\frac{1}{8} & \frac{1}{2\sqrt{2}} & \frac{3\sqrt{3}}{8}\\ \frac{1}{2\sqrt{2}} & -\frac{3}{10} & \frac{3}{10}\sqrt{\frac{3}{2}}\\ \frac{3\sqrt{3}}{8} & \frac{3}{10}\sqrt{\frac{3}{2}} & \frac{7}{40}\end{pmatrix}. \tag{1.28}$$

As a result of the leading-$\ln Q^2$ approximation, at the lower end of the Green's function Σ the two ladder system $T_{(ij)(kl)}$ ends up with the momentum configuration $\boldsymbol{k}_i = -\boldsymbol{k}_j \equiv \boldsymbol{l}$ and $\boldsymbol{k}_k = -\boldsymbol{k}_l \equiv \boldsymbol{l}'$.

For the coupling of this Green's function to the transition vertex we introduce the nine component vector $\boldsymbol{V}$: $\boldsymbol{V}^{\mathrm{T}} = (\boldsymbol{v}^{\mathrm{T}}, \boldsymbol{v}^{\mathrm{T}}, \boldsymbol{v}^{\mathrm{T}})$ with

$$\boldsymbol{v}^{\mathrm{T}} = (2,\, 4\sqrt{2},\, 6\sqrt{3})\,. \tag{1.29}$$

This vector is obtained from (1.25) by applying the color projectors listed in appendix A. As a result, our function D_4^{I}, written as a (transposed) nine component vector, takes the form:

$$\begin{aligned}\boldsymbol{D}_4^{\mathrm{I},t}(\omega, Q_0^2/Q^2) \;=\; & \frac{1}{\omega}(D_2^t \otimes \boldsymbol{V}^{\mathrm{T}})(\omega, Q^2)^{\tau=4} + \\ & + a_2^t \sum_f e_f^2 \frac{\sqrt{8}}{2\pi} 2\sqrt{2}\alpha_s^3 \left(\frac{Q_0^2}{Q^2}\right)^2 \int\frac{\mathrm{d}\tilde{\nu}}{2\pi\mathrm{i}}\left(\frac{Q^2}{Q_0^2}\right)^{\tilde{\nu}} \frac{1}{\omega\tilde{\nu}}\frac{1}{(\omega\tilde{\nu} - \gamma_2)} \cdot \boldsymbol{V}^{\mathrm{T}}\,\Sigma(\omega\tilde{\nu})\;.\end{aligned} \tag{1.30}$$

Finally, the four-gluon system has to be coupled to the proton. In modelling this coupling we take, as a guideline, the structure of D_4: to be definite, we assume that the coupling to the proton has the same symmetry properties as D_4, the coupling of the four gluon state to a perturbative target, e.g. to a virtual photon or to a heavy onium state. The decomposition in (1.16) reflects the different contributions: apart from totally symmetrical (under the combined interchange of color and momenta) terms which are contained in D_4^{I} and D_4^{R}, we have a term with mixed symmetry

properties which occurs only in $D_4^{\rm R}$. For the symmetrical part we make the simplest ansatz, which contains only the color singlet representation. For the term with mixed symmetry we simply follow the perturbative ansatz. This leads to:

$$\varphi_4^{abcd} = \varphi_{4\rm S}^{abcd} + \varphi_{4\rm A}^{abcd} \tag{1.31}$$

with

$$\varphi_{4\rm S}^{abcd} = \frac{1}{3\cdot 8}\frac{1}{k_1^2k_2^2k_3^2k_4^2}\Big(\delta^{ab}\delta^{cd} f_{\rm S}(1,2;3,4;\omega) + \delta^{ac}\delta^{bd} f_{\rm S}(1,3;2,4;\omega) + \delta^{ad}\delta^{bc} f_{\rm S}(1,4;2,3;\omega)\Big) \tag{1.32}$$

and

$$\varphi_{4\rm A}^{abcd} = -\frac{1}{3\cdot 8}\frac{1}{k_1^2k_2^2k_3^2k_4^2}\Big(f^{abm}f^{mcd} f_{\rm A}(1,2;3,4;\omega) + \\ + f^{acm}f^{mbd} f_{\rm A}(1,3;2,4;\omega) + f^{adm}f^{mbc} f_{\rm A}(1,4;2,3;\omega)\Big) \tag{1.33}$$

with positive-valued functions $f_{\rm S}$ and $f_{\rm A}$. The signs can be derived with the help of the AGK rules which will be discussed below in more detail. The pre-factors 1/8 and 1/3 are convenient for color and for statistics, resp. We immediately see that the $\varphi_{4\rm A}$-term does not couple to $D_4^{\rm I}$ but only to $D_4^{\rm R}$, and we will come back to this term when we discuss $D_4^{\rm R}$.

In order to discuss the momentum structure of the ansatz $\varphi_{4\rm S}$, let us recall that in the usual DIS leading-twist ladder the lowest rung has only a longitudinal integration, and the integration over the virtuality of the lowest parton is absorbed into the initial condition $\varphi_2(Q_0^2,x)$. In evaluating our four-gluon system in the DLA we treat each gluon ladder of our auxiliary potential $T_{(ij)(kl)}$ in the same way as the leading-twist ladder. Let the lowest potential be $T_{(12)(34)}$. At its lower end we have the momentum factor $(\boldsymbol{k}_1\boldsymbol{k}_2)(\boldsymbol{k}_3\boldsymbol{k}_4)$. In the function $f_{\rm S}(i,j;k,l;\omega)$ of our ansatz (1.31) the main contribution comes from the region where

$$\boldsymbol{k}_i = \boldsymbol{l}+\boldsymbol{r}, \quad \boldsymbol{k}_j = -\boldsymbol{l}+\boldsymbol{r}, \quad \boldsymbol{k}_k = \boldsymbol{m}-\boldsymbol{r}, \quad \boldsymbol{k}_l = -\boldsymbol{m}-\boldsymbol{r}, \\ r^2 \ll l^2,\, m^2\,. \tag{1.34}$$

Combining these functions with the momentum factors from the auxiliary potential $T_{(12)(34)}$ we are lead to the following definition of our initial condition:

$$Q_0^2\,\varphi_{4\rm S}(Q_0^2;\omega) = \int^{Q_0^2}\!\mathrm{d}r^2 \int_{r^2}^{Q_0^2}\frac{\mathrm{d}l^2}{l^4}\int_{r^2}^{Q_0^2}\frac{\mathrm{d}m^2}{m^4} l^2m^2 f_{\rm S}(k_i,k_j;k_k,k_l;\omega). \tag{1.35}$$

E.g. if we set $\boldsymbol{k}_1 = \boldsymbol{l}+\boldsymbol{r}$, $\boldsymbol{k}_2 = -\boldsymbol{l}+\boldsymbol{r}$, $\boldsymbol{k}_3 = \boldsymbol{m}-\boldsymbol{r}$ and $\boldsymbol{k}_4 = -\boldsymbol{m}-\boldsymbol{r}$ in (1.32) and perform the integrations as in (1.35) we get a factor

$$\frac{1}{3\cdot 8}\left(\delta^{ab}\delta^{cd} + \frac{1}{2}\delta^{ac}\delta^{bd} + \frac{1}{2}\delta^{ad}\delta^{bc}\right) Q_0^2\cdot\varphi_{4\rm S}(Q_0 r;\omega), \tag{1.36}$$

where the factors 1/2 in front of the second and the third term are due to the angular integrations over $\boldsymbol{l}$ and $\boldsymbol{m}$ (a similar definition holds for the functions $\varphi_{4\rm A}$ and $f_{\rm A}$). As to the longitudinal integrals, since we work in ω-space we allow the function $\varphi_{4\rm S}$ to depend on ω: if we assume a single

ladder to rise as $(1/x)^\lambda$, $\varphi_{4\mathrm{S}}$ should have a pole at $\omega = 2\lambda$, i.e. the initial distribution rises twice as strong as the leading-twist gluon structure function at the same scale.

Finally we couple (1.31) to D_4^{I} in (1.30). Projecting onto the color eigenstates and introducing the nine-component vector

$$\mathbf{\Phi}_{4\mathrm{S}}(Q_0^2,\omega) = \begin{pmatrix} \boldsymbol{w} \\ \boldsymbol{w} \\ \boldsymbol{w} \end{pmatrix} \cdot \varphi_{4\mathrm{S}}(Q_0^2;\omega), \qquad \boldsymbol{w} = \frac{1}{3\cdot 8}\begin{pmatrix} 9 \\ 2\sqrt{2} \\ 3\sqrt{3} \end{pmatrix} \tag{1.37}$$

we arrive at the following expression for our twist-four contribution to the structure function in the (ω,ν)-representation:

$$\begin{aligned} \Delta F_t^{\mathrm{I}} &= -\frac{1}{128\pi^2}\frac{Q^2}{Q_0^2} D_4^{\mathrm{I};abcd}(\omega,\nu)\varphi_4^{abcd}(\omega) = \\ &= -\frac{a_2^t}{16}\frac{\alpha_{\mathrm{s}}^3}{\pi^3}\sum_f e_f^2 \frac{Q_0^2}{Q^2}\int\frac{\mathrm{d}\tilde{\nu}}{2\pi\mathrm{i}}\left(\frac{Q^2}{Q_0^2}\right)^{\tilde{\nu}} \frac{1}{\omega\tilde{\nu}}\frac{1}{(\omega\tilde{\nu}-\gamma_2)}\varphi_{4\mathrm{S}}(\omega) \\ &\quad -\frac{a_2^t}{32}\frac{\alpha_{\mathrm{s}}^3}{\pi^3}\sum_f e_f^2 \frac{Q_0^2}{Q^2}\int\frac{\mathrm{d}\tilde{\nu}}{2\pi\mathrm{i}}\left(\frac{Q^2}{Q_0^2}\right)^{\tilde{\nu}} \frac{1}{\omega\tilde{\nu}}\frac{1}{(\omega\tilde{\nu}-\gamma_2)}\cdot \boldsymbol{V}^{\mathrm{T}}\,\Sigma(\omega\tilde{\nu})\,\mathbf{\Phi}_{4\mathrm{S}}(\omega), \end{aligned} \tag{1.38}$$

and an analogous expression in the longitudinal case. After performing the inversion within $\Sigma = (G^{-1} - \frac{1}{2}S)^{-1}$ we get explicit expressions for the components of vector $\Sigma\boldsymbol{V}$. They are listed in appendix A.

As one of the most striking features of (1.38) we note that Σ has a leading singularity in the $\tilde{\nu}$-plane at [29, 47]

$$\tilde{\nu} = 4(1+\delta)\frac{N_{\mathrm{c}}\alpha_{\mathrm{s}}}{\pi\omega}\ , \tag{1.39}$$

where $\delta = 0.009549$. Using the usual saddle point approximation, this pole leads to the following asymptotic small x_{B} behavior:

$$D_4^{\mathrm{I}} \sim \left(\frac{Q_0^2}{Q^2}\right)^2 \exp\left(2\left(1+\frac{\delta}{2}\right)\sqrt{\frac{4N_c}{\pi}\alpha_{\mathrm{s}}\ln(1/x)\ln(Q^2/Q_0^2)}\right)\ . \tag{1.40}$$

This rise at small x_{B} is approximately twice as strong as that of the leading-twist gluon structure function, and at sufficiently small x_{B} the four-gluon higher-twist term will certainly become as strong as the leading-twist term, despite its suppression due to the extra power in α_{s} and the $1/Q^2$ factor. This strong rise at small x_{B} is the reason why the four-gluon operator, (1.1), is expected to be so important in the small x_{B}, low Q^2-region.

Besides the leading pole (1.39), there are more singularities in the $\tilde{\nu}$-plane, which have been discussed in some detail in ref. [48]. There are three cuts in the $\tilde{\nu}$-plane. The first one stems from the singlet-part of matrix γ (eqn. (1.28)). It starts at $\tilde{\nu} = 0$ and goes up to the point $\tilde{\nu} = 4\frac{N_{\mathrm{c}}\alpha_{\mathrm{s}}}{\pi\omega}$ which is very close to the leading pole (1.39). It overlaps with the symmetrical color octet cut, which is located in the interval $[0, \frac{6\alpha_{\mathrm{s}}}{\pi\omega}]$. The cut of the color 27plet goes from $-\frac{4\alpha_{\mathrm{s}}}{\pi\omega}$ to 0.

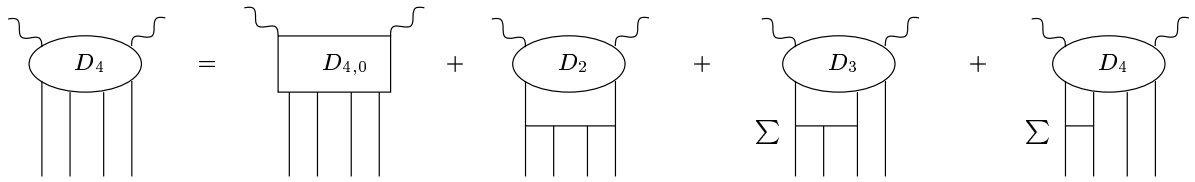

FIG. 1.3: The integral equation for D_4. The sums denote couplings to the gluon lines in all possible ways.

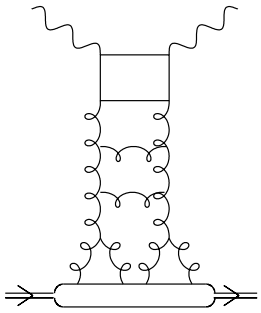

FIG. 1.4: The reggeizing part of the four-gluon amplitude has the same evolution as the two-gluon amplitude but is suppressed by one factor α_s.

Finally, we return to (1.16) and we discuss the *reducible* part D_4^R. From [29, 30] we have:

$$
\begin{aligned}
&D_4^{\rm R}(\boldsymbol{k}_1,\boldsymbol{k}_2,\boldsymbol{k}_3,\boldsymbol{k}_4) = \qquad\qquad (1.41)\\
&= \frac{g^2}{2\sqrt{2}}\Big\{\;\; d^{abcd}\big[D_2(\boldsymbol{k}_1,\boldsymbol{k}_2+\boldsymbol{k}_3+\boldsymbol{k}_4)+D_2(\boldsymbol{k}_4,\boldsymbol{k}_1+\boldsymbol{k}_2+\boldsymbol{k}_3)\,-\,D_2(\boldsymbol{k}_1+\boldsymbol{k}_4,\boldsymbol{k}_2+\boldsymbol{k}_3)\big]+\\
&\qquad + d^{abdc}\big[D_2(\boldsymbol{k}_2,\boldsymbol{k}_1+\boldsymbol{k}_3+\boldsymbol{k}_4)+D_2(\boldsymbol{k}_3,\boldsymbol{k}_1+\boldsymbol{k}_2+\boldsymbol{k}_4)\,-\,D_2(\boldsymbol{k}_1+\boldsymbol{k}_2,\boldsymbol{k}_3+\boldsymbol{k}_4)\,-\\
&\qquad\qquad -\,D_2(\boldsymbol{k}_1+\boldsymbol{k}_3,\boldsymbol{k}_2+\boldsymbol{k}_4)\big]\Big\},
\end{aligned}
$$

where the color tensor d^{abcd} is given in appendix A. It contains both symmetrical and anti-symmetrical parts: one easily recognizes the structures (1.32) and (1.33). Convoluting D_4^R with our ansatz (1.31) we find that φ_{4S} couples only to the symmetrical and φ_{4A} only to the mixed-symmetrical part of D_4^R. With the help of the same arguments as before, cf. (1.35), we arrive at

$$
\begin{aligned}
\Delta F_t^{\rm R} &= -\frac{1}{128\omega\pi^2}\left(\frac{Q^2}{Q_0^2}\right) D_4^{{\rm R};abcd}\,\varphi_4^{abcd}(\omega)^{\tau=4} =\\
&= \frac{a_2^t}{32}\frac{\alpha_s^2}{\pi^2}\sum_f e_f^2\,\frac{1}{\omega}\left(\frac{Q_0^2}{Q^2}\right)\exp\left(\frac{\gamma_2}{\omega}\ln(Q^2/Q_0^2)\right)\frac{1}{3}[14\varphi_{4S}(\omega)-9\varphi_{4A}(\omega)]\,. \qquad (1.42)
\end{aligned}
$$

Here φ_{4A} is defined in analogy with φ_{4S} in (1.35). It is important to note that the negative sign in front of φ_{4A} is dictated by the AGK rules (see below). Note that, at lowest order in α_s, it is this contribution D_4^R that contains the diagrams with four elementary gluon lines between the quark-loop and the proton (fig. 1.2).

After we have given the DLA expressions for the four-gluon twist-four contributions, let us briefly return to the operator product expansion. As before, the ladder diagrams denote the $\ln Q^2$ evolution

in the DLA, but instead of writing the four-gluon amplitude as an evolution equation in $\ln Q^2$ we have used the closed expression in the (ω,ν)-representation. Twist-four corresponds to the point $\nu=-2$. $D_4^{\rm I}$ then has the following interpretation: the upper two-gluon ladder (evaluated near $\nu=-2$) describes the evolution of operator (1.2), the $2\to 4$ vertex the mixing between (1.1) and (1.2), and the Green's function Σ the evolution of the four-gluon operators (1.1). The three auxiliary potentials $T_{(12)(34)}$, $T_{(13)(24)}$, $T_{(14)(23)}$ seem to correspond to the three operators in the first, second, and third line of (1.1), and what we have called "switching from $(ij)(kl)$ to $(ik)(jl)$" has to be interpreted as the mixing between these three different four-gluon operators. If we were to go beyond DLA, there would also be a transition from the four-gluon state back to two gluons (this vertex could again be derived from (1.19) and (1.22), by expanding about $\nu=1$), and eventually these transitions would be iterated and exponentiated in the t-channel. A remarkable feature of the small $x_{\rm B}$ approximation (upon which the DLA is based) is the fact that the four-gluon operator has no direct coupling to the quark loop.

The interpretation of the contribution $D_4^{\rm R}$, on the other hand, is more subtle. As stated before, this term has its origin in the reggeization of the gluon: from the point of view of DIS the appearance of reggeization is a "novel" phenomenon since at the leading-twist level it has played only an indirect rôle (e.g. as part of the NLO anomalous dimension of the gluon). From the point of view of Q^2 evolution, $D_4^{\rm R}$ belongs to the two-gluon operator (1.2). Including $D_4^{\rm R}$, therefore, at first sight seems like adding a non-leading correction to (1.15), and within the DLA we better should restrict ourselves to the leading term (1.15). On the other hand, the analysis in [30] clearly shows that $D_4^{\rm I}$ and $D_4^{\rm R}$ have the same origin (diagrams with four gluons in the t-channel) and support the same powers of logarithms. We, therefore, got the feeling that for the twist-four calculations – which necessarily have to include t-channel states with four gluons – we have to keep $D_4^{\rm R}$ as a separate contribution, in addition to (1.15).

A better understanding of why we have to keep this contribution can be obtained by looking at the evolution of the gluonic operator in (1.2). The mixing between (1.1) and (1.2) is of order $\alpha_{\rm s}^2$ in the anomalous dimension matrix, i.e. in total the correction to the evolution of (1.2) due to the transition from (1.2) to (1.1) and back to (1.2) is a NNLO effect of order $\alpha_{\rm s}^3$. To be consistent, we, therefore, have to include NNLO corrections also in the anomalous dimension $\gamma^{\tau=4}$ in (1.8) and in the coefficient function. They are not available yet. On the other hand, $D_4^{\rm R}$ can be viewed as a particular part of these corrections, connected with the reggeization of the gluon. Moreover, there are reasons to expect that $D_4^{\rm R}$ will be dominating within these corrections. Since we are studying t-channel states with four gluons, $D_4^{\rm R}$ provides contributions from the "decay of a reggeizing gluon into two or three gluons" which then become partons inside the proton. In other words, we are encountering the two- and three-particle states in the gluon trajectory function, appearing at the lower end of the two-gluon ladder. Clearly, these higher-order particle states in the trajectory function can appear not only at the lower end of the two-gluon ladder (as taken into account by $D_4^{\rm R}$) but everywhere between the proton and the photon. Such a contribution would then be part of the NNLO corrections to the gluon rung, i.e. to the anomalous dimension $\gamma^{\tau=4}$ in (1.8) mentioned above. In this sense, $D_4^{\rm R}$ counts those NNLO corrections to the two-gluon kernel which are connected with four-gluon states in the t-channel, and these corrections are taken into account only at the lower end of the ladder. When running $\alpha_{\rm s}$ and the strong ordering of the transverse momenta is taken into account, we expect these corrections to be largest when they appear at the lower end of the ladder. For these reasons our incomplete treatment of the NNLO corrections in the evolution of the two-gluon operator (1.2) may not be such a bad approximation.

1.3 Contributions with Three t-channel Gluons

There is no three-gluon operator that might contribute to our twist-four analysis of the unpolarized structure functions. On the other hand one can compute contributions with three t-channel gluons. The corresponding amplitude D_3 has been computed in ref. [30] and as it turns out, it reggeizes completely. Keeping the discussion above in mind, where we have argued that the reggeizing part of the four-gluon amplitude should be related to NNLO corrections of the two-gluon operator, we have to interpret D_3 as a part of the NLO corrections to the contributions of this operator. Due to (1.40) we expect ΔF^{I} to give the main twist-four contributions. On the other hand, it couples to the same initial distribution as ΔF^{R}. Within our numerical analysis we will, therefore, be able to compare these two contributions. As it turns out, ΔF^{R} is in general not negligible compared to ΔF^{I}. Using the foregoing discussion, we conclude that we also cannot neglect the contribution of D_3. Its particular form is given by the following equation [30] (cf. (1.41)):

$$D_3(\boldsymbol{k}_1,\boldsymbol{k}_2,\boldsymbol{k}_3) = \frac{g}{4\sqrt{2}} f^{abc} \left(D_2(\boldsymbol{k}_1+\boldsymbol{k}_2,\boldsymbol{k}_3) + D_2(\boldsymbol{k}_1,\boldsymbol{k}_2+\boldsymbol{k}_3) - D_2(\boldsymbol{k}_1+\boldsymbol{k}_3,\boldsymbol{k}_2)\right) . \tag{1.43}$$

The convolution with the initial distribution of the proton requires a new function, $\varphi_3(\omega)$. One ends up with functions $\Delta F^3_{(t,\ell)}$ which have the same dependence on variables as (1.42) (with a different constant factor in front of the r.h.s.; it will be absorbed into the unknown initial distribution φ_3).

1.4 Running α_{s}

Since in DLA the leading-twist two-gluon amplitude must coincide with the DGLAP solution, it is clear (in this case) how one can consider the fact that α_{s} is running. One has to exchange the value of fixed α_{s} by $\bar{\alpha}_{\mathrm{s}} \equiv 4\pi/\beta_0$ ($\gamma_2 \to 12/\beta_0$) and the expression Q^2/Q_0^2 by t/t_0, where $t = \ln(Q^2/\Lambda^2)$ and $t_0 = \ln(Q_0^2/\Lambda^2)$. This procedure should be applicable for the bare four-gluon amplitude (i.e. the amplitude without two-gluon amplitude and vertex at the top of fig. 1.1b), as well, since the addition of one rung is always performed by convolution with the common BFKL kernel. This means that each time α_{s} comes with a factor $\ln(t/t_0)$ it has to be replaced by $\bar{\alpha}_{\mathrm{s}}$.

There are three powers of α_{s} in eqn. (1.38): One stems from the quark-loop, which (in the longitudinal case at leading order) is proportional to a logarithm. The remaining two powers stem from the coupling of the four-gluon to the two-gluon amplitude via the Vertex V (fig. 1.1b). Here we get only one logarithm. We write this coupling symbolically as

$$D_4^{\mathrm{I},\ell} = \int_{\tau_0}^{\tau} \mathrm{d}\tau' \exp[\gamma_2(\tau-\tau')] f \alpha_{\mathrm{s}}^2 \int \frac{\mathrm{d}\nu}{2\pi\mathrm{i}} \exp[\nu(\tau'-\tau_0)] G(\nu) , \tag{1.44}$$

where $\tau = \ln t$ etc., $G(\nu)$ is understood as the *four-gluon amplitude Greens-function* and f shall contain all remaining factors. In eqn. (1.44) one factor α_{s} needs to be replaced by $\alpha_{\mathrm{s}}(t')$ and the other one by $\bar{\alpha}_{\mathrm{s}}$. If, on the other hand, we go back to fixed α_{s}, we have to replace τ and τ' in eqn. (1.44) by t and t', resp. Performing the t'-integration and comparing with eqn. (1.38), we can identify the quantities G and f. By this way, we come to the following conclusions: For running α_{s} the factor $(Q^2/Q_0^2)^\nu$ in eqn. (1.38) has to be replaced by $(t/t_0)^\nu$, one power α_{s} has to be evaluated as $\alpha_{\mathrm{s}}(Q^2)$, while (in the longitudinal case) the remaining two powers are replaced by $\bar{\alpha}_{\mathrm{s}}$. In the denominators we have to replace the factor $(\omega\nu - \gamma_2)$ by $(\omega\nu - \omega - \gamma_2)$.

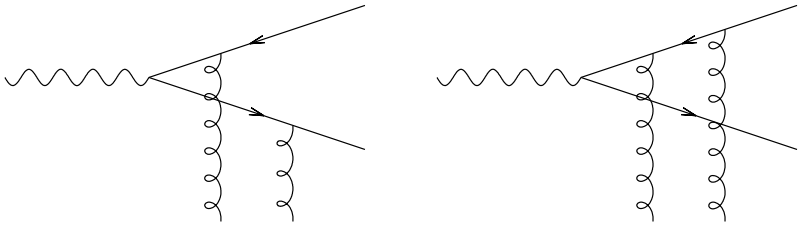

FIG. 1.5: Two of the four diagrams which enter into diffractive $q\bar{q}$-production at leading order.

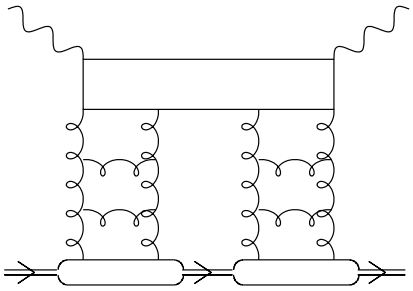

FIG. 1.6: The twist-four part of diffractive $q\bar{q}$-production is described by exchange of gluon ladders.

Repeating in (1.30) the standard saddle point analysis (cf. eqn. (1.39)), we arrive at a small $x_{\rm B}$ behavior of the form

$$D_4^{\rm I} \sim \left(\frac{Q_0^2}{Q^2}\right)^2 \exp\left[2\left(1+\frac{\delta}{2}\right)\sqrt{\frac{48}{\beta_0}\,\ln\frac{1}{x}\,\ln\frac{t}{t_0}}\right]\,. \tag{1.45}$$

Apart from the small δ-correction, this small $x_{\rm B}$ behavior is just the square of the well-known leading-twist double scaling formula [50, 51]. Therefore, in the kinematical regime in which $D_4^{\rm I}$ gives the main contribution to twist-four, higher-twist is expected to increase much faster with decreasing $x_{\rm B}$ than leading-twist and to decrease slower than $1/Q^2$.

We end this section with a brief summary. All in all we have collected four different contributions (both for the transverse and the longitudinal structure function). In our notation

$$\Delta F = \Delta F^{(2)} + \Delta F^3 + \Delta F^{\rm R} + \Delta F^{\rm I}\,, \tag{1.46}$$

where we have suppressed labels t and ℓ. As far as the Q^2-evolution is concerned, the first three terms belong to the twist-four two-gluon operator (1.2) whereas the last one denotes the four-gluon operator (1.1). This last contribution is of particular interest, since at small $x_{\rm B}$ it rises stronger than the other ones and, therefore, may potentially become large. However, we have already seen that the four contributions in (1.46) come with alternating signs, which hints at the possibility of strong cancellations.

2 Diffractive Dissociation

Up to now, we have been describing the four twist-four contributions, which we believe to dominate at small $x_{\rm B}$: $\Delta F^{\rm R}$, $\Delta F^{\rm I}$, ΔF^3 and the twist-four part of the two-gluon amplitude ΔF^2. In each

Contribution	Sign	$\ln(Q^2/Q_0^2)$	$\beta \to 1$
Trans. $\tau = 2$	$+$	non-pert.	vanishes
Trans. $\tau = 4$	$-$	no	vanishes
Long. $\tau = 2$	vanishes	vanishes	vanishes
Long. $\tau = 4$	$+$	yes	constant

TABLE 1.2: The four contributions to diffractive $q\bar{q}$-production up to twist $\tau = 4$ enter with different signs into the diffractive cross section. The table shows also which contributions have leading logarithms, and how they behave for $\beta \to 1$.

of the equations defining these amplitudes, viz. (1.15), (1.38), (1.42) and (1.43), enters a non-perturbative initial distribution φ. Since these initial distributions yield a large number of free parameters, a naive fit to experimental data seems to be impossible. It is, therefore, worthwhile to analyse exclusive amplitudes which are known to belong to higher-twist. The best candidates for this are diffractive final states, in particular the production of longitudinal vector particles and the production of jets with large transverse momenta. In this section we, therefore, give a brief overview of the rôle of higher-twist in DIS diffraction. In particular, we will discuss the relation between the higher-twist pieces of diffractive cross sections and the higher-twist contributions to F_t and F_ℓ from the previous section. In our numerical analysis these relationships will be used to estimate the initial distribution $\varphi_{4\mathrm{S,A}}$, cf. (1.31).

2.1 Diffractive $q\bar{q}$-Production

It is useful to divide the kinematical regime into different regions of the variable $\beta \equiv Q^2/(M^2+Q^2)$, where M is the invariant mass of the diffractive system. We begin with the small mass region ($\beta \to 1$), where the $q\bar{q}$-production process is known to give the main contribution to diffraction. Those contributions to the cross section, which can be described perturbatively, can be viewed as follows. Seen from the angle of the proton rest frame the virtual photon splits into a $q\bar{q}$-pair, which interacts with the proton before the quarks result into the two jets. For diffraction the interaction between the $q\bar{q}$-pair and the proton must be colorless and, therefore, in the small x_{B} regime where gluons are expected to dominate, at least two gluons need to be exchanged (fig. 1.5). The cross section can, now, be computed by coupling the gluons in fig. 1.5 to the proton and by squaring the diagrams afterwards. This leads to the following expressions in the case of zero momentum transfer ($t = 0$) [52, 53]:

$$\left.\frac{\mathrm{d}\sigma^t}{\mathrm{d}M^2\,\mathrm{d}t\,\mathrm{d}p_t^2}\right|_{t=0} = \sum_f e_f^2 \frac{\alpha_{\mathrm{em}}\pi^2\alpha_{\mathrm{s}}^2}{12}\frac{1}{M^4}\frac{\left(1-\frac{2p_t^2}{M^2}\right)}{\sqrt{1-\frac{4p_t^2}{M^2}}}\left[-\int\frac{\mathrm{d}l^2}{l^2}\mathcal{F}_{\mathrm{G}}(x_{\mathbb{P}},l^2)\,\mathcal{I}^t(Q^2,M^2,p_t^2,l^2)\right]^2 \tag{2.1}$$

and

$$\left.\frac{\mathrm{d}\sigma^\ell}{\mathrm{d}M^2\,\mathrm{d}t\,\mathrm{d}p_t^2}\right|_{t=0} = \sum_f e_f^2 \frac{\alpha_{\mathrm{em}}\pi^2\alpha_{\mathrm{s}}^2}{3}\frac{4}{Q^2M^2}\frac{p_t^2}{M^2}\frac{1}{\sqrt{1-\frac{4p_t^2}{M^2}}}\left[-\int\frac{\mathrm{d}l^2}{l^2}\mathcal{F}_{\mathrm{G}}(x_{\mathbb{P}},l^2)\,\mathcal{I}^\ell(Q^2,M^2,p_t^2,l^2)\right]^2. \tag{2.2}$$

Here $\boldsymbol{p}_t$ is the transverse part (in the Sudakov decomposition) of the quark-momenta, $x_{\mathbb{P}} = x_{\rm B}/\beta$,

$$\mathcal{I}^t(Q^2, M^2, p_t^2, l^2) = \frac{M^2 - Q^2}{M^2 + Q^2} + \frac{l^2 + \frac{p_t^2}{M^2}(Q^2 - M^2)}{\sqrt{\left[l^2 + \frac{p_t^2}{M^2}(Q^2 - M^2)\right]^2 + 4p_t^4 \frac{Q^2}{M^2}}}\,, \tag{2.3}$$

$$\mathcal{I}^\ell(Q^2, M^2, p_t^2, l^2) = \frac{Q^2}{M^2 + Q^2} - \frac{p_t^2 Q^2}{M^2\sqrt{\left[l^2 + \frac{p_t^2}{M^2}(Q^2 - M^2)\right]^2 + 4p_t^4 \frac{Q^2}{M^2}}} \tag{2.4}$$

and $\mathcal{F}_{\rm G}$ represents the unintegrated gluon distribution of the proton

$$\int^{Q^2} {\rm d}l^2\, \mathcal{F}_{\rm G}(x_{\mathbb{P}}, l^2) = x_{\mathbb{P}}\, g(x_{\mathbb{P}}, Q^2)\,. \tag{2.5}$$

In order to establish a connection with the deep inelastic structure functions we have to integrate over M^2 (or β), p_t^2 and t. Integrating eqns. (2.1) and (2.2) over p_t^2- and M^2 one arrives at the quark-loop at the top of fig. 1.6, with the constraint that the two-gluon systems at the r.h.s. and at the l.h.s. are in a color singlet state. In section 1 we denoted the quark-loop that enters into the four-gluon amplitude as $D_{4,0}$. Here, we use the superscript $(1,+,+)$ in order to indicate that the two gluon-systems are in the color singlet: $D_{4,0}^{(1,+,+)}$. In terms of $D_{4,0}^{(1,+,+)}$ the integrated diffractive cross section becomes:

$$\left.\frac{{\rm d}\sigma^{q\bar{q}}}{{\rm d}t}\right|_{t=0} = \frac{4\pi^2\alpha_{\rm em}}{128\pi^2}\int\frac{{\rm d}l^2}{l^2}\int\frac{{\rm d}m^2}{m^2} D_{4,0}^{(1,+,+)}(\boldsymbol{l}, -\boldsymbol{l}, \boldsymbol{m}, -\boldsymbol{m})\mathcal{F}_{\rm G}(x_{\mathbb{P}}, l^2)\mathcal{F}_{\rm G}(x_{\mathbb{P}}, m^2) \tag{2.6}$$

(we have suppressed the distinction between longitudinal and transverse polarization). As shown in [30], $D_{4,0}^{(1,+,+)}(\boldsymbol{k}_1, \boldsymbol{k}_2, \boldsymbol{k}_3, \boldsymbol{k}_4)$ can be written as a sum of $D_{2,0}$ expressions with appropriate evaluation of momenta:

$$\begin{aligned} D_{4,0}^{(1,+,+)}(\boldsymbol{k}_1, \boldsymbol{k}_2, \boldsymbol{k}_3, \boldsymbol{k}_4) = g^2\frac{\sqrt{2}}{3}\big\{ \;& D_{2,0}(\boldsymbol{k}_1, \boldsymbol{k}_2 + \boldsymbol{k}_3 + \boldsymbol{k}_4) + D_{2,0}(\boldsymbol{k}_2, \boldsymbol{k}_1 + \boldsymbol{k}_3 + \boldsymbol{k}_4) + \\ & + D_{2,0}(\boldsymbol{k}_3, \boldsymbol{k}_1 + \boldsymbol{k}_2 + \boldsymbol{k}_4) + D_{2,0}(\boldsymbol{k}_4, \boldsymbol{k}_1 + \boldsymbol{k}_2 + \boldsymbol{k}_3) - \\ & - D_{2,0}(\boldsymbol{k}_1 + \boldsymbol{k}_2, \boldsymbol{k}_3 + \boldsymbol{k}_4) - D_{2,0}(\boldsymbol{k}_1 + \boldsymbol{k}_3, \boldsymbol{k}_2 + \boldsymbol{k}_4) - \\ & - D_{2,0}(\boldsymbol{k}_1 + \boldsymbol{k}_4, \boldsymbol{k}_2 + \boldsymbol{k}_3)\big\}\,. \end{aligned} \tag{2.7}$$

Here $\boldsymbol{k}_1, \ldots, \boldsymbol{k}_4$ are the transverse components of the gluon momenta at the lower end of the quark-loop. In our case the quark-loop couples to the proton via the unintegrated gluon structure function $\mathcal{F}_{\rm G}$ (cf. (2.1) and (2.2)), and we have to substitute $\boldsymbol{k}_1 = -\boldsymbol{k}_2 = \boldsymbol{l}$ and $\boldsymbol{k}_3 = -\boldsymbol{k}_4 = \boldsymbol{l}'$ and integrate over $\boldsymbol{l}$ and $\boldsymbol{l}'$. For the determination of leading-twist and twist-four contributions we simply expand in powers of $1/Q^2$.

Before we describe the formal expansion in the reciprocal value of Q^2, let us give a qualitative description [54]. We begin with a discussion of the p_t^2-integration of the transverse cross section (2.1) and keep M^2 fixed. As long as p_t^2 is not small, the leading contribution of the $\boldsymbol{l}$-integration comes from the region of small $l^2 < p_t^2(M^2 + Q^2)/M^2$ where $\mathcal{I}^t/l^2$ behaves like a constant. The $\boldsymbol{l}$-integration, therefore, simply leads to a factor $x_{\mathbb{P}}g(x_{\mathbb{P}}, p_t^2(Q^2 + M^2)/M^2)$, and the transverse cross

section falls as $[1/p_t^2\, x_{I\!P}\, g(x_{I\!P}, p_t^2(Q^2+M^2)/M^2]^2$. Using naive dimensional arguments it follows that this region belongs to higher-twist. Considering the integration over p_t^2 one finds dominance of the low p_t^2 region where perturbation theory breaks down. The leading-twist part of the transverse cross section is obtained by extending the convergent p_t^2-integral up to infinity. The twist-four term arises as a correction: the correct upper limit of the p_t^2-integration is $Q^2(1-\beta)/\beta$, i.e. we have to subtract the integral from $Q^2(1-\beta)/\beta$ to infinity. The subtracted quantity is the negative twist-four correction to the transverse cross section. The convergence of the p_t^2-integration implies also that there is no factor $\ln Q^2$ in the twist-four contribution to the transverse cross section.

Turning to the longitudinal cross section, one notices in (2.2) the extra p_t^2 factor in front of the square brackets: this changes, compared to the transverse case, the p_t^2-behavior of the cross section in two ways. When integrating over p_t^2, the small p_t^2 region no longer dominates, whereas in the large p_t^2-region we encounter a logarithmic divergence. This explains the $1/Q^2$-suppression of the cross section and the appearance of a factor $\ln Q^2$. The β (or M^2) dependence of the two cross sections can be determined if we have a closer look at the two formulae (2.1) and (2.2): while the transverse cross section (both leading- and higher-twist) vanishes near $\beta = 1$, the longitudinal one stays finite. This leads to the conclusion that the longitudinal cross section (which for $\beta \ll 1$ is much smaller than the transverse one) dominates in the large β-region. In other words, the diffractive $q\bar{q}$ cross section near $\beta = 1$ is mainly longitudinal and belongs to twist-four. Results of this discussion are summarized in table 1.2.

In order to obtain quantitative expressions for the higher-twist cross sections (and to verify our intuitive arguments), we return to the p_t^2 and β-integrated expressions in (2.7) and perform a formal expansion in powers of $1/Q^2$. Inserting the (ω,ν)-representation of $D_{2,0}$ (cf. (1.11)) in (2.7) and expanding about the twist-four point $\nu = -2$ yields in the transverse case

$$\frac{1}{\omega} D_{4,0}^{t(1,+,+)}(\omega, l^2, l'^2)^{\tau=4} = a_2^t \frac{4\pi\sqrt{2}}{3} \frac{1}{\omega} \sum_f e_f^2 \frac{\sqrt{8}}{2\pi} \alpha_{\rm s}^2 \left\{ 2l^4 + 2l'^4 - (\boldsymbol{l}+\boldsymbol{l}')^4 - (\boldsymbol{l}-\boldsymbol{l}')^4 \right\} . \tag{2.8}$$

Similarly, in the longitudinal case we get

$$\frac{1}{\omega} D_{4,0}^{\ell(1,+,+)}(\omega, l^2, l'^2)^{\tau=4} = -b_2^\ell \frac{4\pi\sqrt{2}}{3} \frac{1}{\omega} \sum_f e_f^2 \frac{\sqrt{8}}{2\pi} \alpha_{\rm s}^2 \Big\{ 2l^4 \ln l^2 + 2l'^4 \ln l'^2 - \\ - (\boldsymbol{l}+\boldsymbol{l}')^4 \ln(\boldsymbol{l}+\boldsymbol{l}')^2 - (\boldsymbol{l}-\boldsymbol{l}')^4 \ln(\boldsymbol{l}-\boldsymbol{l}')^2 \Big\} . \tag{2.9}$$

Here, l^2 and l'^2 are normalized by Q^2. Working in DLA, we have for the unintegrated gluon structure function $\mathcal{F}_{\rm G}$ an expression of the form

$$\mathcal{F}_{\rm G}(x, l^2) = \frac{1}{Q^2} \frac{\partial}{\partial l^2} \int \frac{{\rm d}\omega}{2\pi{\rm i}} \left(\frac{1}{x}\right)^\omega \exp\left(\frac{\gamma_2}{\omega} \ln l^2/q_0^2\right) \varphi_2(\omega)^{\tau=2} , \tag{2.10}$$

where $\varphi_2(\omega)$ is the initial distribution of the gluon structure function and $q_0^2 = Q_0^2/Q^2$. Multiplying (2.8) with functions $\mathcal{F}_{\rm G}(l^2)$ and $\mathcal{F}_{\rm G}(l'^2)$ and performing the integrations over $\boldsymbol{l}$ and $\boldsymbol{l}'$, we arrive at the following higher-twist correction to the differential diffractive cross section:

$$\Delta \frac{{\rm d}\sigma^{q\bar{q},t}}{{\rm d}t}\bigg|_{t=0} = -\frac{4\pi^2\alpha_{\rm em}}{Q^4} \frac{a_2^t}{6\pi^2} \frac{\alpha_{\rm s}^2}{\omega} \sum_f e_f^2 \exp\left(2\frac{\gamma_2}{\omega} \ln Q^2/Q_0^2\right) [\varphi_2(Q_0^2, \omega)]^2 . \tag{2.11}$$

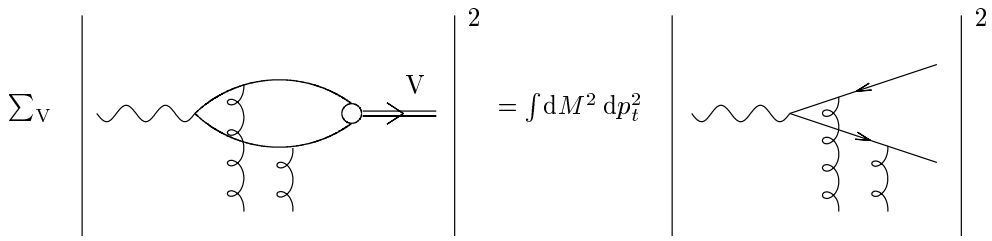

FIG. 1.7: Duality relates the diffractive vector meson production cross section to the diffractive $q\bar{q}$-production cross section.

For the longitudinal case the $\boldsymbol{l}$, $\boldsymbol{l}'$ integrations are slightly more complicated, since (2.9) contains logarithms. In order to obtain the maximum number of logarithms, we split the integration interval into subintervals $l^2 < l'^2$ and $l'^2 < l^2$. The result is

$$\Delta \frac{\mathrm{d}\sigma^{q\bar{q},\ell}}{\mathrm{d}t}\bigg|_{t=0} = \frac{4\pi^2\alpha_{\rm em}}{Q^4}\frac{b_2^\ell}{6\pi^2}\frac{\alpha_{\rm s}^2}{2\gamma_2}\sum_f e_f^2 \left\{1 - \exp\left(2\frac{\gamma_2}{\omega}\ln Q^2/Q_0^2\right)\right\}\left[\varphi_2(Q_0^2,\omega)\right]^2 . \tag{2.12}$$

Before we can draw the relation between the two initial distributions entering into the inclusive and diffractive structure functions, we still have to integrate over the momentum transfer t. Repeating the discussion in the sequel of eqn. (1.30), we note that in DLA the nonzero momentum transfer enters only into the lowest part of the ladders, the initial distributions φ_2. Integration in (2.11) or (2.12) over t, therefore, simply means replacing φ_2^2 by $\int \mathrm{d}^2\boldsymbol{q}\,\varphi_2^2$, i.e. by an effective new initial condition. Moreover, if we allow for diffractive dissociation of the target proton, this initial condition will again be modified into a new initial condition which we denote by $\varphi_4^{\rm diff}(\omega)$:

$$\Delta\sigma^{q\bar{q},\ell} = \frac{4\pi^2\alpha_{\rm em}}{Q^2}\frac{b_2^\ell}{6\pi^2}\frac{\alpha_{\rm s}^2}{2\gamma_2}\sum_f e_f^2\frac{Q_0^2}{Q^2}\left\{1 - \exp\left(2\frac{\gamma_2}{\omega}\ln Q^2/Q_0^2\right)\right\}\varphi_4^{\rm diff}(Q_0^2,\omega) \tag{2.13}$$

(and a similar expression for the transverse cross section). Further below we shall discuss how this diffractive cross section contributes to the structure functions $F_{\ell,t}$. In particular, we will derive a relation between $\varphi_4^{\rm diff}(\omega)$ and $\varphi_{\rm 4S,A}(\omega)$ introduced in (1.31).

2.2 Diffractive Vector Meson Production

Let us, now, turn to those diffractive processes which have been examined most intensively both theoretically and experimentally: the diffractive production of vector mesons: $\gamma^* + p \to V + p$, where V can be any vector meson. For the longitudinal photon this process has been shown to be calculable within perturbative QCD [7–10]:

$$\frac{\mathrm{d}\sigma^\ell_{\gamma^* p\to {\rm V}p}}{\mathrm{d}t}\bigg|_{t=0} = \frac{12\pi^3\alpha_{\rm s}^2}{N_{\rm c}^2\,\alpha_{\rm em}}\frac{M_{\rm V}}{Q^6}\Gamma_{{\rm V}\to e^+e^-}T(Q^2)\eta_{\rm V}^2\left|\left(1 + {\rm i}\frac{\pi}{2}\frac{\mathrm{d}}{\mathrm{d}\ln x}\right)xg(x,Q^2)\right|^2 . \tag{2.14}$$

Experiments show that after summing over all vector particles one gets a significant (about 20 %) contribution to the total diffractive cross section. As can be seen in (2.14), for an individual vector particle, the cross section behaves as $1/Q^6$. In ref. [10] it has been shown that the production cross

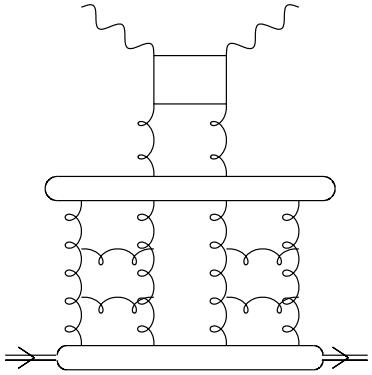

FIG. 1.8: The (integrated) $q\bar{q}g$-production amplitude is given by an expression which is symbolized by this figure. Note that the effective $2 \to 4$ transition vertex is not the same as in fig. 1.1b for D_4^{I}.

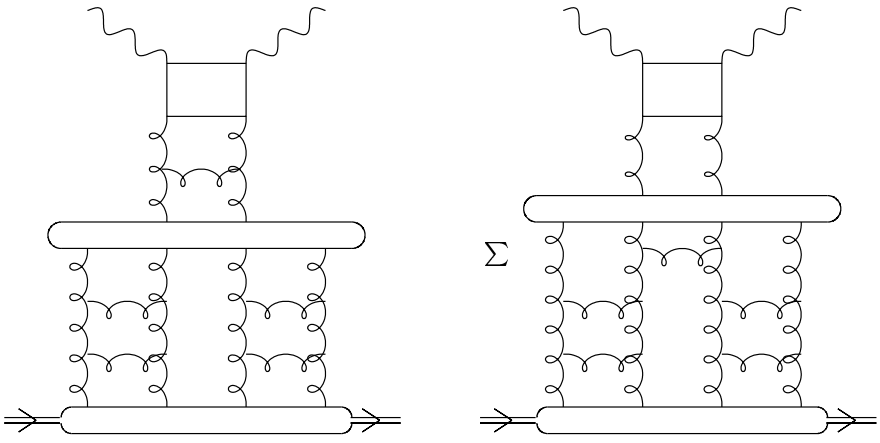

(a) (b)

FIG. 1.9: Same as in fig. 1.8 but now for $q\bar{q}gg$-production. The sum denotes all possible couplings between systems (12) and (34).

Contribution	Sign	$\ln(Q^2/Q_0^2)$	
Trans. $\tau = 2$	+	$\ln(Q^2/Q_0^2)$	non-pert.
Trans. $\tau = 4$	+	$\ln(Q^2/Q_0^2)$	
Long. $\tau = 2$	+	no	non-pert.
Long. $\tau = 4$	−	$(\ln(Q^2/Q_0^2))^2$	

TABLE 1.3: The four contributions to diffractive $q\bar{q}g$-production. We list the sign structure and powers of $\ln Q^2$.

section of a single vector particle can also be obtained if one starts with open $q\bar{q}$-production and projects onto the corresponding angular momentum and parity quantum numbers. This suggests to apply a simple duality argument and to set, for the mass range $m_\rho < M < M_c$, the sum over vector particle production cross sections (2.14) equal to the M^2- (and p_t^2-) integrated cross section of open $q\bar{q}$-production (2.2) (we illustrate this equality in fig. 1.7). In this way, the sum over the vector particle cross sections turns into a twist-four contribution: the additional factor $1/Q^2$ in (2.14) is due to the projection onto the vector particle wave function. As a result of this argument, taking the measured vector particle cross section and summing over all vector particles, we can use the obtained numbers in order to obtain a lower bound of the integrated longitudinal $q\bar{q}$ cross section [55], which belongs to twist-four.

2.3 Diffractive $q\bar{q}g$-Production and Multi-Jet Processes

Diffractive $q\bar{q}$-production is expected to be dominant near $\beta = 1$. If we go to $\beta < 1$, we have to consider also gluon production processes ($q\bar{q}g$-, $q\bar{q}gg$-,...-jets). Cross sections for these processes have been calculated in different kinematical regions: for very small β (the triple Regge region) in [30, 56], for strong ordering in the transverse momenta in [57, 58]. The latter calculation allows to describe the whole β-interval, but only the first one contains both leading-twist and twist-four. In this section, therefore, we make use only of the results obtained in [56] and discuss the higher-twist contributions to diffractive $q\bar{q}g$-production. The calculations are similar to those for the $q\bar{q}$-production process discussed above: we keep all powers in the transverse momenta, but we restrict ourselves to the leading logarithms in M^2 (or $1/\beta$). An example of the Feynam diagrams is shown in fig. 1.10a. A complete description can be found in [56]. In general, the s-channel gluon can be emitted anywhere from one of the t-channel gluons.

The analytic expressions for the cross section formulae [56] are to lengthy to be repeated here. We follow the same logic as in the sequel of (2.1) and (2.2). After integration over the momenta of the outgoing quarks and the gluon the result [30] takes the form illustrated in fig. 1.8, where eqns. (1.41) and (1.43) have been used. The result can be illustrated with the help of diagrams which have a fermion-loop $D_{2,0}$ at the top, and the (final state) s-channel gluon is contained in an effective vertex function which is similar (but not identical) to the $2 \to 4$ gluon vertex in (1.19) (fig. 1.1b). Comparing the further derivation with the derivation of (2.8) and (2.9) we, now, have instead of

(2.7) the expression [30]

$$D^{\ell,t}_{q\bar{q}g,0}(\boldsymbol{l},\boldsymbol{l}')\Big|_{t=0} = \frac{3g^2}{4\sqrt{2}} D^{\ell,t}_{2,0} \otimes \big\{ 2G(\boldsymbol{l},-\boldsymbol{l}) + 2G(\boldsymbol{l}',-\boldsymbol{l}') + 2G(\boldsymbol{l},\boldsymbol{l}') + 2G(\boldsymbol{l},-\boldsymbol{l}') + \\ + G(\boldsymbol{l}+\boldsymbol{l}',-\boldsymbol{l}-\boldsymbol{l}') + G(\boldsymbol{l}-\boldsymbol{l}',-\boldsymbol{l}+\boldsymbol{l}') - 2G(\boldsymbol{l},-\boldsymbol{l}+\boldsymbol{l}') \\ - 2G(\boldsymbol{l},-\boldsymbol{l}-\boldsymbol{l}') - 2G(\boldsymbol{l}',\boldsymbol{l}-\boldsymbol{l}') - 2G(\boldsymbol{l}',-\boldsymbol{l}-\boldsymbol{l}') \big\} . \qquad (2.15)$$

Here $G(\boldsymbol{a},\boldsymbol{b})$ is the same function that enters into the convolution $D_2 \otimes V$ (eqns. (1.18), (1.19)). The ladders at the lower end of this vertex in fig. 1.8, again, denote (leading-twist) gluon structure functions (2.10).

Since we did not present the explicit formulae for the (unintegrated) diffractive cross sections, we only briefly sketch the qualitative picture (details can be found in [56]). Let $\boldsymbol{k}_2$ be the transverse momentum of the gluon, and $\boldsymbol{k}_1$, $-(\boldsymbol{k}_1+\boldsymbol{k}_2)$ those of the quarks. The easiest way is to start with the hard region (i.e. the transverse momenta of quarks and gluons are large), and to consider configurations where the momenta are ordered: $k_2^2 < k_1^2$. In this region, the transverse cross sections goes as $\mathrm{d}\sigma^t \sim 1/[k_1^2 k_2^4] \cdot [x_{\mathbb{P}} g(x_{\mathbb{P}}, k_2^2)]^2$ and the longitudinal cross section behaves as $\mathrm{d}\sigma^\ell \sim 1/[k_1^4 k_2^4] \cdot [x_{\mathbb{P}} g(x_{\mathbb{P}}, k_2^2)]^2$. Using dimensional counting, one observes that this region belongs to twist-four. Leading-twist can be obtained if one realizes that the integration over the gluon momentum $\boldsymbol{k}_2$ is dominated by the small momentum region, i.e. by nonperturbative physics. The remaining $\boldsymbol{k}_1$-integration provides, for the transverse photon, a $\ln Q^2$-enhancement, whereas for the longitudinal photon it does not (table 1.3).

As indicated before, the derivation of the twist-four contributions of the integrated cross section, now, follows the same way as for $q\bar{q}$-production. We use the (ω,ν)-representation of (2.15), and get for the twist-four (near $\nu=-2$) contribution of the transverse photon

$$\frac{1}{\omega} D^t_{q\bar{q}g,0}(\omega, l^2, l'^2)^{\tau=4} = -a_2^t \frac{9}{\pi}\frac{1}{\omega} \sum_f e_f^2 \alpha_{\mathrm{s}}^3 \frac{Q^2}{Q_0^2} \Big\{ 2l^4 \ln l^2 + 2l'^4 \ln l'^2 \\ - \Big[2l^4 + 2l'^4 - 8l^2 l'^2 \Big] \ln \Big[\max(l^2, l'^2) \Big] \Big\} . \qquad (2.16)$$

Similarly, for the longitudinal photon we obtain

$$\frac{1}{\omega} D^\ell_{q\bar{q}g,0}(\omega, l^2, l'^2)^{\tau=4} = \frac{b_2^\ell}{2}\frac{9}{\pi}\frac{1}{\omega} \sum_f e_f^2 \alpha_{\mathrm{s}}^3 \frac{Q^2}{Q_0^2} \Big\{ 2l^4 \ln^2 l^2 + 2l'^4 \ln^2 l'^2 \\ - \Big[2l^4 + 2l'^4 - 8l^2 l'^2 \Big] \ln^2 \Big[\max(l^2, l'^2) \Big] \Big\} . \qquad (2.17)$$

The integration over $\boldsymbol{l}$, $\boldsymbol{l}'$ is done in the same way as described after (2.10). With (2.10) for the unintegrated structure function we find

$$\Delta \frac{\mathrm{d}\sigma^{q\bar{q}g,t}}{\mathrm{d}t}\bigg|_{t=0} = -\frac{4\pi^2\alpha_{\mathrm{em}}}{Q^4} \frac{9 a_2^t}{16\pi^3} \frac{\alpha_{\mathrm{s}}^3}{2\gamma_2} \frac{1}{\omega} \sum_f e_f^2 \left\{ 1 - \exp\left(\frac{2\gamma_2}{\omega} \ln \frac{Q^2}{Q_0^2} \right) \right\} \varphi_2^2(\omega) \qquad (2.18)$$

and

$$\Delta \frac{\mathrm{d}\sigma^{q\bar{q}g,\ell}}{\mathrm{d}t}\bigg|_{t=0} = \frac{4\pi^2\alpha_{\mathrm{em}}}{Q^4} \frac{9 b_2^\ell}{32\pi^3} \frac{\alpha_{\mathrm{s}}^3}{2\gamma_2^2} \sum_f e_f^2 \left\{ \exp\left(\frac{2\gamma_2}{\omega} \ln \frac{Q^2}{Q_0^2} \right) - 1 - \frac{2\gamma_2}{\omega} \ln \frac{Q^2}{Q_0^2} \right\} \varphi_2^2(\omega) \qquad (2.19)$$

for the transverse and for the longitudinal photon, resp. Finally, performing the integration over t and replacing φ_2^2 by $\varphi_4^{\rm diff}$ leads to our final expressions for the twist-four corrections to the diffractive structure functions.

An important feature of these results is the sign structure (summarized in table 1.3). For both the transverse and the longitudinal contributions we find the opposite signs compared to $q\bar{q}$-production (table 1.2). This implies that when we are calculating the total twist-four corrections to the diffractive cross section – either transverse or longitudinal – we are adding two terms ($q\bar{q}$ and $q\bar{q}g$) of opposite signs. Moreover, switching from transverse to longitudinal diffractive cross sections results also in sign changes. This already hints at the possibility of substantial cancellations, in particular in the corrections to $F_2^{\rm D} = F_\ell^{\rm D} + F_t^{\rm D}$.

After we have been discussing diffractive $q\bar{q}$- and $q\bar{q}g$-production, it is not difficult to find the generalization with the production of more gluons. These processes are likely to become important in the region of very small β. For example, for the (integrated) production cross section of two gluons we have to calculate the diagrams shown in fig. 1.9. As before, eqns. (1.41) and (1.43) have been used. In this way all diagrams in fig. 1.9 can be rearranged in terms of the vertex (2.15), and they can be grouped into two classes. Beginning with the fermion-loop at the top of the diagram, we have, in the case of fig. 1.9a, one BFKL rung which contains one of the (final state) s-channel gluons. The second s-channel gluon is contained in the vertex (2.15) which couples to the BFKL rung at the top and the two gluon-ladders (for the unintegrated gluon structure functions) at the bottom. In the case of fig. 1.9b, there is no rung between the fermion-loop and the vertex (2.15). Instead the second s-channel gluon is contained in one of the four possible rungs at the bottom of the vertex. Extending these considerations to the case of three final state gluons there are three possibilities: 1) two gluon rungs between the quark-loop and the vertex, 2) one rung at the top and one rung at the bottom of the vertex, 3) two rungs at the bottom of the vertex.

2.4 Connection with the Structure Functions $F_{\ell,t}$ and the AGK Cutting Rules

After we have discussed the different diffractive cross sections, we, now, turn to the question of how these contributions enter into the inclusive cross section (1.17). An important ingredient are the AGK cutting rules [42].

We first return to the total cross section (1.17) and recapitulate how the AGK rules work. Let us, for the moment, replace the proton by a virtual photon, i.e. we consider the elastic scattering of a virtual photon off another virtual photon. This process can be treated perturbatively. For the time being we do not expand in powers of Q_0^2/Q^2, but consider the Regge limit at large but finite Q^2. In order to study the AGK rules, we start with the discontinuity across the four-gluon t-channel intermediate state. Disregarding all unnecessary details, this discontinuity takes the form

$$\mathrm{disc}_\omega \, F_{\gamma^*\gamma^*} \sim \frac{1}{4!} C_4^* \otimes C_4 \tag{2.20}$$

where $F_{\gamma^*\gamma^*}$ denotes the t-channel partial wave for the $\gamma^*\gamma^*$ scattering process, $C_4(k_1,k_2,k_3,k_4;\omega) = (\omega - \sum \beta(k_i)) D_4(k_1,k_2,k_3,k_4;\omega)$ is the amputated $\gamma^*\gamma^* \to 4$-gluons partial wave, and the convolution "$\otimes$" contains all phase space factors. For C_4 we have the same decomposition (eqn. (1.16)) as for D_4, and $C_4^{\rm R}$ contains a completely symmetric part and a part with mixed symmetry (cf. the discussion after (1.41)). In the unitarity integral (2.20), we take from both C_4 and C_4^* either the symmetric part or the part with mixed symmetry, i.e. there is no interference term.

First, consider the symmetric parts, e.g. $C_4^{\rm I}$ for both factors in (2.20). Writing $C_4^{\rm I}$ in terms of the auxiliary potentials $T_{(ij)(kl)}$ from our discussion above, we have in our unitarity integral on the r.h.s. of (2.20) the three identical 'diagonal' terms $T_{(12)(34)} \otimes T_{(12)(34)}$, $T_{(13)(24)} \otimes T_{(13)(24)}$, and $T_{(14)(23)} \otimes T_{(14)(23)}$. Together with the statistical factor 1/4!, this gives a weight factor $1/2(1/2)^2$ for the diagonal term (this counting does not include color). Similarly, 'nondiagonal' terms, $T_{(12)(34)} \otimes T_{(13)(24)}$ etc., yield the weight factor $(1/2)^2$. In order to verify the AGK cutting rules we compare $2\,{\rm Im}\,T_{\gamma^*\gamma^*}$ of this amplitude with the different cuts, σ_0, σ_1, and σ_2 (the subscripts refer to the number of cut ladders). The (diagonal) "diffractive cut" σ_0 has the cutting line between the gluon lines '2' and '3'. Its contribution is positive and has the weight $(1/2)^2$ (due to the statistical factors inside the ladders). For the "double multiperipheral" cut σ_2 the cutting line runs also between gluons '2' and '3', but its (positive) contribution has the weight $2(1/2)^2$. Finally, the "absorptive cut" σ_1 is negative; the cutting line runs between line '1' and '2' or '3' and '4', and the counting gives $-2 \cdot 3 \cdot 1/3! = -1$. Adding all these contributions, we arrive at $-(1/2)^2$, i.e. minus the diffractive cross section σ_1. The result agrees with $2\,{\rm Im}\,T_{\gamma^*\gamma^*}$, as anticipated by the AGK rules. Two features of these results are important for us: in total, the four-gluon t-channel state gives a *negative* correction to the single-ladder contribution (this justifies the minus sign in (1.17)), and its absolute value equals the 'diffractive cut' σ_0. It is easy to verify that the same conclusion also holds for nondiagonal parts $T_{(12)(34)} \otimes T_{(13)(24)}$ etc.

Next, the part with mixed symmetry: in (2.20) we put $C_4^{\rm R}$ for both C_4-factors, and we take the terms with the anti-symmetric structure constants ($f^{abc'} f^{c'cd}$ etc.). Their color and momentum structure is the same as in (1.33). They are connected with the odd signature reggeized gluon. Again, in the unitarity integral we have diagonal terms of the type $f_{\rm A}(12,34) \otimes f_{\rm A}(12,34)$. Their total weight is $2(1/2)^2$. In the counting of the nondiagonal terms we encounter several cancellations: the weight factor turns out to be 1/2. Now, we compare this with the cuts σ_0, σ_1, and σ_2. For the diagonal σ_0 and σ_2 contributions where the cutting line runs between gluons '2' and '3', we find the weight factors $(1/2)^2$ and $2(1/2)^2$, resp. They are the same as the counting factors for the even signature ladders which we have discussed before. In particular, we again have the negative sign for the sum of the three cuts. There is, however, an important difference between even and odd signature reggeons: for odd signature the real part of the signature dominates, and the leading contribution σ_0 is contained in the LO BFKL equation. The only contribution to σ_0 from the four gluon intermediate state comes from the 'diagonal' partss which present the two gluon contributions to the gluon trajectory functions. Consistency, therefore, requires that the magnitude of this term is linked to the leading order BFKL ladder. One can check from (1.41) that this condition is, indeed, satisfied.

In summary, the AGK rules allow us to determine the sign of our initial conditions. We return to deep inelastic scattering off the proton, consider the twist-four term in the expansion in powers of Q_0^2/Q^2 and replace, in (2.20), the second C_4 factor by our general ansatz (1.31), i.e. by our non-perturbative initial conditions $\varphi_{4\rm S}$ and $\varphi_{4\rm A}$. In order to preserve the sign structure dictated by the AGK rules, both functions have to be positive. Moreover, since $\varphi_{4\rm A}$ is connected with the reggeization of the gluon trajectory function, it is linked to the size of the twist-four part in the BFKL ladder, $\Delta F^{(2)}$. In this first attempt to estimate the higher-twist contribution, we will consider two different values for $\varphi_{4\rm A}$ which corresponds to a reasonable range.

Next we attempt to relate these unknown initial conditions to the diffractive $q\bar{q}$ cross section (2.13), in order to obtain an estimate of their magnitude. The easiest way is a comparison of the two-ladder diagrams in ΔF^4 with the diffractive cross section (fig. 1.6). Taking in ΔF^4 the color singlet part

of the ladders, projecting onto twist-four, and equating the diffractive cut of this contribution with the cross section (2.13) we arrive at the equation:

$$\frac{5}{4}\varphi_{4\mathrm{S}} - \frac{3}{4}\varphi_{4\mathrm{A}} = \varphi_4^{\mathrm{diff}}. \tag{2.21}$$

This result is quite remarkable, since – at first sight – it does not seem to agree with the AGK rules. Naively one might have expected that $\varphi_{4\mathrm{S}} = \varphi_4^{\mathrm{diff}}$, i.e. the four-gluon contribution equals (up to the overall minus sign which we have extracted already in (1.17)) the diffractive cross section. Let us recapitulate the origin of (2.21): from (1.16) we deduced that QCD diagrams for $T_{\gamma^*\gamma^*}$ with four gluons in the t-channel have to be decomposed according to their symmetry under permutation of color and momenta (the antisymmetric terms have their origin in the reggeization of the gluon). The same argument forces us to use the ansatz (1.31)-(1.33), i.e. we have the two functions $\varphi_{4\mathrm{S}}$ and $\varphi_{4\mathrm{A}}$. The AGK rules work for each term separately, but the t-channel state with four reggeized gluons couples only to $\varphi_{4\mathrm{S}}$. Finally, when computing the two-ladder diagrams in $T_{\gamma^*\gamma^*}$, we find for the coupling of two ladders to the proton the combination on the l.h.s. of (2.21) (the fact that the factor in front of $\varphi_{4\mathrm{S}}$ equals $5/4$ and not 1 is due to the second and third term in (1.32)).

An important consequence of this analysis is that, from this single condition (2.21), we cannot fix both initial conditions $\varphi_{4\mathrm{S}}$ and $\varphi_{4\mathrm{A}}$. We, therefore, propose to proceed as follows. The longitudinal cross section for diffractive $q\bar{q}$-production allows to estimate $\varphi_4^{\mathrm{diff}}$. From our discussion above we know that $\varphi_{4\mathrm{A}}$ is connected with the reggeization of the gluon: in our numerical analysis we will vary $\varphi_{4\mathrm{A}}$ in such a way that its correction to the leading-twist structure function ranges between 20 % and 100 % (see below). Together with the variation of $\varphi_{4\mathrm{A}}$ we also find a change in the strength of $\varphi_{4\mathrm{S}}$ and ΔF^{I}.

2.5 The Sign Structure

It may be helpful to briefly recapitulate the sequence of our arguments, in particular the sign structure. The easiest way is to start with the twist-four corrections to the diffractive cross sections; their signs are summarized in tables 1.2 and 1.3. Starting with $q\bar{q}$-production, in the transverse case twist-four is a correction to leading-twist and has a negative sign. The longitudinal cross section starts with twist-four and is positive. Next diffractive $q\bar{q}g$-production: all signs change, compared to $q\bar{q}$-production. This is due to the vertex (2.15) which has an intrinsic minus sign.

In the next step we have argued that when generalising to an arbitrary number of gluons in the diffractive final state and allowing for evolution in the unintegrated gluon structure function we generate all diagrams contained in ΔF^4: although there is no direct correspondence between the splitting $\Delta F^4 = \Delta F^{\mathrm{R}} + \Delta F^{\mathrm{I}}$ and the different diffractive final states. As a memo we nevertheless can say that ΔF^{R} "is related to" (i.e. gets the same sign as) the cross section for $q\bar{q}$-production, and a similar correspondence holds for ΔF^{I} and diffractive $q\bar{q}g$-, $q\bar{q}gg$-, ...,-production.

In the last step we have to remember that it is not only the diffractive states which contribute to the structure functions. Making use of the AGK rules we conclude that taking into account all other energy discontinuities simply means changing the sign of the (total) diffractive contributions. The results are summarized in table 1.4.

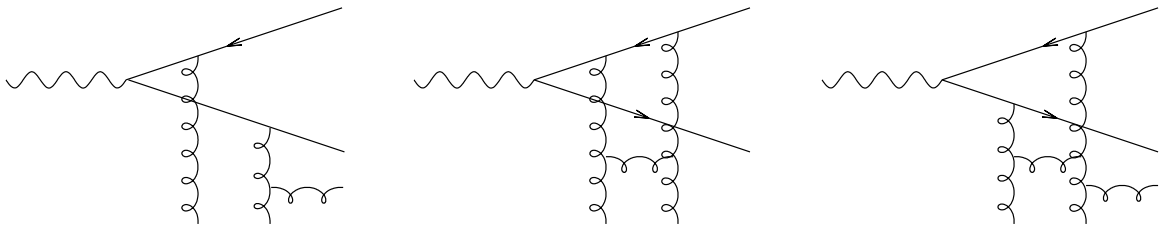

FIG. 1.10: Three sample diagrams which contribute to D_4 at order α_s^3 ((a) and (b)) and at order α_s^4 (c). Diagrams (a) and (c) enter also into diffractive $q\bar{q}g$-production at leading- and next-to-leading order, resp. For the diffractive process the two t-channel gluons must certainly be in the color singlet, while there are also contributions from other color states which enter into D_4.

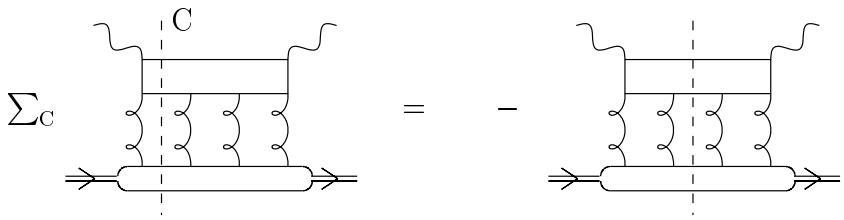

FIG. 1.11: The AGK rules: The sum over the three cuts, which is necessary for the computation of the inclusive structure function, gives a contribution that is equal to minus one times the term where only the diffractive cut is applied.

3 Numerical Results

3.1 General Procedure and Determination of Initial Parton Distributions

Using the framework outlined above we have performed a numerical analysis. The first step to be discussed is how to fix the free parameters in the various initial distributions φ. From our discussion it should have become clear that we have to determine five initial distributions, viz. φ_2 for ΔF^2, φ_3 for the three-gluon correction to ΔF^2, and φ_4 which couples to both ΔF^{R} and ΔF^{I}. Moreover φ_4 consists of a symmetrical part and a part with mixed symmetry, cf. eqn. (1.31). All initial distributions depend on ω, and a pole at some positive ω-value corresponds to a rising (in $1/x_{\mathrm{B}}$) initial condition.

Let us begin with a detailed discussion of the four-gluon case. As indicated before, we relate φ_4 directly to the diffractive $q\bar{q}$ cross section (eqs. (2.13) and (2.21)), and the latter can be estimated with the help of the measured cross section of longitudinal vector production if we sum over all vector mesons in the final state [55]. Let us assume that – after integration over t, p_t^2 and M^2, and including diffractive dissociation of the proton – this cross section reaches a few per cent of the inclusive (transverse) leading-twist cross section at $x_{\mathrm{B}} = 10^{-3}$, $Q^2 = 10\,\mathrm{GeV}^2$. Using this estimate we fix the initial condition $\varphi_4^{\mathrm{diff}}$ and, with the help of (2.21), also the combination of the initial conditions $\varphi_{4\mathrm{S}}$ and $\varphi_{4\mathrm{A}}$, which enter into the four-gluon amplitude. Since the outlined procedure fixes only the difference $5\varphi_{4\mathrm{S}} - 3\varphi_{4\mathrm{A}}$ (cf. (2.21)) we still have some freedom for determining the ratio of $\varphi_{4\mathrm{S}}$ and $\varphi_{4\mathrm{A}}$. In a perturbative toy model, namely deep inelastic scattering off a virtual photon, $\varphi_{4\mathrm{A}}$ is linked to the leading-twist amplitude: it provides the t-channel four-gluon state inside the BFKL amplitude (cf. the discussion in section 2.4) and, hence, can be derived from the size of the leading-twist contribution. However, when replacing the (target) virtual photon by the proton, this connection becomes somewhat uncertain, and we, therefore, consider different values for the ratio $\varphi_{4\mathrm{A}}/\varphi_{4\mathrm{S}}$. Starting with the toy model, we find it reasonable to expect that $\varphi_{4\mathrm{A}}$ should not be smaller than $\varphi_{4\mathrm{S}}$. We, therefore, set $\varphi_{4\mathrm{A}} = \lambda\varphi_{4\mathrm{S}}$ and consider the range $1.0 < \lambda < 1.5$. Eqn. (2.21) indicates that this seemingly small variation will nevertheless have a large effect: if λ reaches the vicinity of $5/3 \approx 1.6$, $\varphi_{4\mathrm{S}}$ increases strongly (for fixed $\varphi_4^{\mathrm{diff}}$). This enhances the contribution of ΔF^{I}, whereas ΔF^{R} changes much less, since it depends on both, $\varphi_{4\mathrm{S}}$ and $\varphi_{4\mathrm{A}}$ (cf. (1.42)). Since ΔF^{I} and ΔF^{R} enter with different signs, a variation of λ between 1 and 1.5 has a large effect on the total twist-four contribution.

Knowing the initial conditions we can, in principle, predict all other higher-twist corrections to the diffractive cross section. In a future analysis of diffractive jet data at HERA it may be possible to measure the twist-four $q\bar{q}$ and $q\bar{q}g$ contributions directly. This will provide an important consistency check of this strategy. As we have said before, due to the cancellations between the $q\bar{q}$ and $q\bar{q}g$ parts the total higher-twist contribution to F_2^{D} may be smaller than the naive estimate based on longitudinal vector production.

As to the other two initial conditions, φ_2 and φ_3, we have not been able to relate them to any direct measurement. Starting with φ_2, for simplicity we assume that at the scale Q_0^2 the initial distribution is the same for the leading-twist case and for twist-four. It follows that the longitudinal twist-four part of the two-gluon amplitude contributes with a negative sign to F_2, since b_2^ℓ in eqn. (1.14) is negative. For the three-gluon amplitude we make an even more ad hoc choice and demand that at $x_{\mathrm{B}} = 10^{-3}$, $Q^2 = 1\,\mathrm{GeV}^2$ its absolute magnitude in ΔF_2^ℓ equals the mean value of ΔF^2 and

	$F_2^{\tau=2}$	ΔF^2	ΔF^3	ΔF^{R}	ΔF^{I}
long.	+	−	+	−	+
trans.	+	+	−	+	−

TABLE 1.4: The various contributions to F_2 enter with different signs.

ΔF^{R}. Our numerical analysis shows that the choice of the point, $x_{\mathrm{B}} = 10^{-3}$, $Q^2 = 1\,\mathrm{GeV}^2$, hardly influences our results, since ΔF^2, ΔF^3 and ΔF^{R} have nearly the same shape (up to factors $\sqrt{\alpha_{\mathrm{s}}(Q^2)}$ and $\alpha_{\mathrm{s}}(Q^2)$).

In principle, for both, $\varphi_2^{\tau=4}$ and the three-gluon term φ_3, not only the absolute magnitude but also the overall signs are undetermined. We have fixed these signs with the help of the following considerations. First, in ΔF^2 there is no reason why there should be a sign change when going from leading-twist to twist-four. As an example, in a toy model, deep inelastic scattering of two virtual photons with virtualities $Q_1^2 \ll Q_2^2$, both leading- and higher-twist have the same sign. Next, as we have argued above, ΔF^3 and ΔF^{R} are supposed to be related to the NLO and NNLO corrections to BFKL. Our choice of signs is consistent with the expectation that these corrections have alternating signs, i.e. ΔF^3 is negative with respect to ΔF^2, and ΔF^{R} is positive again. The sign of ΔF^{R}, on the other hand, has to be consistent with (1.42) and the AGK cutting rules, i.e. posititive for the transverse part. All in all we, therefore, believe that our choice of signs should be on a rather safe ground. Table 1.4 summarizes the sign structure of the various leading- and next-to-leading twist parts in F_2.

As one of the results of our analysis we observe that ΔF^{R} and ΔF^{I} enter with opposite signs and, depending on the choice of parameters, can weaken each other: although we got some freedom for determining the relative contribution of $\varphi_{4\mathrm{S}}$ and $\varphi_{4\mathrm{A}}$, both, ΔF^{R} and ΔF^{I}, are in most cases sizeable and enter with opposite sign. But despite these cancellations the total twist-four contribution becomes sizeable near $Q^2 = 1\,\mathrm{GeV}^2$. In total, it seems that twist-four is negative and the contribution of the transverse photon is larger than that of the longitudinal one.

In our numerical analysis we have used our formulae in order to perform, in the kinematical regime of HERA, a "semiquantitative" numerical study of the potential rôle of twist-four at small x_{B} and low Q^2. As we have emphasised several times the limitations due to the DLA are severe. On the leading-twist level it is known that this approximation, which in the anomalous dimension retains only the most singular (near $\omega = 0$) term, is insufficient to describe HERA data at small x_{B} and low Q^2: it is, at least, necessary to keep also the constant term within the gluon anomalous dimension. We, therefore, expect that a similar level of accuracy will be needed also for a realistic estimation of twist-four corrections. We can only hope that, as long as we restrict ourselves to a comparison of leading-twist and twist-four (i.e. the ratio of both), at least a part of the uncertainty drops out, and the results may describe the trend correctly on a semiquantitative level.

As outlined above, we are using the diffractive vector production cross section to estimate twist-four contributions to F_2. To be precise, we assume that the longitudinal twist-four $q\bar{q}$ cross section (2.13) reaches three per cent at $Q^2 = 10\,\mathrm{GeV}^2$, $x_{\mathrm{B}} = 10^{-3}$ relative to the inclusive transverse leading-twist contribution. As to the choice of the starting scale Q_0^2, our limitations due to the DLA are causing a particular problem. In DLA, the four-gluon amplitude ΔF^{I} vanishes at $Q^2 = Q_0^2$, and it needs some Q^2 evolution before it "forgets" about its starting condition. In a more accurate analysis, we

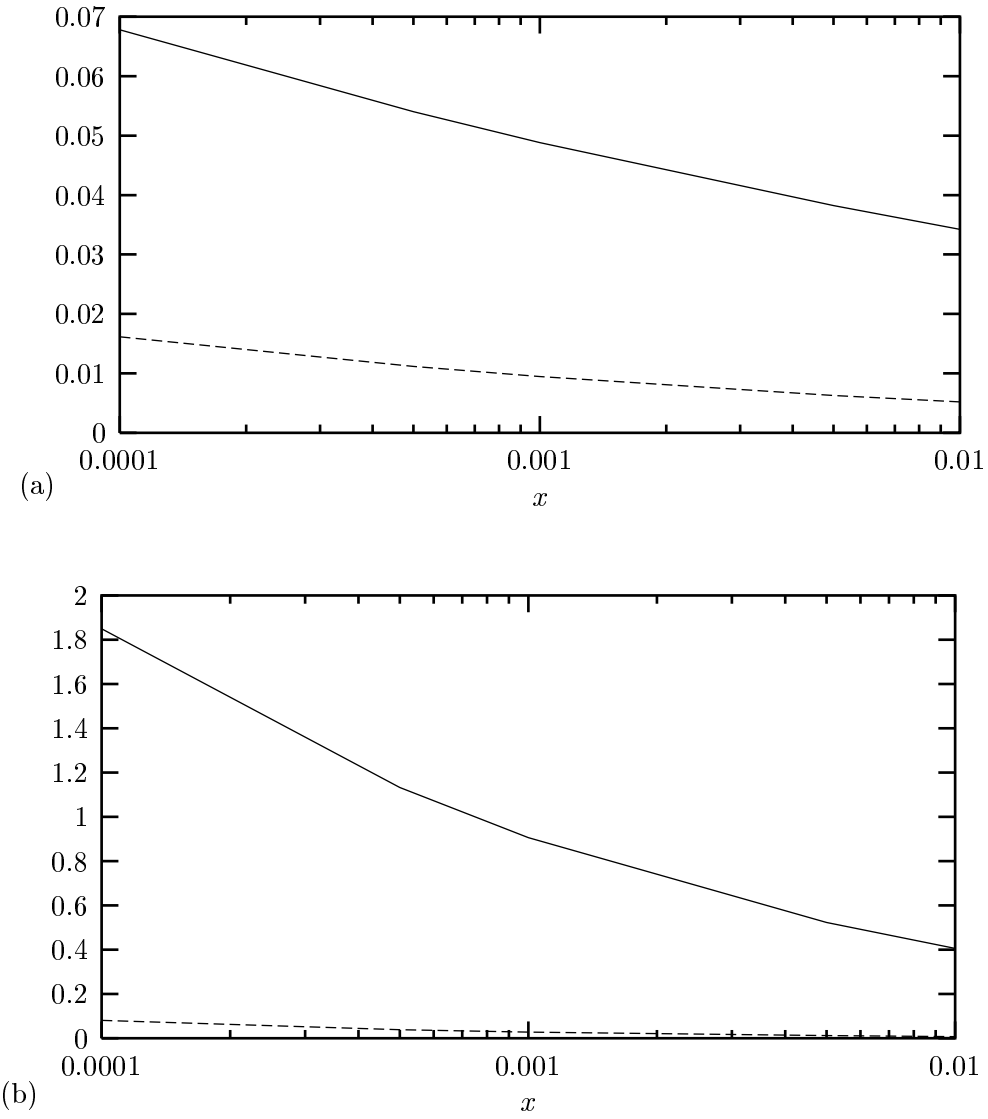

FIG. 1.12: Transverse leading-twist structure function in DLA (solid line) in comparison with the longitudinal twist-four contribution to F_2 of the diffractive $q\bar{q}$-production process as a function of x_{B} at (a) $Q^2 = 1\,\mathrm{GeV}^2$ and (b) $Q^2 = 10\,\mathrm{GeV}^2$. For this scenario, we have chosen constant initial distributions at $Q_0^2 = 0.5\,\mathrm{GeV}^2$.

would start with some nonzero value. In order to escape from this unrealistic behavior near Q_0^2 we have chosen a very small value for the input scale, viz. $Q_0^2 = 0.5\,\mathrm{GeV}^2$, and hope that for Q^2 values greater than, say, $0.8\,\mathrm{GeV}^2$, these unwanted effects are suppressed. For the numerical computation of the double Mellin transforms we have extended the method outlined in ref. [62] (see appendix B for more details). The numerical results of our analysis strongly depend upon the x_B-shape of the initial distributions, both for the leading-twist and for the twist-four correction. We, therefore, compare three different scenarios, two with constant initial conditions with different choices for the ratio $\lambda = \varphi_{4\mathrm{A}}/\varphi_{4\mathrm{S}}$, and one with rising initial conditions.

3.2 Constant Initial Parton Distributions

Following a presently popular trend in analysing HERA data, we first assume that the leading-twist gluon structure function at the input scale Q_0^2 is flat at small x_B. In two subsections we will consider the results for two different choices of the ratio $\lambda \equiv \varphi_{4\mathrm{A}}/\varphi_{4\mathrm{S}}$, viz. $\lambda = 1$ and $\lambda = 1.5$. First, we show in figs. 1.12a and 1.12b the x_B-dependence of the transverse leading-twist structure function in comparison with the twist-four contribution due to diffractive longitudinal $q\bar{q}$-production, eqn. (2.13). In the lower figure the point $x_\mathrm{B} = 10^{-3}$ is our point of comparison: the higher-twist term has reached 3 % of F_2. The comparison of the two figures shows the expected behavior: higher-twist becomes more important at low Q^2. If there would be only this twist-four contribution, we would have a 20 % correction at $Q^2 = 1\,\mathrm{GeV}^2$.

3.2.1 Weak Anti-Symmetrical Initial Distribution ($\lambda = 1$)

The picture changes quite substantially if we include the other twist-four contributions. We start with a discussion of the longitudinal part. Fig. 1.13a shows how this twist-four part is composed of the four contributions (the twist-four part of the two-gluon amplitude ΔF^2, ΔF^3, ΔF^R and ΔF^I) at $Q^2 = 1\,\mathrm{GeV}^2$. In order to simplify comparisons, we have normalized all twist-four contributions by the corresponding transverse leading-twist values. As can be seen, two of the four contributions (ΔF^3 and ΔF^I) enter with positive and the remaining two with negative signs, so that the sum (solid line) gives a very small contribution. Let us take a closer look at the cancellations, in particular those between ΔF^R and ΔF^I. As we argued before, after we have set $\varphi_{4\mathrm{A}} = \varphi_{4\mathrm{S}}$, the relative sign as well as the relative magnitude are fixed: in fig. 1.13a (at $Q^2 = 1\,\mathrm{GeV}^2$) ΔF^R and ΔF^I almost compensate each other. Due to (1.45) ΔF^I will become dominating at very small x_B. In our calculations this region is not yet reached.

The sign of each longitudinal twist-four contribution does not change when we go to higher Q^2-values (fig. 1.13b), but the total sum, now, becomes positive in the full x_B-interval. A look at the absolute values, which are not shown here, tells us that the twist-four contributions have actually increased compared to the case at $Q^2 = 1\,\mathrm{GeV}^2$ – the $1/Q^2$ suppression sets in rather late. But since leading-twist has increased as well, the relative contributions have decreased. Moreover, since ΔF^I is the twist-four contribution with the strongest evolution (cf. (1.45)) the total twist-four contribution is positive and reaches up to 1.5 % of leading-twist (fig. 1.13b). As to the other pair of contributions (ΔF^2 and ΔF^3), they enter also with opposite signs and, approximately, the same strength. But this clearly depends very much on our choice of the initial conditions. For example, a smaller choice of φ_3, the initial distribution of the three-gluon amplitude, which, as outlined in

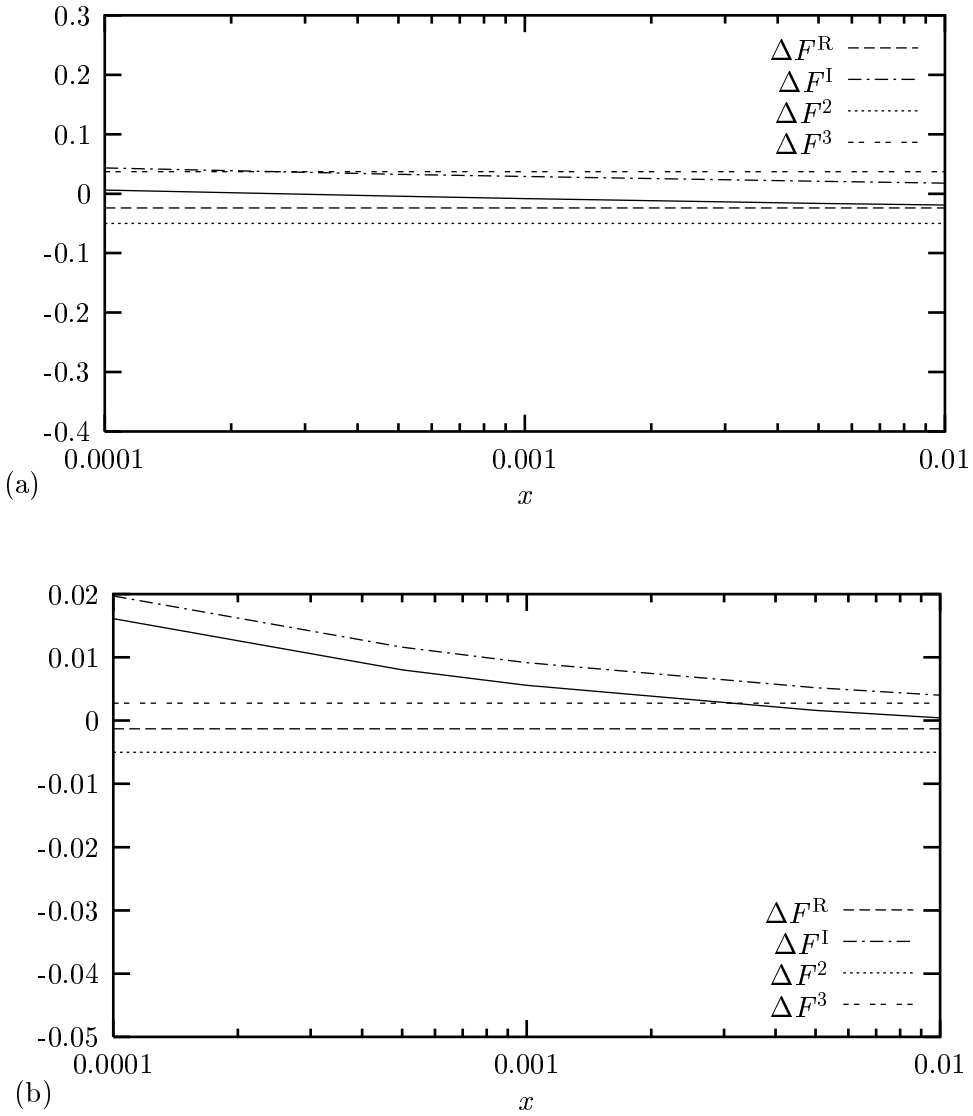

FIG. 1.13: Longitudinal part of the twist-four contributions (solid line) and the four terms they are composed of as a function of x_{B} at (a) $Q^2 = 1\,\mathrm{GeV}^2$ and (b) $Q^2 = 10\,\mathrm{GeV}^2$. Normalization with transverse leading-twist values.

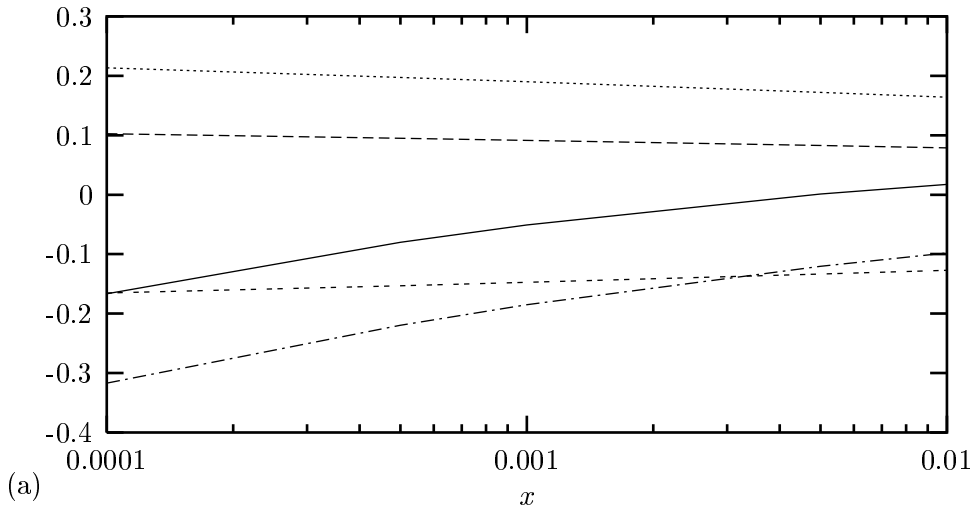

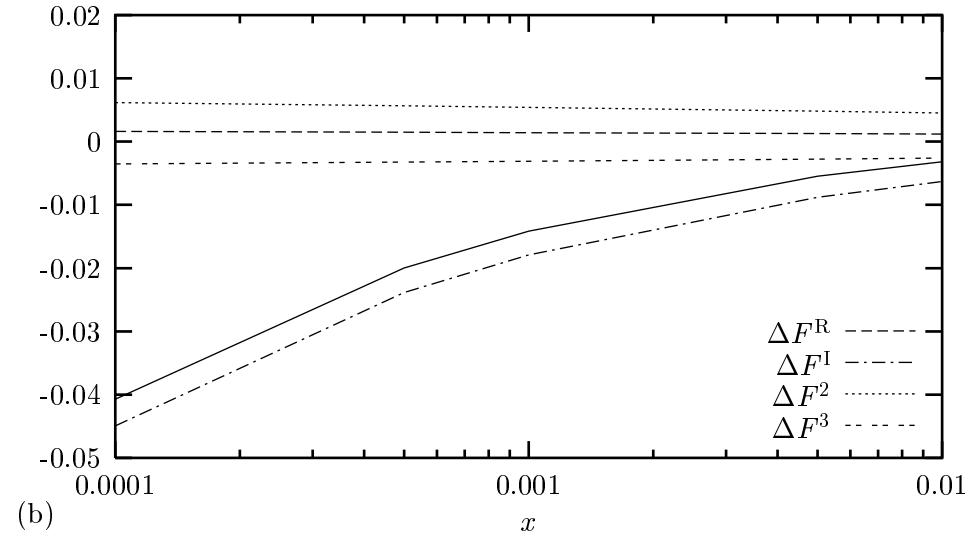

FIG. 1.14: Same as in fig. 1.13 but, now, for the transverse twist-four contributions.

section 3.1, cannot be related to any experimental measurement, results in significant smaller values of ΔF_ℓ.

Next, we take a look at the transverse contributions (fig. 1.14). As always in our discussion, this contribution represents the DLA, and as we discussed before, it is suppressed by one power of $\ln(Q^2/Q_0^2)$ in comparison to the longitudinal (twist-four) contribution. Nevertheless, our results for ΔF_t represent the leading term for the transverse structure function. We plot our results in the same way as we did for the longitudinal case, and the $x_{\rm B}$ distributions for the two values $Q^2 = 1\,{\rm GeV}^2$ and $Q^2 = 10\,{\rm GeV}^2$ are shown in figs. 1.14a and b, resp. First, one notices that for each separate (with leading-twist normalized) twist-four contribution the transition from $Q^2 = 1\,{\rm GeV}^2$ to $Q^2 = 10\,{\rm GeV}^2$ results in a much stronger decrease than in the longitudinal case. This is certainly due to the absence of the $\ln Q^2$-factor, which makes the Q^2-evolution weaker. Altogether, at $Q^2 = 1\,{\rm GeV}^2$ the transverse twist-four terms, which enter into the correction to F_t are of much larger size than in the longitudinal case and the sum of all four terms, now, gives a negative contribution.

In our scenario the transverse twist-four contribution (fig. 1.14a) gives a negative correction with an amount of up to fifteen per cent of leading-twist. The main reason for this is that, now, $\Delta F^{\rm I}$ is the dominating contribution. If we would go to even smaller values of $x_{\rm B}$ the dominance of $\Delta F^{\rm I}$ would become even more pronounced but one has to keep in mind that in this case even higher twist contributions (twist-six, etc.) will, very likely, become important, as well. If we, now, have a look at the curves for $Q^2 = 10\,{\rm GeV}^2$ (fig. 1.14b) we see that the transverse twist-four contribution enters with an amount of up to four per cent compared to leading-twist. Altogether, with these results we expect that, in the twist-four case, the transverse photon always dominates over the longitudinal one, even if we go beyond the DLA and take into account sub-leading terms of the longitudinal photon. Moreover, with these results, we can determine the contribution (within $\Delta F^{\rm R}$) due to the initial distribution with mixed symmetry. Using (1.42) and the numerical values in fig. 1.14 we deduce that (for the transverse photon at $Q^2 = 1\,{\rm GeV}^2$) this contribution has an amount of about 20 % of leading-twist. We believe that this is a rather low value, since $\lambda < 1$ seems to be rather unlikely.

Finally, figs. 1.15a and b show the Q^2-dependence of the longitudinal and transverse twist-four contributions at $x_{\rm B} = 10^{-3}$. As a general feature, we observe the interplay between the $1/Q^2$ suppression factor and the rise in the Q^2-evolution. In both figures, the change of the sign in the sum of all contributions is due to the increase of $\Delta F^{\rm I}$. Since we have performed our computations in DLA, the various twist-four contributions either vanish for $Q^2 \to Q_0^2$ or become a small constant. Moreover, $\Delta F^{\rm I}$ goes much faster to zero than all other contributions. As discussed before, this is a special problem of the DLA approximation of $\Delta F^{\rm I}$. If we would take into account also sub-leading terms, this decrease of $\Delta F^{\rm I}$ for low Q^2 would be less distinct. It is, therefore, likely that the dominance of $\Delta F^{\rm I}$ in the twist-four corrections to F_2 is, in fact, stronger than found in the DLA.

In summary, we have seen that in this scenario the longitudinal twist-four contribution remains small compared to transverse leading-twist in the whole kinematical regime under consideration, while the transverse twist-four contribution gives a negative correction with an amount of up to fifteen per cent of leading-twist at $Q^2 = 1\,{\rm GeV}^2$. The reason for the smallness of the longitudinal part is that the various twist-four contributions enter with different signs. In particular, $\Delta F^{\rm R}$ contributes with a rather large amount compared to $\Delta F^{\rm I}$. We can, therefore, justify in retrospect that we have also taken twist-four contributions of ΔF^2 and ΔF^3 into account. If we argue that

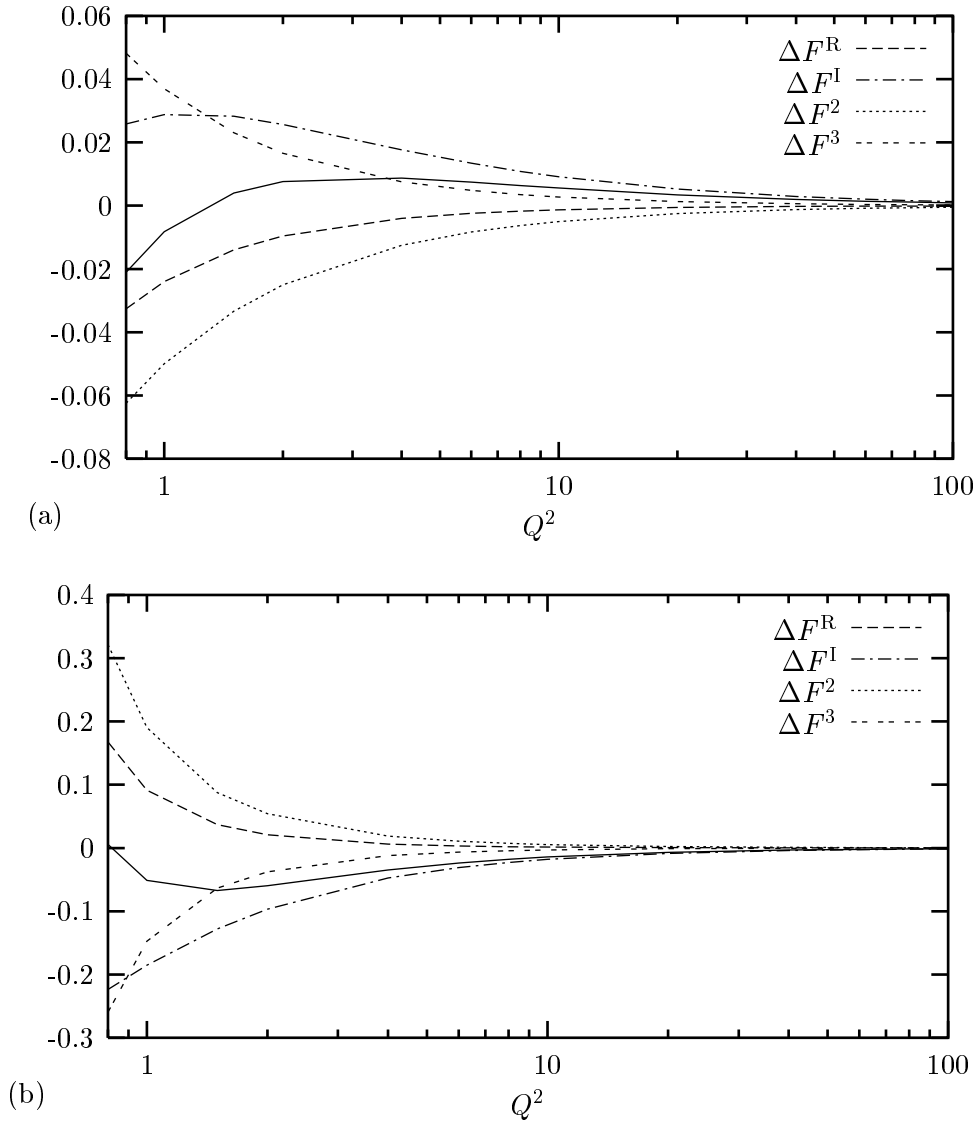

FIG. 1.15: Q^2-dependence of the (a) longitudinal and (b) transverse twist-four contributions (solid line) and the four terms they are composed of at $x_{\mathrm{B}} = 10^{-3}$. Normalization with transverse leading-twist values.

ΔF^3 should be related to the next-to-leading order corrections of the BFKL amplitude, ΔF^{R} would correspond even to NNLO corrections, while ΔF^{I} is the first term which contributes with a stronger power-behavior (cf. eqn. (1.45)).

3.2.2 Strong Anti-Symmetrical Initial Distribution ($\lambda = 1.5$)

The numerical results shown so far are all based on the assumption that $\varphi_{4\mathrm{S}} = \varphi_{4\mathrm{A}}$. As discussed above, this might be a rather small choice for $\varphi_{4\mathrm{A}}$. In this subsection we, therefore, present our results for setting $\varphi_{4\mathrm{A}} = 1.5\,\varphi_{4\mathrm{S}}$. Since φ^{diff} is a fixed quantity, our new scenario results in larger values for both $\varphi_{4\mathrm{S}}$ and $\varphi_{4\mathrm{A}}$, cf. (2.21). As we have outlined above, ΔF^{I} couples only to $\varphi_{4\mathrm{S}}$, while ΔF^{R} couples to both $\varphi_{4\mathrm{S}}$ and $\varphi_{4\mathrm{A}}$. If we, now, have a look at eqn. (1.42), we realize that an increase in $\varphi_{4\mathrm{A}}$ with a corresponding increase in $\varphi_{4\mathrm{S}}$ results in a decrease of ΔF^{R}, while ΔF^{I} increases substantially. This statement gets confirmed if we have a look at the numerical values, which are shown in fig. 1.16 for the longitudinal and transverse contributions at $Q^2 = 1\,\mathrm{GeV}^2$. Both, in the longitudinal and in the transverse case, ΔF^{I} is, now, the dominating twist-four contribution. This results in a total positive twist-four contribution of up to fifteen per cent in the longitudinal case, while we get a negative transverse twist-four contribution which reaches up to more than one hundred per cent of leading-twist. Certainly, if this scenario is realistic, the consideration of quantities up to twist-four is not sufficient. As far as twist-four reaches, say, fifty per cent of leading-twist, it will become necessary to consider also contributions with twist larger than four. Using, again, (1.42) we deduce that for this scenario (for the transverse photon at $Q^2 = 1\,\mathrm{GeV}^2$) the contribution (within ΔF^{R}) due to the initial distribution with mixed symmetry reaches about 130 % of leading-twist, i.e. $\lambda = 1.5$ corresponds to an upper limit of $\varphi_{4\mathrm{A}}$.

With the results presented so far, we believe the largest uncertainties are due to the freedom in choosing the ratio $\varphi_{4\mathrm{A}}/\varphi_{4\mathrm{S}}$. As we have demonstrated, a slightly stronger choice of $\varphi_{4\mathrm{A}}$ compared to $\varphi_{4\mathrm{S}}$ has a large effect on the relative contributions of ΔF^{I} and ΔF^{R}, and, therefore, on the total twist-four contributions. Other sources of possible unaccuracies are our choice of the size of ΔF^3, and the double logarithmic approximation. Moreover, as outlined above, it seems possible that ΔF^{I} at very low Q^2 would even be larger if one would take into account also sub-leading terms. This means we expect that ΔF^{I} dominates at small Q^2 and the longitudinal twist-four part gives a significant positive contribution. Therefore, it remains possible that there are still cancellations: in this case between longitudinal and transverse contributions. Our results, on the other hand, seem to confirm that the flattening of structure functions for decreasing Q^2 is due to an interplay of leading- and higher-twist, and that the transverse twist-four contributions are the dominating corrections. In any case, however, the opposite sign of ΔF^{R} weakens the influence of ΔF^{I}. One might also question our *three per cent choice* for determining the initial distribution of the four-gluon amplitude. It seems that a slightly stronger or weaker choice of $\varphi_4^{\mathrm{diff}}$ would crucially influence our results. This problem could probably be overcome if one takes also other measurable twist-four quantities into account.

3.3 Increasing Initial Parton Distributions

As an alternative, we have considered a scenario with an initial gluon distribution which increases at small x_{B}: $x_{\mathrm{B}} g(x_{\mathrm{B}}, Q_0^2) \sim (1/x_{\mathrm{B}})^{\omega_0}$. For the twist-four part of the two-gluon amplitude and

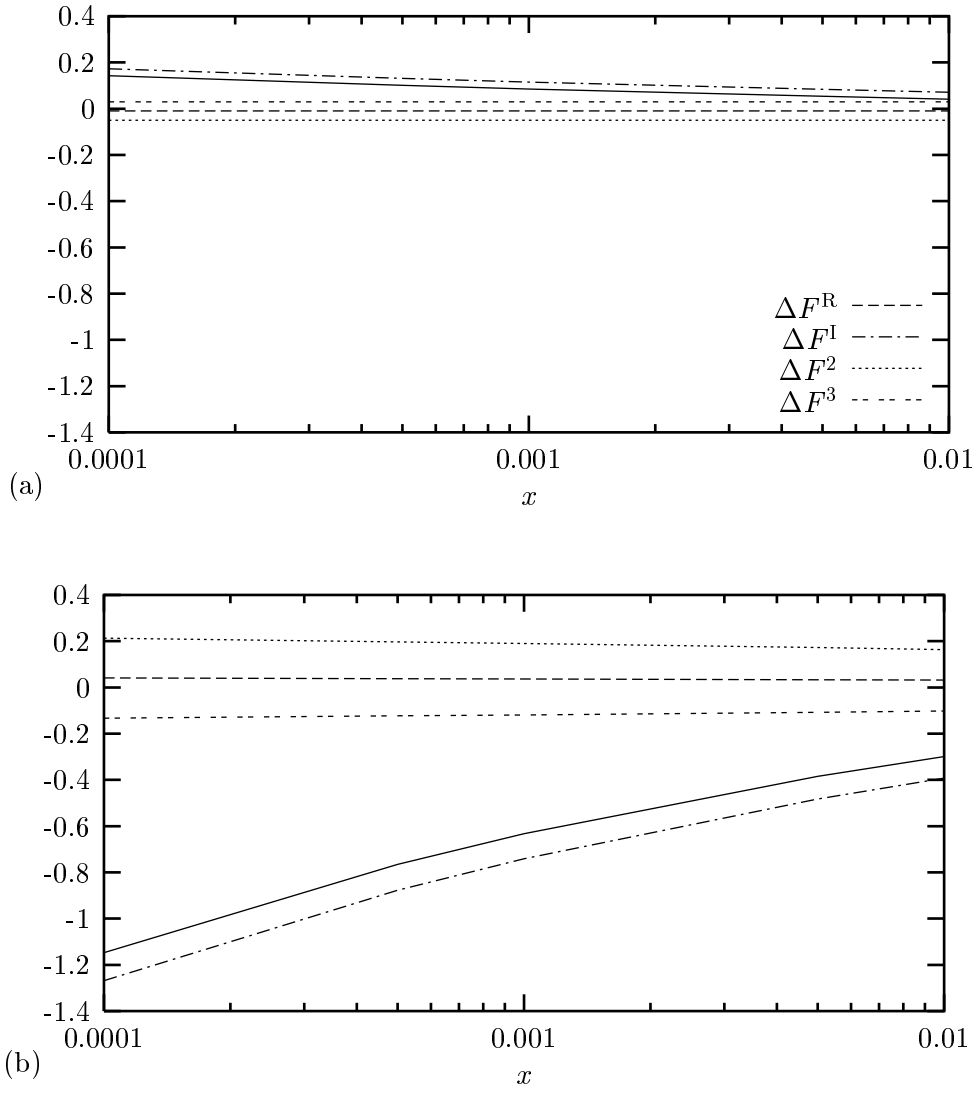

FIG. 1.16: (a) longitudinal and (b) transverse twist-four contributions as a function of x_{B} at $Q^2 = 1\,\mathrm{GeV}^2$. For this scenario, we have chosen constant initial distributions with a strong choice of the anti-symmetrical initial distribution that enters into ΔF^4. The two diagrams, shown here, correspond to diagrams 1.13a and 1.14a in the previous scenario. Normalization with transverse leading-twist values.

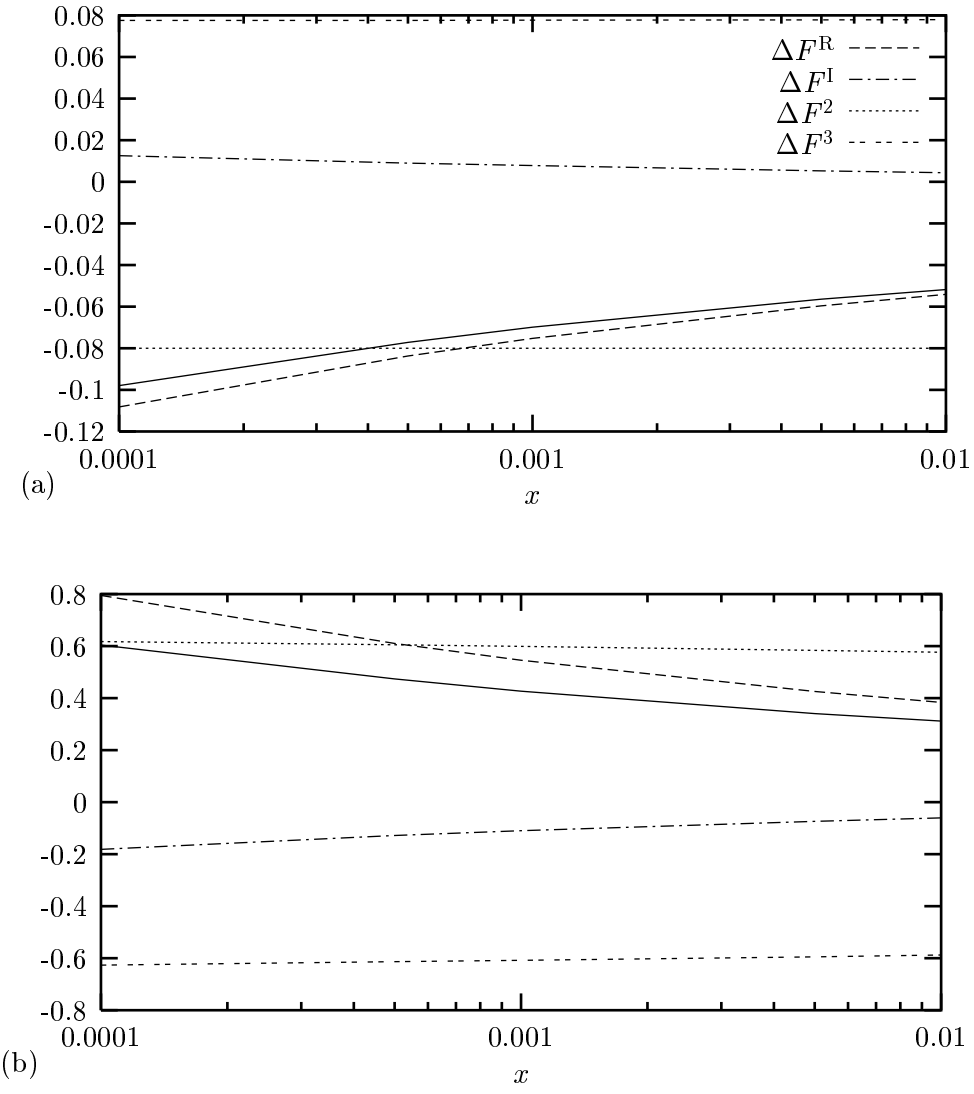

FIG. 1.17: (a) longitudinal and (b) transverse twist-four contributions as a function of x_{B} at $Q^2 = 1\,\mathrm{GeV}^2$. For this scenario, we have chosen increasing initial distributions ($\omega_0 = 0.2$) at $Q_0^2 = 0.8\,\mathrm{GeV}^2$. Normalization with transverse leading-twist values.

for the three-gluon contribution we assume the same power-behavior of the initial contribution as in the leading-twist case, and we have set $\omega_0 = 0.2$. As to the ΔF^4 contributions, the situation is slightly more subtle. Since the four-gluon operator in $\Delta F^{\rm I}$ is closely related to the double-exchange of DGLAP ladders, it seems reasonable to assume that the initial distribution of the four-gluon amplitude behaves like $(1/x_{\rm B})^{2\omega_0}$, i.e. the functions $\varphi_4(\omega)$ in (1.31) are assumed to have a pole at $2\omega_0$. For $\Delta F^{\rm R}$ there is an ambiguity: on the one hand, the lowest order diagram is the four-gluon exchange, i.e. the evolution should start with φ_4 which rises as $\sim (1/x_{\rm B})^{2\omega_0}$. On the other hand, if we consider $\Delta F^{\rm R}$ as a NNLO correction to the two-gluon operator (1.2), one might argue that we should have the same initial conditions as for the twist-four part of the two-gluon amplitude, i.e. $\sim (1/x_{\rm B})^{\omega_0}$. In our numerical analysis we have chosen the first option. Finally, since it seems unrealistic to assume an increasing initial distribution at $Q_0^2 = 0.5\,{\rm GeV}^2$, we, now, set $Q_0^2 = 0.8\,{\rm GeV}^2$. Moreover we return to our initial convention and set $\varphi_{4{\rm S}} = \varphi_{4{\rm A}}$.

Fig. 1.17 shows the twist-four contributions at $Q^2 = 1\,{\rm GeV}^2$ for the longitudinal and transverse photon. Compared to our first scenario, the twist-four corrections are, now, much larger. In order to understand this growth of the twist-four corrections we return to the first scenario (figs.1.13a and 1.14a). Due to the increasing initial distribution, all four contributions are larger than in the first case. In particular, ΔF^2 and ΔF^3 are magnified by a similar factor, and the approximate cancellation works in the same way as before. For $\Delta F^{\rm R}$ and $\Delta F^{\rm I}$, on the other hand, the approximate balance is distorted: at $Q^2 = 1\,{\rm GeV}^2$ we are close to the initial scale, and $\Delta F^{\rm I}$ is still small. Moreover, $\Delta F^{\rm R}$ has a stronger rise in $1/x_{\rm B}$ than ΔF^2 and ΔF^3 and, therefore, dominates. As result, the twist-four corrections at $Q^2 = 1\,{\rm GeV}^2$ are dominated by $\Delta F^{\rm R}$ which is, now, much less balanced than in the previous scenario. If we choose a weaker $x_{\rm B}$-dependence within $\Delta F^{\rm R}$ at the initial scale and set our initial scale, as before, to $Q_0^2 = 0.5\,{\rm GeV}^2$, it is possible to partly restore the balance and to obtain a somewhat smaller twist-four correction.

However, we got the feeling that the following trend is correct. Initial parton distributions which increase at small $x_{\rm B}$ tend to increase the twist-four corrections at low Q^2. Although it is, again, the transverse photon that leads to the main twist-four contributions, $\Delta F^{\rm R}$ is much stronger than $\Delta F^{\rm I}$. This results in positive transverse twist-four contributions in the kinematical regime under consideration.

If these tentative conclusions are correct, we have to interpret the scenario with rising initial conditions to be unstable. As discussed before, twist-four corrections could, in principle, provide an explanation for the observed change in the small $x_{\rm B}$ behavior at low Q^2. With decreasing Q^2, a negative transverse higher-twist could, because of its stronger rise at small $x_{\rm B}$, overcome the $1/Q^2$ suppression and interfere with the rising leading-twist contribution. In this scenario, we found that the opposite sign for transverse higher-twist is more likely, and leading- and higher-twist are adding up rather than compensating each other.

4 Conclusions

We have made a first attempt to estimate twist-four corrections to the gluon structure function at small $x_{\rm B}$ and low Q^2. For this, we have collected all presently available information on the gluonic twist-four evolution equations and defined the terms which need to be included. Up to now, DLA is the only approximation for which closed expressions exist. In addition, we have outlined how to use DIS diffractive dissociation (in particular the production of longitudinal vector mesons)

for a determination of the free parameters, i.e. the initial conditions. For this determination it was necessary to use the AGK cutting rules and the result, eqn. (2.21), deviates from the naive expectation.

One of the main results is the sign structure of the different twist-four corrections to the structure functions. We find, both in the transverse and in the longitudinal structure functions, terms with opposite sign which tend to compensate each other. Although our results are, at best, only "semiquantitative", we observe – in the scenarios with constant initial distributions – significant cancellations. The total longitudinal twist-four contribution is very small compared to transverse leading-twist. The total transverse twist-four contribution is negative and enters with a significant amount. In detail, we have considered three scenarios. For two of these scenarios we have chosen constant initial parton distributions at the input scale Q_0^2. In both cases the transverse photon led to the main twist-four contributions and in both cases they turned out to be negative. Altogether, the transverse twist-four contribution entered with an amount of fifteen to hundred per cent (relative to the transverse leading-twist contribution) at $x_{\mathrm{B}} = 10^{-4}$, $Q^2 = 1\,\mathrm{GeV}^2$. If these results are a sufficient approximation, a fit of DIS structure functions in the regime of these small x_{B}, low Q^2 values has to be considered as in-accurate. In addition, we have considered a scenario with increasing initial distributions, which turned out to be rather unstable. This instability might disappear if one could go beyond the DLA.

The results presented here are very tentative due to the limitations of the DLA. Before firm conclusions can be drawn, several improvements have to be made. Most desirably, one would like to use the full LO expressions for the gluonic twist-four coefficient functions and evolution kernels. They do not yet exist. In the second part of this thesis we present the first step in the direction of such a complete analysis. But it will take some time before one can start with numerical calculations. As can be seen already from eqn. (1.38), for a numerical analysis the amount of computer work necessary to calculate the Q^2 evolution of the gluon operators is substantially larger than in the leading-twist case. Finally, as discussed above, experimental information on specific final states is needed in order to restrict the arbitrariness in the choice of the initial conditions. In this first attempt we have used only the diffractive longitudinal vector meson production in order to obtain a first hint on the magnitude of twist-four. Besides this, other information on final states might be useful; a promising candidate might be a measurement of the two-particle correlation function as a function of rapidity [59].

Part 2

Twist-Four Gluon-Operators

The numerical results presented in the first part of this thesis give an insight into the possible contributions of gluonic higher-twist operators to inclusive DIS structure functions. For a more accurate analysis it is, first, necessary to analyse the contributions of these operators with the help of more formal methods. Such an analysis could be based on the OPE, i.e. one classifies all gluonic twist-four operators and computes the corresponding coefficient functions and anomalous dimensions.

On the other hand, one can make use of a rather intuitive approach. We have, therefore, extended EFP's [19] method in order to extract gluonic twist-four contributions to inclusive DIS structure functions in LO. The method provides a way to the factorization of gluonic coefficient functions and matrix elements of gluon-operators between proton states. When dealing with a certain class of operators the power behavior of the corresponding amplitudes is not immediately clear, since there can be trace terms which yield an even higher $1/Q^2$ suppression. Moreover, one has to handle target-mass corrections. For our analysis we are neglecting the target-mass corrections and we do not classify the twist-four contributions in the classical way, i.e. twist is equal to dimension minus spin, but as corrections which are suppressed by one power of $1/Q^2$. By this way we can use a dimensional analysis in order to show that our derivation is consistent in so far as diagrams with more than four t-channel gluons lead to contributions of, at least, twist-six. For this first analysis, we are not considering the evolution of the different contributions.

Since, thanks to the optical theorem, the inclusive structure functions are proportional to the imaginary part of the forward Compton scattering amplitude, our computations are based on the diagrams in fig. 2.1, i.e. we are considering amplitudes with two, three and four t-channel gluons. This is quite different from the analysis in the first part of this thesis. The diagrams in fig. 2.1 are *real* Feynman diagrams and we, first, consider them without any restrictions. The multi-gluon amplitude diagrams of part one correspond actually to diagrams with reggeized gluons in the t-channel with an application of multiple s-channel cuts. Only in DLA these reggeized gluons become *real* gluons.

We are working in the axial gauge, and we can show that, within this gauge, it is sufficient to restrict oneself to the diagrams in fig. 2.1 for a consistent treatment of twist-four gluon-operators. In this first analysis we do not compute explicit expressions for the upper quark-loop parts in the diagrams

of fig. 2.1. Instead we derive some general expressions for the corresponding amplitudes and make use only of the color-, Lorentz- and momentum structure of theses quark-loops. Moreover, in the four-gluon case we restrict ourselves to the color structure of the one-loop amplitude, while for two and three gluons the relations are of more general validity.

For our discussion it is useful to clarify the terms leading-order and next-to-leading order. The diagrams in figs. 2.1b and c are suppressed by factors g and g^2, resp., compared to the diagram in fig. 2.1a. Within our derivations we will factor these constants out and absorb them within the expressions for the lower blobs. By this way we can treat all three quark-loop expressions as if they were of the same order in α_s. On the other hand, computing these quark-loop expressions (we are not doing this here) one will get terms proportional to logarithms in Q^2 and terms which are just constants. In our conventions we call those terms which are proportional to logarithms, LO quark-coefficient functions convoluted by Altarelli-Parisi splitting functions, while we denote the constants as NLO gluon-coefficient functions. In this context it is also necessary to clarify the rôle of diagrams which involve three- and four-gluon vertices like those in fig. 2.2. For this first analysis we restrict ourselves to quark-loop diagrams which are one particle irreducible (1PI). The three- and four-gluon vertices in fig. 2.2 have, therefore, to be considered as if they were absorbed by the lower blobs and are part of the evolution. For a consistent analysis which takes also contributions of diagrams like those in fig. 2.2 into account one has to extend the Ward identities which will be derived in section 8.

5 EFP's Approach

Since the approach used here is based on methods developed by EFP [19], let us, first, summarize EFP's results. The computations in [19] can coarsely be divided into two steps. In the first step the authors consider the relevant diagrams – i.e. diagrams with four t-channel partons on the Born level – and perform the factorization of the coefficient functions and matrix elements of the relevant operators. In particular, these operators are (we are ignoring terms which involve a matrix γ_5):[1]

$$A^\rho(\lambda) = \frac{1}{4}\langle p|\mathrm{T}\left\{\bar\psi(0)\gamma^\rho\psi(\lambda n)\right\}|p\rangle\,, \tag{5.1}$$

$$B^{\rho\mu}(\eta,\lambda) = \frac{1}{4}\langle p|\mathrm{T}\left\{\bar\psi(0)\gamma^\rho \mathrm{D}^\mu(\eta n)\psi(\lambda n)\right\}|p\rangle\,, \tag{5.2}$$

$$C^{\rho\mu\nu}(\omega,\eta,\lambda) = \frac{1}{4}\langle p|\mathrm{T}\left\{\bar\psi(0)\gamma^\rho \mathrm{D}^\mu(\omega n)\mathrm{D}^\nu(\eta n)\psi(\lambda n)\right\}|p\rangle \tag{5.3}$$

and

$$Q(\omega,\eta,\lambda) = \frac{1}{16}g^2\langle p|\mathrm{T}\left\{\left[\bar\psi(0)\not{n}t^a\psi(\omega n)\right]\left[\bar\psi(\eta n)\not{n}t^a\psi(\lambda n)\right]\right\}|p\rangle\,. \tag{5.4}$$

Moreover, EFP outline how one can find the relation between the expressions which involve operators (5.1)-(5.4) and the OPE if one takes moments.

In the second step, EFP used equations of motion in order to write the contributions of the two-quark operators (5.1)-(5.3) with the help of quantities which are linearly independent. For this

[1] Cf. eqns. (2.45)-(2.50) and (5.23)-(5.24) in [19]. The calculations are performed in the axial gauge with the gauge vector n_μ. Since we are interested in the general structure of the results, we postpone the definition of various quantities until later sections.

they studied the longitudinal (which corresponds to the canonical basis in [17]) and transverse basis separately. While the expressions within the longitudinal basis turned out to be rather complicated, the twist-four contributions of the two-quark operator to the transverse and longitudinal structure functions $F_{\rm T}$ and $F_{\rm L}$ in the transverse basis can be expressed with the help of the quantities

$$\Lambda^2 \boldsymbol{T}_1(x) = \frac{1}{4}\int \frac{\mathrm{d}\lambda}{2\pi} \mathrm{e}^{\mathrm{i}\lambda x} \langle p|\mathrm{T}\left\{\bar\psi(0)\gamma_\mu \not{n}\gamma_\nu d^{\mu\mu'}\mathrm{D}_{\mu'}(0) d^{\nu\nu'}\mathrm{D}_{\nu'}(\lambda n)\psi(\lambda n)\right\}|p\rangle \tag{5.5}$$

and

$$\Lambda^2 \boldsymbol{T}_2(x_2,x_1) = \frac{1}{4}\int \frac{\mathrm{d}\lambda}{2\pi}\frac{\mathrm{d}\eta}{2\pi} \mathrm{e}^{\mathrm{i}\eta(x_2-x_1)}\mathrm{e}^{\mathrm{i}\lambda x_1} \langle p|\mathrm{T}\left\{\bar\psi(0)\gamma_\mu \not{n}\gamma_\nu d^{\nu\nu'}\mathrm{D}_{\nu'}(\eta n) d^{\mu\mu'}\mathrm{D}_{\mu'}(\eta n)\psi(\lambda n)\right\}|p\rangle\,, \tag{5.6}$$

such that the twist-four contributions to $F_{\rm T}$ and $F_{\rm L}$ are (we are neglecting the proton mass)

$$F_{\rm T}^{\tau=4} = \frac{\Lambda^2}{Q^2}\left[4\boldsymbol{T}_1(x_{\rm B}) - x_{\rm B}\int \mathrm{d}x_1\mathrm{d}x_2 \frac{\delta(x_{\rm B}-x_2)-\delta(x_{\rm B}-x_1)}{x_2-x_1}\boldsymbol{T}_2(x_2,x_1)\right]\,, \tag{5.7}$$

$$F_{\rm L}^{\tau=4} = 4\frac{\Lambda^2}{Q^2}\boldsymbol{T}_1(x_{\rm B}) \tag{5.8}$$

plus terms involving the four-quark operator (5.4). Compared to EFP, we have performed only the first step. For the second step one has to compute expressions for the quark-loops in fig. 2.1, first.

6 Conventions

Before we go into details, let us specify our conventions. The QCD Lagrangian is given by

$$\mathscr{L}_{\rm QCD} = -\frac{1}{4}F^a_{\mu\nu}(x)F^{a\mu\nu}(x) + \sum_{j=\text{flavors}} \bar q_j(x)\left[\mathrm{i}\gamma_\mu \mathrm{D}^\mu(x) - m_j\right] q_j(x) \tag{6.1}$$

and the covariant derivative applied to a gluon-operator has the form

$$\mathrm{D}^{ab}_\mu F^b_{\rho\sigma} = \left(\delta^{ab}\partial_\mu - g f^{abc}A^c_\mu\right)F^b_{\rho\sigma}\,. \tag{6.2}$$

For our computations it is convenient to use the axial gauge, i.e. we are introducing a light-like vector n^μ such that

$$n_\mu A^\mu_a = 0\,. \tag{6.3}$$

We are using the same vector n within the decomposition of momentum vectors into Sudakov variables:

$$k_i^\mu = x_i p^\mu + \alpha_i n^\mu + k^\mu_{i,\rm T}\,, \qquad p^2 = n^2 = p\cdot k_{i,\rm T} = n\cdot k_{i,\rm T} = 0\,, \qquad p\cdot n = 1\,. \tag{6.4}$$

Here p represents the momentum of the target hadron, which we assume to be massless throughout this thesis. For the color factors occurring in different quantities, we have chosen a normalization such that the Gell-Mann matrices t^a satisfy

$$\mathrm{tr}\, t^a t^b = \frac{1}{2}\delta^{ab} \tag{6.5}$$

and we set the number of colors $N_{\rm c} = 3$.

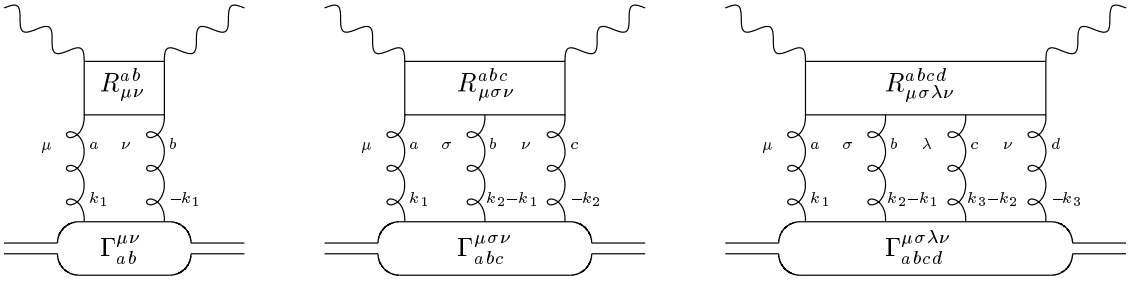

(a) (b) (c)

FIG. 2.1: For a systematic analysis of the twist-four contributions of gluonic operators it is sufficient to consider the contributions of the three diagrams shown here. The quark-loops symbolize the coupling of the gluons in all possible ways and the propagators of the gluon-lines belong to the lower blobs. We take all gluon momenta to be outgoing of the proton.

7 Factorization

As outlined in the introduction it is our aim to specify twist-four gluon operators, write them in covariant form and perform the factorization of coefficient functions and matrix elements of these operators between proton states. We will argue that it is sufficient to consider the diagrams in fig. 2.1. Here the upper parts represent the quark-loops with two, three and four t-channel gluons. They are amputated in the gluon lines and we denote them by $R^{ab}_{\mu\nu}(k_1)$, $R^{abc}_{\mu\sigma\nu}(k_1,k_2)$ and $R^{abcd}_{\mu\sigma\lambda\nu}(k_1,k_2,k_3)$, resp. These quark-loops will contribute to both: the next-to-leading order twist-four gluon-coefficient functions and the leading-order twist-four quark-coefficient functions convoluted by Altarelli-Parisi splitting functions. We can derive some general results for the twist-four contributions of the diagrams in fig. 2.1 without knowing explicit expressions for these quark-loops. All we need are some general properties of the functions R concerning the Lorentz-, color- and momentum-structure.

The lower parts in fig. 2.1 are denoted by $\Gamma^{\mu\nu}_{ab}(k_1)$, $\Gamma^{\mu\sigma\nu}_{abc}(k_1,k_2)$ and $\Gamma^{\mu\sigma\lambda\nu}_{abcd}(k_1,k_2,k_3)$, resp., and with these conventions the contributions of the diagrams in fig. 2.1 are given by

$$\tilde{H}_1(x_{\rm B},Q^2) = \int\frac{{\rm d}^4k_1}{(2\pi)^4}R^{ab}_{\mu\nu}(k_1)\Gamma^{\mu\nu}_{ab}(k_1)\,, \tag{7.1}$$

$$\tilde{H}_2(x_{\rm B},Q^2) = \int\frac{{\rm d}^4k_1}{(2\pi)^4}\frac{{\rm d}^4k_2}{(2\pi)^4}R^{abc}_{\mu\sigma\nu}(k_1,k_2)\Gamma^{\mu\sigma\nu}_{abc}(k_1,k_2)\,, \tag{7.2}$$

$$\tilde{H}_3(x_{\rm B},Q^2) = \int\frac{{\rm d}^4k_1}{(2\pi)^4}\frac{{\rm d}^4k_2}{(2\pi)^4}\frac{{\rm d}^4k_3}{(2\pi)^4}R^{abcd}_{\mu\sigma\lambda\nu}(k_1,k_2,k_3)\Gamma^{\mu\sigma\lambda\nu}_{abcd}(k_1,k_2,k_3)\,, \tag{7.3}$$

where we have dropped the photon indices. As we will show in section 10 expressions (7.1)-(7.3) contain leading-twist and twist-four contributions of gluonic operators as well as some parts with twist larger than four. The twist-four parts can be projected out if one performs a dimensional analysis. Here, the convenience of the axial gauge becomes most explicit.

The lower blobs in fig. 2.1 can be written as matrix elements of gluon-operators between proton

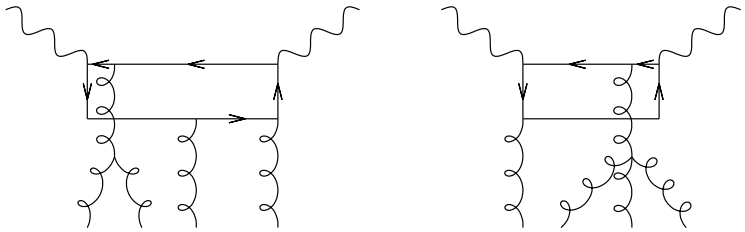

FIG. 2.2: Sample diagrams which contain three- and four-gluon vertices.

states:

$$\Gamma^{\mu\nu}_{ab}(k_1) = \int \mathrm{d}^4 z_1 \, \mathrm{e}^{\mathrm{i}k_1\cdot z_1} \langle p|\mathrm{T}\{A^\nu_b(0)A^\mu_a(z_1)\}|p\rangle \,, \tag{7.4}$$

$$\Gamma^{\mu\sigma\nu}_{abc}(k_1,k_2) = \int \mathrm{d}^4 z_1 \, \mathrm{d}^4 z_2 \, \mathrm{e}^{\mathrm{i}k_1\cdot z_1} \mathrm{e}^{\mathrm{i}(k_2-k_1)\cdot z_2} \langle p|\mathrm{T}\{A^\nu_c(0)A^\sigma_b(z_2)A^\mu_a(z_1)\}|p\rangle \,, \tag{7.5}$$

$$\Gamma^{\mu\sigma\lambda\nu}_{abcd}(k_1,k_2,k_3) = \int \mathrm{d}^4 z_1 \, \mathrm{d}^4 z_2 \, \mathrm{d}^4 z_3 \, \mathrm{e}^{\mathrm{i}k_1\cdot z_1} \mathrm{e}^{\mathrm{i}(k_2-k_1)\cdot z_2} \mathrm{e}^{\mathrm{i}(k_3-k_2)\cdot z_3} \langle p|\mathrm{T}\{A^\nu_d(0)A^\lambda_c(z_3)A^\sigma_b(z_2)A^\mu_a(z_1)\}|p\rangle \,. \tag{7.6}$$

Here T denotes the time ordered product and expressions (7.4)-(7.6) contain the propagators of the gluon lines in fig. 2.1.

In order to perform the factorization procedure with expressions (7.1)-(7.3) it is, now, most convenient to expand the expressions for the quark-loops about the longitudinal components of the gluon-momenta (cf. (6.4)):

$$R^{ab}_{\mu\nu}(k_1) = R^{ab}_{\mu\nu}(x_1 p) + \frac{\partial R^{ab}_{\mu\nu}(x_1 p)}{\partial k_1^\sigma}(k_1 - x_1 p)^\sigma + \frac{1}{2}\frac{\partial^2 R^{ab}_{\mu\nu}(x_1 p)}{\partial k_1^\sigma \partial k_1^\lambda}(k_1 - x_1 p)^\sigma (k_1 - x_1 p)^\lambda + \cdots \,, \tag{7.7}$$

$$R^{abc}_{\mu\sigma\nu}(k_1,k_2) = R^{abc}_{\mu\sigma\nu}(x_1 p, x_2 p) + \sum_{i=1}^{2} \frac{\partial R^{abc}_{\mu\sigma\nu}(x_1 p, x_2 p)}{\partial k_i^\lambda}(k_i - x_i p)^\lambda + \cdots \,, \tag{7.8}$$

$$R^{abcd}_{\mu\sigma\lambda\nu}(k_1,k_2,k_3) = R^{abcd}_{\mu\sigma\lambda\nu}(x_1 p, x_2 p, x_3 p) + \cdots \,. \tag{7.9}$$

We will justify in section 10 that we can neglect further terms in these series if we are interested only in terms up to twist-four.

Before we give the results of the factorization procedure, we compute some Ward identities for the derivatives in eqns. (7.7) and (7.8), show how the expressions for the lower blobs Γ can be expressed with the help of gluonic $F^{\mu\nu}_a$-operators and perform a dimensional analysis of the expressions (7.1)-(7.3) in the next three sections.

8 Ward Identities

In order to find relations for the derivatives of the quark-loops in eqns. (7.7) and (7.8) we will make use of Ward identities. Although these identities can be derived diagrammatically on the one

loop level, this is a rather tedious task. We, therefore, make a digression into the path-integral formulation of QCD and derive these Ward identities in the most general way. For this, we, first, derive a relation for the generating functional of perturbatively calculated vertex functions V in the next subsection. This relation, viz. eqn. (8.9), will then be used to derive the desired equations in the following two subsections.

The Ward identities which will be derived in this section are only valid for 1PI vertex functions. They can, therefore, not be applied naively to expressions for quark-loops which involve three- and four-gluon vertices like those in fig. 2.2.

8.1 Generating Functional

The generating functional for Green's functions in the axial gauge can be written as [60, 61]

$$W[J^a_\mu, K^a] = \mathcal{N} \int \mathcal{D}A^a_\mu \, \mathcal{D}\lambda^a \, \exp\left\{ \mathrm{i} \int \mathrm{d}^4x \left[\mathcal{L}_{\mathrm{QCD}} - \lambda^a \, n \cdot A^a + A^a_\mu J^\mu_a + \lambda^a K^a \right] \right\} . \tag{8.1}$$

Here $\mathcal{N}$ is some normalization factor, J^a_μ and K^a are sources, the term $\lambda^a \, n \cdot A^a$ has been introduced in order to define the axial gauge and the Lagrangian $\mathcal{L}_{\mathrm{QCD}}$ is given by eqn. (6.1). The generating functional must be invariant under gauge transformations, which for infinitesimal $\omega(x)$ can be written as

$$A^a_\mu \to A^a_\mu + \mathrm{D}^{ab}_\mu(A)\omega^b = A^a_\mu + \partial_\mu \omega^a - g f^{abc} A^c_\mu \omega^b \, . \tag{8.2}$$

Using standard arguments, i.e. inserting (8.2) into (8.1), substituting fields that occur as factors within the integral by functional derivatives and making use of the arbitrariness of ω, one gets

$$0 = \mathrm{D}^{ab}_\mu(J) \left(n^\mu \frac{\delta}{\mathrm{i}\delta K^b(x)} - J^\mu_b(x) \right) W[J^a_\mu, K^a] \, , \tag{8.3}$$

where the covariant derivative is given by

$$\mathrm{D}^{ab}_\mu(J) = \delta^{ab}\partial_\mu - g f^{abc} \frac{\delta}{\mathrm{i}\delta J^\mu_c} \, . \tag{8.4}$$

For our analysis we need the generating functional V for perturbatively calculated vertex functions. This can be obtained with the help of the following procedure. First, define the functional $\tilde{V}$ via Legendre transformation

$$\tilde{V}[A^a_\mu, \Lambda^a] = Z[J^a_\mu, K^a] - \int \mathrm{d}^4x \, \left[A^a_\mu J^\mu_a + K_a \Lambda^a \right] \, , \tag{8.5}$$

where Z is defined as

$$Z[J^a_\mu, K^a] = -\mathrm{i} \ln W[J^a_\mu, K^a] \, . \tag{8.6}$$

With these definitions we get from (8.3)

$$\mathrm{D}^{ab}_\mu(A) \left(n^\mu \Lambda_b + \frac{\delta \tilde{V}}{\delta A^\mu_b} \right) = 0 \, . \tag{8.7}$$

Now, V can be obtained via subtraction [60,61]:

$$V[A^a_\mu,\Lambda^a] = \tilde{V}[A^a_\mu,\Lambda^a] + \int \mathrm{d}^4x\, \Lambda_a\, n\cdot A^a \tag{8.8}$$

and the Ward identity (8.7) finally becomes

$$\mathrm{D}^{ab}_\mu(A)\frac{\delta V}{\delta A^b_\mu} = 0\,. \tag{8.9}$$

8.2 Relations Between Two- and Three-Gluon Quark-Loops

We are, now, deriving an equation which relates the derivative of the two-gluon quark-loop $R^{ab}_{\mu\nu}$ with the three-gluon quark-loop $R^{abc}_{\mu\sigma\nu}$. The relation between the perturbatively computed quark-loops and the generating functional V is as follows (see fig. 2.1 for our conventions on the gluon momenta):

$$\int \mathrm{d}^4x_1\,\mathrm{d}^4x_2\,\mathrm{e}^{\mathrm{i}k_1\cdot x_1}\mathrm{e}^{\mathrm{i}k_2\cdot x_2}\frac{\delta^2 V[0]}{\delta A^\mu_a(x_1)\delta A^\nu_b(x_2)} = (2\pi)^4\delta(k_1+k_2)R^{ab}_{\mu\nu}(k_1)\,, \tag{8.10}$$

$$\int \mathrm{d}^4x\,\mathrm{d}^4x_1\,\mathrm{d}^4x_2\,\mathrm{e}^{\mathrm{i}k_1\cdot x_1}\mathrm{e}^{\mathrm{i}k\cdot x}\mathrm{e}^{\mathrm{i}k_2\cdot x_2}\frac{\delta^3 V[0]}{\delta A^\mu_a(x_1)\delta A^\sigma_b(x)\delta A^\nu_c(x_2)} = (2\pi)^4\delta(k+k_1+k_2)R^{abc}_{\mu\sigma\nu}(k_1,k+k_1)\,, \tag{8.11}$$

$$\int \mathrm{d}^4x\,\mathrm{d}^4x_1\,\mathrm{d}^4x_2\,\mathrm{d}^4x_3\,\mathrm{e}^{\mathrm{i}k_1\cdot x_1}\mathrm{e}^{\mathrm{i}(k_2-k_1)\cdot x}\mathrm{e}^{\mathrm{i}(k_3-k_2)\cdot x_2}\mathrm{e}^{\mathrm{i}k_4\cdot x_3}\frac{\delta^4 V[0]}{\delta A^\mu_a(x_1)\delta A^\sigma_b(x)\delta A^\lambda_c(x_2)\delta A^\nu_d(x_3)} = \\ = (2\pi)^4\delta(k_3+k_4)R^{abcd}_{\mu\sigma\lambda\nu}(k_1,k_2,k_3)\,. \tag{8.12}$$

Relabelling Lorentz- and color indices in eqn. (8.9) and differentiating the equation by $A^\mu_a(x_1)$ and $A^\nu_c(x_2)$ one gets

$$\partial^\sigma\frac{\delta^3 V[0]}{\delta A^\mu_a(x_1)\delta A^\sigma_b(x)\delta A^\nu_c(x_2)} = g\left\{f^{abb'}\delta(x-x_1)\frac{\delta^2 V[0]}{\delta A^\mu_{b'}(x)\delta A^\nu_c(x_2)} - f^{bcb'}\delta(x-x_2)\frac{\delta^2 V[0]}{\delta A^\mu_a(x_1)\delta A^\nu_{b'}(x)}\right\}. \tag{8.13}$$

Now, multiplying eqn. (8.13) by the same exponentials which enter into (8.11), integrating over x, x_1 and x_2 and keeping eqns. (8.10) and (8.11) in mind one ends up with

$$-\mathrm{i}\,k^\sigma R^{abc}_{\mu\sigma\nu}(k_1,k+k_1) = g\left\{f^{abb'}R^{b'c}_{\mu\nu}(k+k_1) - f^{bcb'}R^{ab'}_{\mu\nu}(k_1)\right\}. \tag{8.14}$$

The two-gluon quark-loop must be in the color singlet. We can, therefore, define

$$R^{ab}_{\mu\nu}(k) \equiv \delta^{ab}R_{\mu\nu}(k)\,. \tag{8.15}$$

With this definition we can take the limit $k\to 0$ in eqn. (8.14) and finally get the desired result:

$$\mathrm{i}\,g f^{abc}\frac{\partial R_{\mu\nu}(k_1)}{\partial k_1^\sigma} = R^{abc}_{\mu\sigma\nu}(k_1,k_1)\,. \tag{8.16}$$

8.3 Relations Between Three- and Four-Gluon Quark-Loops

Relations between derivatives of the three-gluon quark-loop $R^{abc}_{\mu\sigma\nu}$ and the four-gluon quark-loop $R^{abcd}_{\mu\sigma\lambda\nu}$ can be obtained in a completely analogous way. If we differentiate (8.9) three times, multiply the resulting equation by adequate exponentials and perform the x_i-integrations, we get, similar to (8.14):

$$-\mathrm{i}\,k^\sigma R^{abcd}_{\mu\sigma\lambda\nu}(k_1,k_1+k,k_2+k) = g\Big\{ f^{abb'} R^{b'cd}_{\mu\lambda\nu}(k_1+k,k_2+k) - f^{bcc'} R^{ac'd}_{\mu\lambda\nu}(k_1,k_2+k) - f^{bdb'} R^{acb'}_{\mu\lambda\nu}(k_1,k_2)\Big\}\,. \tag{8.17}$$

Before we can take the limit $k \to 0$ we have to explore the color structure of $R^{abc}_{\mu\sigma\nu}$. We, first, restrict ourselves to the one-loop case. Since $R^{abc}_{\mu\sigma\nu}$ is the sum of all diagrams with three external gluons, we can, in the one-loop case, always group two diagrams together. For each diagram there is another diagram which gives the same momentum dependence (up to the sign) but different color structure (see fig. 2.3 for illustration). Since the gluon-system must have even C-parity this color structure is always of the form[2]

$$\mathrm{tr}(t^a t^b t^c) - \mathrm{tr}(t^c t^b t^a) = \mathrm{i}\,\frac{1}{2}\,f^{abc} \tag{8.18}$$

for each pair of diagrams. We, therefore, define

$$R^{abc}_{\mu\lambda\nu}(k_1,k_2) \equiv g f^{abc} R_{\mu\lambda\nu}(k_1,k_2)\,, \tag{8.19}$$

where the factor g has been factored out for convenience. The amplitude has to be in the color singlet. We, therefore, expect that eqn. (8.19) also holds beyond the one-loop level. If we, now, insert (8.19) into (8.17) and make use of the Jacobi identity,

$$f^{abc'} f^{c'cd} - f^{acc'} f^{c'bd} + f^{adc'} f^{c'bc} = 0\,, \tag{8.20}$$

we can take the limit $k \to 0$ and obtain

$$\mathrm{i}\,g^2 \left\{ f^{abc'} f^{c'cd} \frac{\partial R_{\mu\lambda\nu}(k_1,k_2)}{\partial k_1^\sigma} + f^{acc'} f^{c'bd} \frac{\partial R_{\mu\lambda\nu}(k_1,k_2)}{\partial k_2^\sigma} \right\} = R^{abcd}_{\mu\sigma\lambda\nu}(k_1,k_1,k_2)\,. \tag{8.21}$$

For our computations we need relations for $R^{abc}_{\mu\lambda\nu}$ derived by k_1 or k_2. Since eqn. (8.21) contains these derivatives only as a sum, we have to project with adequate color tensors. Now, we realize that there is more than one color tensor which projects out the desired quantity in eqn. (8.21). E.g. both

$$P_1^{abcd} \equiv \delta^{ac}\delta^{bd} \tag{8.22}$$

and

$$P_2^{abcd} \equiv d^{acc'} d^{c'bd} \tag{8.23}$$

[2] In the case of odd C-parity the coupling of the gluon to quarks and anti-quarks involves a sign change. In this case, one, therefore, gets a factor $\mathrm{tr}(t^a t^b t^c) + \mathrm{tr}(t^c t^b t^a) = \frac{1}{2} d^{abc}$.

project out $\partial R_{\mu\lambda\nu}/\partial k_1^\sigma$. This fact will lead to some important restrictions for the four-gluon quark-loop $R^{abcd}_{\mu\sigma\lambda\nu}$ (eqn. (8.28) below).

For the remainder of this section we will restrict ourselves to the one-loop case. In this case we can use the same arguments that led to the definition (8.19). For four gluons we, now, define the quantity (cf. (8.18))

$$\begin{aligned} d^{abcd} &\equiv \mathrm{tr}\left[t^a t^b t^c t^d\right] + \mathrm{tr}\left[t^d t^c t^b t^a\right] = \\ &= -\frac{1}{4} f^{abc'} f^{c'cd} + \frac{1}{4} d^{abc'} d^{c'cd} + \frac{1}{6}\delta^{ab}\delta^{cd}\,. \end{aligned} \tag{8.24}$$

We realize that there are three linearly independent tensors d, which can be obtained by permutation of color indices in eqn. (8.24) and, therefore, write the color structure of $R^{abcd}_{\mu\sigma\lambda\nu}$ as

$$R^{abcd}_{\mu\sigma\lambda\nu}(k_1,k_2,k_3) \equiv g^2\left\{d^{abcd}R^1_{\mu\sigma\lambda\nu}(k_1,k_2,k_3) + d^{abdc}R^2_{\mu\sigma\lambda\nu}(k_1,k_2,k_3) + d^{acbd}R^3_{\mu\sigma\lambda\nu}(k_1,k_2,k_3)\right\}. \tag{8.25}$$

Each diagram that contributes to $R^{abcd}_{\mu\sigma\lambda\nu}$ on the one-loop level enters into one of the functions $R^i_{\mu\sigma\lambda\nu}$.

If we, now, insert (8.25) into (8.21) and project with the tensors P_1^{abcd} and P_2^{abcd} we end up with two equations, viz.

$$24\mathrm{i}\,\frac{\partial R_{\mu\lambda\nu}(k_1,k_2)}{\partial k_1^\sigma} = -\frac{4}{3}R^1_{\mu\sigma\lambda\nu}(k_1,k_1,k_2) + \frac{32}{3}R^2_{\mu\sigma\lambda\nu}(k_1,k_1,k_2) + \frac{32}{3}R^3_{\mu\sigma\lambda\nu}(k_1,k_1,k_2)\,, \tag{8.26}$$

$$20\mathrm{i}\,\frac{\partial R_{\mu\lambda\nu}(k_1,k_2)}{\partial k_1^\sigma} = -\frac{40}{9}R^1_{\mu\sigma\lambda\nu}(k_1,k_1,k_2) + \frac{50}{9}R^2_{\mu\sigma\lambda\nu}(k_1,k_1,k_2) + \frac{50}{9}R^3_{\mu\sigma\lambda\nu}(k_1,k_1,k_2)\,. \tag{8.27}$$

These two equations can simultaneously be fulfilled only if the following equation holds:[3]

$$R^1_{\mu\sigma\lambda\nu}(k_1,k_1,k_2) + R^2_{\mu\sigma\lambda\nu}(k_1,k_1,k_2) + R^3_{\mu\sigma\lambda\nu}(k_1,k_1,k_2) = 0\,. \tag{8.28}$$

Notice that this equation holds only true if one of the gluon-momenta vanishes (see fig. 2.1 for our conventions on the gluon-momenta). Inserting the latter equation into eqn. (8.26) we end up with the desired results:

$$\mathrm{i}\,\frac{\partial R^{abc}_{\mu\lambda\nu}(k_1,k_2)}{\partial k_1^\sigma} = -\frac{1}{2}gf^{abc}R^1_{\mu\sigma\lambda\nu}(k_1,k_1,k_2) = -\frac{1}{2}gf^{abc}R^3_{\mu\lambda\sigma\nu}(k_1,k_2,k_2) \tag{8.29}$$

and

$$\mathrm{i}\,\frac{\partial R^{abc}_{\mu\sigma\nu}(k_1,k_2)}{\partial k_2^\lambda} = -\frac{1}{2}gf^{abc}R^1_{\mu\sigma\lambda\nu}(k_1,k_2,k_2) = -\frac{1}{2}gf^{abc}R^3_{\mu\lambda\sigma\nu}(k_1,k_1,k_2)\,. \tag{8.30}$$

Here we have also projected out the term which derives $R^{abc}_{\mu\sigma\nu}$ by k_2 in eqn. (8.21) and we have used the fact that we have some freedom in relating the generating functional V and the four-gluon quark-loop in eqn. (8.12). $R^{abcd}_{\mu\sigma\lambda\nu}$ must be invariant under simultaneous exchange of momentum

[3] There are more tensors than those in eqns. (8.22) and (8.23) which project out $\partial R_{\mu\lambda\nu}/\partial k_1^\sigma$ in (8.21). Using these gives a consistent picture but no new results.

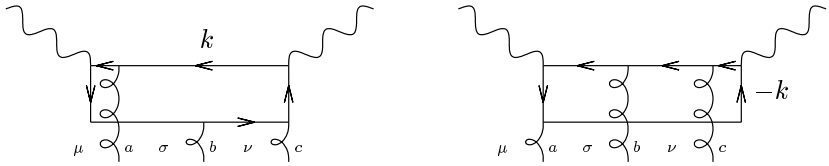

FIG. 2.3: Two sample diagrams which enter into $R^{abc}_{\mu\sigma\nu}$ at leading order in α_s. With an adequate choice of the loop integration variable the traces over Dirac-matrices give the same (up to the sign) momentum dependence for both diagrams. The first diagram contributes with a color factor $\mathrm{tr}\, t^a t^b t^c$ while the second one contributes with a color factor $\mathrm{tr}\, t^c t^b t^a$.

variables, Lorentz- and color indices. This leads to the possibility to express the derivatives of $R^{abc}_{\mu\lambda\nu}$ in eqns. (8.29) and (8.30) either by $R^1_{\mu\sigma\lambda\nu}$ or by $R^3_{\mu\lambda\sigma\nu}$. We are discussing this symmetry in more detail in section 11.

Finally, differentiating eqn. (8.16) by k_1^λ and using (8.29) and (8.30) we get

$$\begin{aligned}\frac{\partial R^{ad}_{\mu\nu}(k_1)}{\partial k_1^\sigma \partial k_1^\lambda} &= \frac{1}{2}\delta^{ad}\left\{R^1_{\mu\sigma\lambda\nu}(k_1,k_1,k_1) + R^3_{\mu\sigma\lambda\nu}(k_1,k_1,k_1)\right\} = \\ &= -\frac{1}{2}\delta^{ad} R^2_{\mu\sigma\lambda\nu}(k_1,k_1,k_1)\,, \end{aligned} \tag{8.31}$$

where we have also made use of (8.28).

9 Gluonic Operators

As outlined in section 7, the lower blobs in fig. 2.1 can be written as matrix-elements of gluonic operators (eqns. (7.4)-(7.6)). Since it is our aim to find expressions for the gluonic twist-four contributions which are explicitly gauge invariant, we have to find relations in which all operators consist of gluonic operators $F^{\mu\nu}_a$ and covariant derivatives D^μ_{ab}. In this section we show how A^μ_a-operators within matrix-elements can be substituted by $F^{\mu\nu}_a$-operators in the axial gauge, where

$$n_\mu F^{\mu\nu}_a = (n\cdot\partial) A^\nu_a\,. \tag{9.1}$$

Let us, first, define[4]

$$\int \mathrm{d}^4z\, \mathrm{d}^4z'\, \mathrm{e}^{\mathrm{i}k\cdot z}\mathrm{e}^{-\mathrm{i}k'\cdot z'}\langle p|\mathrm{T}\left\{A^\nu_b(z')A^\mu_a(z)\right\}|p\rangle \equiv (2\pi)^4\delta(k-k')G^{\mu\nu}_{ab}(k)\,, \tag{9.2}$$

and examine the expression

$$\begin{aligned}&\int \mathrm{d}^4z\, \mathrm{d}^4z'\, \mathrm{e}^{\mathrm{i}k\cdot z}\mathrm{e}^{-\mathrm{i}k'\cdot z'}\langle p|\mathrm{T}\left\{(n\cdot\partial')A^\nu_b(z')(n\cdot\partial)A^\mu_a(z)\right\}|p\rangle = \\ &\qquad = -\mathrm{i}\, n\cdot k\, \mathrm{i}\, n\cdot k' \int \mathrm{d}^4z\, \mathrm{d}^4z'\, \mathrm{e}^{\mathrm{i}k\cdot z}\mathrm{e}^{-\mathrm{i}k'\cdot z'}\langle p|\mathrm{T}\left\{A^\nu_b(z')A^\mu_a(z)\right\}|p\rangle = \\ &\qquad = n\cdot k\, n\cdot k'(2\pi)^4\delta(k-k')G^{\mu\nu}_{ab}(k)\,, \end{aligned} \tag{9.3}$$

[4]We are not writing the p-dependence of function $G^{\mu\nu}_{ab}$ explicitly.

where we have used partial integration. If we, now, perform the integration over k' in eqn. (9.3), keep (9.1) in mind and insert $x = n \cdot k$, we end up with

$$\int \mathrm{d}^4 z \, \mathrm{e}^{\mathrm{i}k\cdot z} \langle p|\mathrm{T}\left\{A_b^\nu(0) A_a^\mu(z)\right\}|p\rangle = \frac{1}{x^2} \int \mathrm{d}^4 z \, \mathrm{e}^{\mathrm{i}k\cdot z} \, n_\alpha n_\beta \langle p|\mathrm{T}\left\{F_b^{\beta\nu}(0) F_a^{\alpha\mu}(z)\right\}|p\rangle \,, \tag{9.4}$$

which is the desired result. In complete analogy, one can find relations for matrix-elements with more than two gluon-operators.

10 Dimensional Analysis

Before we present the results of the factorization procedure we, first, perform the dimensional analysis in this section, in order to justify that we have restricted ourselves to diagrams with up to four t-channel gluons (fig. 2.1) and to those terms in the expansions of the quark-loop expressions R which are given in eqns. (7.7)-(7.9). By this way we also get an insight into how the various twist contributions can be obtained from the expressions under consideration.

As we will show in the next section, after factorization the upper and lower parts of the diagrams in fig. 2.1 are connected by one-dimensional integrals, which we can symbolically write as

$$H_1 = \int \mathrm{d}x_1 \, R_{\mu\nu}(x_1 p) \, {}_2G^{\mu\nu}(x_1) \,, \tag{10.1}$$

$$H_2 = \int \mathrm{d}x_1 \mathrm{d}x_2 \, R_{\mu\sigma\nu}(x_1 p, x_2 p) \, {}_3G^{\mu\sigma\nu}(x_1, x_2) \,, \tag{10.2}$$

$$H_3 = \int \mathrm{d}x_1 \mathrm{d}x_2 \mathrm{d}x_3 \, R_{\mu\sigma\lambda\nu}(x_1 p, x_2 p, x_3 p) \, {}_4G^{\mu\sigma\lambda\nu}(x_1, x_2, x_3) \,. \tag{10.3}$$

For convenience we are using these relations already in this section. The functions G will be given below in eqns. (11.6), (11.11) and (11.26). The functions H_i are not the same as the functions $\tilde{H}_i$ in (7.1)-(7.3). For the functions H_i the number of Lorentz-indices occurring on the right-hand-sides correspond to the number of gluon-lines plus the number of derivatives.

Our argument is based on the assumption that, after factorization, the only dimensional quantity the quark-loops R can depend on is Q^2. We expect an infrared cut-off to enter only within logarithms. On the other hand, the only dimensional quantity the matrix-elements G can depend on is Λ. If we, therefore, determine the dimension of one particular function R with Lorentz indices projected out, we can relate this dimension to the powers of $1/Q^2$ this function must be proportional to.

A simple analysis shows that the dimension of the quark-loops is given by the expression

$$\dim R = 2 - B \,, \tag{10.4}$$

where B is the number of gluon-lines plus the number of derivatives:

$$B = n_\mathrm{G} + n_\mathrm{D} \,. \tag{10.5}$$

With the help of (10.1)-(10.3) we conclude that

$$\dim {}_4G = \dim {}_3G + 1 = \dim {}_2G + 2 \,. \tag{10.6}$$

10.1 Two Gluons

In order to split up H_1, (10.1), into leading- and next-to-leading twist expressions, we, now, explore the tensor structure of ${}_2G^{\mu\nu}$ (which is given by eqn. (11.6), below):

$$ {}_2G^{\mu\nu}(x_1) = d^{\mu\nu} A_1(x_1) + n^\mu n^\nu A_2(x_1)\,, \tag{10.7} $$

where we have ignored terms proportional $n_\alpha p_\beta \varepsilon^{\mu\nu\alpha\beta}$. Since we are working in the axial gauge, i.e. $n \cdot A = 0$, there can be no terms proportional p^μ in (10.7) (cf. (7.4)). The tensor

$$ d^{\mu\nu} \equiv g^{\mu\nu} - p^\mu n^\nu - n^\mu p^\nu \tag{10.8} $$

has been introduced since it serves as a projector, such that

$$ A_1 = \frac{1}{2} d_{\mu\nu}\, {}_2G^{\mu\nu}\,, \tag{10.9} $$

$$ A_2 = p_\mu p_\nu\, {}_2G^{\mu\nu}\,. \tag{10.10} $$

Now, since $\dim p = 1$, $\dim d^{\mu\nu} = 0$ and $\dim n = -1$, we conclude with the help of (10.6) that $\dim A_1 = 0$ and, therefore, $A_1 \sim \Lambda^0$, while $\dim A_2 = 2$, such that $A_2 \sim \Lambda^2$. Keeping the discussion above in mind, we conclude that in eqn. (10.7) it is the term proportional A_1 which gives the leading-twist contribution, while the term proportional A_2 contributes to twist-four, i.e. in (10.1) the corresponding expression is proportional to Λ^2/Q^2.

10.2 Three Gluons

The twist analysis of (10.2) can be performed in complete analogy. Exploring the tensor structure of ${}_3G^{\mu\sigma\nu}$ (which is given by eqn. (11.11), below) one gets

$$ {}_3G^{\mu\sigma\nu} = d^{\mu\nu} n^\sigma\, B_1^1 + d^{\mu\sigma} n^\nu\, B_1^2 + d^{\nu\sigma} n^\mu\, B_1^3 + n^\mu n^\nu n^\sigma B_2\,, \tag{10.11} $$

where we have, again, neglected terms proportional $\varepsilon^{\mu\sigma\lambda\nu}$. Moreover, we have made use of the fact that

$$ n_{\alpha_i}\, {}_3G^{\alpha_1\alpha_2\alpha_3} = 0\,, \tag{10.12} $$

since the indices of ${}_3G^{\mu\sigma\nu}$ belong either to terms like A^α or like $\omega^\alpha_{\alpha'}\partial^{\alpha'}$ and $n_\alpha \omega^\alpha_{\alpha'} = 0$ (cf. (11.7)). The various terms in (10.11) can be projected out in the following way

$$ B_1^1 = \frac{1}{2} d_{\mu\nu} p_\sigma\, {}_3G^{\mu\sigma\nu} \quad \text{etc.}, \tag{10.13} $$

$$ B_2 = p_\mu p_\nu p_\sigma\, {}_3G^{\mu\sigma\nu} \tag{10.14} $$

and a dimensional analysis shows that the terms proportional B_1^i contribute to twist-four, while the term proportional B_2 contributes to twist-six.

10.3 Four Gluons

The tensor structure of ${}_4G^{\mu\sigma\lambda\nu}$ is given by

$$ {}_4G^{\mu\sigma\lambda\nu} = d^{\mu\nu}d^{\sigma\lambda}C_1^1 + \text{perm.} + d^{\mu\nu}n^\sigma n^\lambda C_2^1 + \text{perm.} + n^\mu n^\nu n^\sigma n^\lambda C_3 \,, \tag{10.15} $$

with

$$ C_1^1 = d_{\mu\nu\sigma\lambda}\,{}_4G^{\mu\sigma\lambda\nu} \quad \text{etc.}, \tag{10.16} $$

$$ C_2^1 = \frac{1}{2} d_{\mu\nu}p_\sigma p_\lambda\,{}_4G^{\mu\sigma\lambda\nu} \quad \text{etc.}, \tag{10.17} $$

$$ C_3 = p_\mu p_\nu p_\sigma p_\lambda\,{}_4G^{\mu\sigma\lambda\nu} \,, \tag{10.18} $$

where

$$ d_{\mu\nu\sigma\lambda} \equiv \frac{1}{8}\left(3d_{\mu\nu}d_{\sigma\lambda} - d_{\mu\sigma}d_{\nu\lambda} - d_{\mu\lambda}d_{\nu\sigma}\right) . \tag{10.19} $$

In this case, C_1^i give the twist-four and C_2^i the twist-six contributions, while C_3 belongs to twist-eight.

With these experiences we can, now, analyse terms with more t-channel gluons and/or derivatives. One term with lowest dimension of the corresponding ${}_5G^{\mu\sigma\lambda\rho\nu}$ would be proportional $d^{\mu\nu}d^{\sigma\lambda}n^\rho$ and, therefore, belong to twist-six. Increasing the number of gluon-lines or derivatives increases also the twist of the lowest-twist term. We can, therefore, justify that we have restricted ourselves to the diagrams in fig. 2.1 and to the terms in eqns. (7.7)-(7.9).

11 Results of the Factorization Procedure

Before we present the results of the factorization procedure, let us summarize the preceding results. Our computations are based on the diagrams in fig. 2.1, where the expressions for the quark-loops R are expanded about the longitudinal components of the gluon-momenta (7.7)-(7.9). For the derivatives in (7.7) and (7.8) we have computed some Ward identities in section 8, viz. (8.16), (8.29), (8.30) and (8.31). For the derivation of these relations we had to explore the color structure of the quark-loop expressions, (8.15), (8.19) and (8.25), which also led to an important relation for the four-gluon quark-loop, (8.28), if one of the gluon-momenta vanishes. In section 9 we have developed a method which is useful in order to exchange A-operators by F-operators within matrix-elements and in section 10 we performed the dimensional analysis of the expressions under consideration. This yielded a scheme for projecting out the different twist contributions.

As outlined before, it is our aim to write the gluonic twist-four contributions to the inclusive deep-inelastic structure functions in an explicitly gauge invariant form. In order to get these expressions it is, now, necessary to reorder the terms which enter into the sum over the contributions of the three diagrams in fig. 2.1. In particular, we write the sum over these contributions as

$$ \tilde{H}_1 + \tilde{H}_2 + \tilde{H}_3 = H_1 + H_2 + H_3 + \mathcal{O}\left(\frac{1}{Q^4}\right) . \tag{11.1} $$

Here H_1 consists only of the zeroth order term in eqn. (7.7) inserted in (7.1), while H_2 is the sum of eqns. (7.1) and (7.2) with restrictions for $R^{ab}_{\mu\nu}$ and $R^{abc}_{\mu\sigma\nu}$ to the first and zeroth order terms, resp., in eqns.(7.7) and (7.8). H_3 consists of the sum of expressions (7.1) through (7.3) where only the zeroth order term in eqn. (7.9), the first order terms in (7.8) and the second order term in (7.7) are taken into account. With these conventions the next steps for H_1 and H_2, in order to write them in an explicitly gauge invariant form, are straight forward, while the situation is more peculiar in the case of H_3. We review the results in the next subsections.

11.1 Two and Three Gluons

Inserting the zeroth order term in eqn. (7.7) into (7.1), we realize that the expression for the quark-loop, now, depends only on the longitudinal component of the four-momentum k_1, and we can simplify the integrations over k_1 and z if we introduce the expression (cf. (6.4)) [19]

$$\int \mathrm{d}^4 k_1 = \int \mathrm{d}^4 k_1 \mathrm{d}x_1 \delta(x_1 - k_1 \cdot n) \tag{11.2}$$

and make use of the relation

$$\int \frac{\mathrm{d}^4 k_1}{(2\pi)^4} \mathrm{e}^{\mathrm{i}k_1 \cdot z} \delta(x_1 - k_1 \cdot n) = \int \frac{\mathrm{d}\lambda}{2\pi} \mathrm{e}^{\mathrm{i}\lambda x_1} \delta^{(4)}(z - \lambda n)\,. \tag{11.3}$$

The result is

$$H_1 = \int \mathrm{d}x_1 R^{ab}_{\mu\nu}(x_1 p) \int \frac{\mathrm{d}\lambda}{2\pi} \mathrm{e}^{\mathrm{i}\lambda x_1} \langle p|\mathrm{T}\left\{A^\nu_b(0) A^\mu_a(\lambda n)\right\}|p\rangle\,. \tag{11.4}$$

Now, with the help of the results of section 9 we can substitute the A-operators by F-operators, and with the help of eqns. (10.7) and (10.10) we can project out the twist-four contribution:

$$H_1|_{\tau=4} = \int \mathrm{d}x_1 n^\mu n^\nu R_{\mu\nu}(x_1 p)\, p_{\mu'} p_{\nu'}\, {}_2G^{\mu'\nu'}(x_1)\,, \tag{11.5}$$

where

$${}_2G^{\mu\nu}(x_1) = \frac{n_\alpha n_\beta}{x_1^2} \int \frac{\mathrm{d}\lambda}{2\pi} \mathrm{e}^{\mathrm{i}\lambda x_1} \langle p|\mathrm{T}\left\{\delta^{ab} F^{\nu\beta}_b(0) F^{\mu\alpha}_a(\lambda n)\right\}|p\rangle\,. \tag{11.6}$$

In the case of H_2 we get the additional factor $(k_1 - x_1 p)^\sigma$ from the first order term in eqn. (7.7). This factor can be written as a derivative applied to the exponential function in (7.4) if we introduce the tensor [19]

$$\omega^\mu_{\mu'} \equiv g^\mu_{\mu'} - p^\mu n_{\mu'}\,, \qquad \omega^\mu_{\mu'} k_1^{\mu'} = (k_1 - x_1 p)^\mu\,, \tag{11.7}$$

which subtracts the longitudinal component of the momentum-vector it is applied to. Now, using partial integration in order to apply this derivative to the gluon operator and making use of eqn. (8.16) we get

$$H_2 = \int \mathrm{d}x_1 \mathrm{d}x_2 R_{\mu\sigma\nu}(x_1 p, x_2 p) \int \frac{\mathrm{d}\lambda}{2\pi} \frac{\mathrm{d}\eta}{2\pi} \mathrm{e}^{\mathrm{i}\lambda x_1} \mathrm{e}^{\mathrm{i}\eta(x_2 - x_1)} \omega^\sigma_{\sigma'} \langle p|\mathrm{T}\left\{A^\nu_c(0) \mathrm{D}^{\sigma'}_{ac}(\eta n) A^\mu_a(\lambda n)\right\}|p\rangle\,, \tag{11.8}$$

where the partial derivative within the covariant derivative is due to the first order term in (7.7) and the gluon operator within $\mathrm{D}^{\sigma'}_{ac}$ is due to the zeroth order term in (7.8). For the derivation of (11.8) we have also made use of the fact that, within the axial gauge, the ω-tensor applied to a gluon-operator yields the same operator:

$$\omega^{\mu}_{\mu'} A^{\mu'}_a = A^{\mu}_a \,. \tag{11.9}$$

Projecting out the twist-four contribution with the help of eqns. (10.11) and (10.13) and applying the method developed in section 9 in order to substitute the A-operators by F-operators we end up with

$$H_2|_{\tau=4} = \int \mathrm{d}x_1 \mathrm{d}x_2 \left\{ d^{\mu\nu} n^{\sigma} R_{\mu\sigma\nu}(x_1 p, x_2 p) \frac{1}{2} d_{\mu'\nu'} p_{\sigma'} \, {}_3G^{\mu'\sigma'\nu'}(x_1, x_2) + \text{perm.} \right\} , \tag{11.10}$$

where

$${}_3G^{\mu\sigma\nu}(x_1, x_2) = \frac{n_\alpha n_\beta}{x_1 \, x_2} \int \frac{\mathrm{d}\lambda}{2\pi} \frac{\mathrm{d}\eta}{2\pi} \mathrm{e}^{\mathrm{i}\lambda x_1} \mathrm{e}^{\mathrm{i}\eta(x_2 - x_1)} \omega^{\sigma}_{\sigma'} \langle p | \mathrm{T} \left\{ F^{\nu\beta}_c(0) \mathrm{D}^{\sigma'}_{ac}(\eta n) F^{\mu\alpha}_a(\lambda n) \right\} | p \rangle \,. \tag{11.11}$$

For the permutation in (11.10) one has to keep eqns. (10.11) and (10.13) in mind, i.e. indices of the projector which is applied to $R_{\mu\sigma\nu}$ and of the projector which is applied to ${}_3G^{\mu'\sigma'\nu'}$ have to be permuted simultaneously. Similar to H_1, (11.5), H_2 contains only contributions of the two-gluon operator.

Although we have restricted ourselves to the leading-order terms for the derivation of H_1 and H_2, eqns. (11.5) and (11.10) are of more general validity. Since the Ward identities, we have used, are valid to all orders and our ansätze for the color structure of $R^{ab}_{\mu\nu}$ and $R^{abc}_{\mu\lambda\nu}$, (8.15) and (8.19), are of the most general nature, eqns. (11.5) and (11.10) are valid to all orders as long as one neglects operator mixing.

11.2 Four Gluons

11.2.1 Basics

The situation is more complicated in the case of H_3. Putting all terms which enter into H_3 together and making use of eqns. (8.29), (8.30) and (8.31) we get

$$\begin{aligned} H_3 = \int \mathrm{d}x_1 \mathrm{d}x_2 \mathrm{d}x_3 \Big\{ & R^{abcd}_{\mu\sigma\lambda\nu}(x_1 p, x_2 p, x_3 p) \, {}_4G^{\mu\sigma\lambda\nu}_{abcd}(x_1, x_2, x_3) + \\ & + \frac{\mathrm{i}}{2} g f^{acd} R^1_{\mu\sigma\lambda\nu}(x_1 p, x_2 p, x_3 p) \, {}_3G^{\mu\sigma\lambda\nu}_{acd,1}(x_1, x_3) \delta(x_1 - x_2) + \\ & + \frac{\mathrm{i}}{2} g f^{abd} R^1_{\mu\sigma\lambda\nu}(x_1 p, x_2 p, x_3 p) \, {}_3G^{\mu\sigma\lambda\nu}_{abd,2}(x_1, x_2) \delta(x_2 - x_3) + \\ & + \frac{1}{4} \delta^{ad} \big[R^1_{\mu\sigma\lambda\nu}(x_1 p, x_2 p, x_3 p) + \\ & \qquad + R^3_{\mu\sigma\lambda\nu}(x_1 p, x_2 p, x_3 p) \big] \, {}_2G^{\mu\sigma\lambda\nu}_{ad}(x_1) \delta(x_1 - x_2) \delta(x_2 - x_3) \Big\} , \end{aligned} \tag{11.12}$$

where

$$ {}_4G^{\mu\sigma\lambda\nu}_{abcd}(x_1,x_2,x_3) = \int \frac{\mathrm{d}\lambda}{2\pi}\frac{\mathrm{d}\eta}{2\pi}\frac{\mathrm{d}\tau}{2\pi} \mathrm{e}^{\mathrm{i}\lambda x_1}\mathrm{e}^{\mathrm{i}\eta(x_2-x_1)}\mathrm{e}^{\mathrm{i}\tau(x_3-x_2)} \langle p|\mathrm{T}\left\{A^\nu_d(0)A^\lambda_c(\tau n)A^\sigma_b(\eta n)A^\mu_a(\lambda n)\right\}|p\rangle\,, \tag{11.13} $$

$$ {}_3G^{\mu\sigma\lambda\nu}_{acd,1}(x_1,x_3) = \omega^\sigma_{\sigma'}\int \frac{\mathrm{d}\lambda}{2\pi}\frac{\mathrm{d}\tau}{2\pi} \mathrm{e}^{\mathrm{i}\lambda x_1}\mathrm{e}^{\mathrm{i}\tau(x_3-x_2)} \langle p|\mathrm{T}\left\{A^\nu_d(0)A^\lambda_c(\tau n)\mathrm{i}\partial^{\sigma'}A^\mu_a(\lambda n)\right\}|p\rangle\,, \tag{11.14} $$

$$ {}_3G^{\mu\sigma\lambda\nu}_{abd,2}(x_1,x_2) = \omega^\lambda_{\lambda'}\int \frac{\mathrm{d}\lambda}{2\pi}\frac{\mathrm{d}\eta}{2\pi} \mathrm{e}^{\mathrm{i}\lambda x_1}\mathrm{e}^{\mathrm{i}\eta(x_2-x_1)} \langle p|\mathrm{T}\left\{A^\nu_d(0)\mathrm{i}\partial^{\lambda'}[A^\sigma_b(\eta n)A^\mu_a(\lambda n)]\right\}|p\rangle\,, \tag{11.15} $$

$$ {}_2G^{\mu\sigma\lambda\nu}_{ad}(x_1) = \omega^\sigma_{\sigma'}\omega^\lambda_{\lambda'}\int \frac{\mathrm{d}\lambda}{2\pi}\mathrm{e}^{\mathrm{i}\lambda x_1} \langle p|\mathrm{T}\left\{A^\nu_d(0)\mathrm{i}\partial^{\lambda'}\mathrm{i}\partial^{\sigma'}A^\mu_a(\lambda n)\right\}|p\rangle\,. \tag{11.16} $$

The derivatives in eqns. (11.14)-(11.16) have to be understood as $\partial^{\sigma'}A(\lambda n) \equiv \mathrm{d}A(z)/\mathrm{d}z_{\sigma'}|_{z=\lambda n}$, etc. Due to our definition (8.25), we can split up eqn. (11.12) into three parts

$$ H_3 = H_3^1 + H_3^2 + H_3^3\,, \tag{11.17} $$

where H_3^i corresponds to those terms in (11.12) which contain the function $R^i_{\mu\sigma\lambda\nu}$. Since we intend to write the expression for H_3 in a form which is explicitly gauge invariant (similar to (11.5) and (11.10)) we have to modify it in such a way that partial derivatives occur only within covariant derivatives. This can most easily be done with the help of the following relation:

$$ f^{acd}A^\lambda_c(\tau n)\partial^\sigma = f^{a'cd}A^\lambda_c(\tau n)\mathrm{D}^\sigma_{a'a}(\eta n) + g f^{aba'}f^{a'cd}A^\lambda_c(\tau n)A^\sigma_b(\eta n)\,. \tag{11.18} $$

Inserting (11.18) into (11.12) we realize that the results for the functions H_3^i consist of terms with two-, three- and four-gluon operators. Now, it is known that, in the spin-averaged case, the three-gluon operator does not contribute. Moreover, the decomposition (11.17) is not unique, since the Ward identities could be expressed with the help of different combinations of the functions $R^i_{\mu\sigma\lambda\nu}$ in eqns. (8.29), (8.30) and (8.31). We could, therefore, also write eqn. (11.12) with different combinations of these functions. By exploring symmetry relations for $R^{abcd}_{\mu\sigma\lambda\nu}(k_1,k_2,k_3)$ we will show how to derive expressions for H_3 which involve only one of the functions R^i and contain no three-gluon operator.

11.2.2 Symmetry Relations of the Four-Gluon Quark-Loop Expression

The expression for the four-gluon quark-loop, $R^{abcd}_{\mu\sigma\lambda\nu}(k_1,k_2,k_3)$, has to be completely symmetrical under simultaneous exchange of gluon-momenta, Lorentz- and color indices. This can be seen in two ways. First, within the path-integral formulation we have defined $R^{abcd}_{\mu\sigma\lambda\nu}(k_1,k_2,k_3)$ in eqn. (8.12). Since the gluon is a boson the derivation operators in (8.12) commute and the proclaimed symmetry follows immediately. Secondly, it can be seen diagrammatically. Clearly, $R^{abcd}_{\mu\sigma\lambda\nu}(k_1,k_2,k_3)$ corresponds to the expression which is obtained if one takes all diagrams up to a specified order into account, i.e. in leading-order one has to consider all permutations for the coupling of four t-channel gluons to quarks and anti-quarks. For example, we consider the diagram in fig. 2.4a. If we set $k_1 = k_2' - k_1'$, $k_2 = k_2'$, $k_3 = k_3'$ and exchange $\mu \leftrightarrow \sigma$ and $a \leftrightarrow b$ we get an analytic expression which is the same as the one we get from the diagram in fig. 2.4b. Since such a relation can be drawn for each diagram that enters into $R^{abcd}_{\mu\sigma\lambda\nu}$ we have in general

$$ R^{abcd}_{\mu\sigma\lambda\nu}(k_1,k_2,k_3) = R^{bacd}_{\sigma\mu\lambda\nu}(k_2-k_1,k_2,k_3)\,. \tag{11.19} $$

	$R^1_{\mu\sigma\lambda\nu}(k_1,k_2,k_3) =$	$R^2_{\mu\sigma\lambda\nu}(k_1,k_2,k_3) =$	$R^3_{\mu\sigma\lambda\nu}(k_1,k_2,k_3) =$
1	$R^2_{\sigma\mu\lambda\nu}(k_2-k_1,k_2,k_3)$	$R^1_{\sigma\mu\lambda\nu}(k_2-k_1,k_2,k_3)$	$R^3_{\sigma\mu\lambda\nu}(k_2-k_1,k_2,k_3)$
2	$R^2_{\mu\sigma\nu\lambda}(k_1,k_2,k_2-k_3)$	$R^1_{\mu\sigma\nu\lambda}(k_1,k_2,k_2-k_3)$	$R^3_{\mu\sigma\nu\lambda}(k_1,k_2,k_2-k_3)$
3	$R^3_{\mu\lambda\sigma\nu}(k_1,k_1-k_2+k_3,k_3)$	$R^2_{\mu\lambda\sigma\nu}(k_1,k_1-k_2+k_3,k_3)$	$R^1_{\mu\lambda\sigma\nu}(k_1,k_1-k_2+k_3,k_3)$
4	$R^2_{\sigma\lambda\mu\nu}(k_2-k_1,k_3-k_1,k_3)$	$R^3_{\sigma\lambda\mu\nu}(k_2-k_1,k_3-k_1,k_3)$	$R^1_{\sigma\lambda\mu\nu}(k_2-k_1,k_3-k_1,k_3)$
5	$R^3_{\lambda\mu\sigma\nu}(k_3-k_2,k_1-k_2+k_3,k_3)$	$R^1_{\lambda\mu\sigma\nu}(k_3-k_2,k_1-k_2+k_3,k_3)$	$R^2_{\lambda\mu\sigma\nu}(k_3-k_2,k_1-k_2+k_3,k_3)$
6	$R^1_{\lambda\sigma\mu\nu}(k_3-k_2,k_3-k_1,k_3)$	$R^3_{\lambda\sigma\mu\nu}(k_3-k_2,k_3-k_1,k_3)$	$R^2_{\lambda\sigma\mu\nu}(k_3-k_2,k_3-k_1,k_3)$
7	$R^1_{\mu\nu\lambda\sigma}(k_1,k_1-k_3,k_1-k_2)$	$R^3_{\mu\nu\lambda\sigma}(k_1,k_1-k_3,k_1-k_2)$	$R^2_{\mu\nu\lambda\sigma}(k_1,k_1-k_3,k_1-k_2)$

TABLE 2.1: Making use of symmetry relations for $R^{abcd}_{\mu\sigma\lambda\nu}(k_1,k_2,k_3)$ one finds relations between the three functions $R^i_{\mu\sigma\lambda\nu}(k_1,k_2,k_3)$.

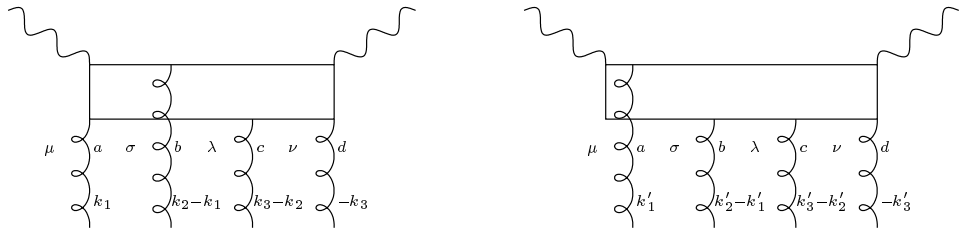

(a) (b)

FIG. 2.4: Two sample diagrams which enter into $R^{abcd}_{\mu\sigma\lambda\nu}$. They are identical if one sets $k_1 = k'_2 - k'_1$, $k_2 = k'_2$, $k_3 = k'_3$ and exchanges $\mu \leftrightarrow \sigma$ and $a \leftrightarrow b$.

Next, with the help of the color structure (8.25) of $R^{abcd}_{\mu\sigma\lambda\nu}$ we can find relations between the three functions $R^i_{\mu\sigma\lambda\nu}$ if we realize that for $a \leftrightarrow b$: $d^{abcd} \to d^{abdc}$, $d^{abdc} \to d^{abcd}$ but $d^{acbd} \to d^{acbd}$, as follows from the definition of d^{abcd}, (8.24). With these relations we get

$$R^1_{\mu\sigma\lambda\nu}(k_1,k_2,k_3) = R^2_{\sigma\mu\lambda\nu}(k_2-k_1,k_2,k_3)\,, \tag{11.20}$$

$$R^2_{\mu\sigma\lambda\nu}(k_1,k_2,k_3) = R^1_{\sigma\mu\lambda\nu}(k_2-k_1,k_2,k_3)\,, \tag{11.21}$$

$$R^3_{\mu\sigma\lambda\nu}(k_1,k_2,k_3) = R^3_{\sigma\mu\lambda\nu}(k_2-k_1,k_2,k_3)\,. \tag{11.22}$$

Exchanging other gluon lines one gets a large number of relations. Some of these are given in table 2.1.

11.2.3 Gauge Invariant Expressions

With the help of the relations in table 2.1 we can, now, write eqn. (11.12) as an explicitly gauge invariant expression. For example, using the relation in row one, column two of table 2.1 we can exchange function $R^2_{\mu\sigma\lambda\nu}$ in the first line of (11.12) by $R^1_{\sigma\mu\lambda\nu}$ and after an adequate transformation of integration variables ($x_1 \to x_2 - x_1$, $\lambda \leftrightarrow \eta$) and an exchange of Lorentz- and color indices a function $R^1_{\mu\sigma\lambda\nu}$ can be factored out. Similarly the terms involving function $R^3_{\mu\sigma\lambda\nu}$ in (11.12) can

be brought into the desired form with the help of the expression in row three, column three of table 2.1. We end up with

$$H_3 = \int \mathrm{d}x_1 \mathrm{d}x_2 \mathrm{d}x_3 \int \frac{\mathrm{d}\lambda}{2\pi}\frac{\mathrm{d}\eta}{2\pi}\frac{\mathrm{d}\tau}{2\pi} \mathrm{e}^{\mathrm{i}\lambda x_1}\mathrm{e}^{\mathrm{i}\eta(x_2-x_1)}\mathrm{e}^{\mathrm{i}\tau(x_3-x_2)} R^1_{\mu\sigma\lambda\nu}(x_1p,x_2p,x_3p)\omega^{\sigma}_{\sigma'}\omega^{\lambda}_{\lambda'} \times$$
$$\times \langle p|\mathrm{T}\big\{A^{\nu}_d(0)\big[g^2 l_1^{abcd} A^{\lambda'}_c(\tau n)A^{\sigma'}_b(\eta n) - \frac{1}{2}\mathrm{D}^{\lambda'}_{ac'}(\tau n)\mathrm{D}^{\sigma'}_{c'd}(\eta n)\big]A^{\mu}_a(\lambda n)\big\}|p\rangle\,, \quad (11.23)$$

where

$$l_1^{abcd} = f^{adc'}f^{c'bc} + \frac{1}{4}\left(\delta^{ab}\delta^{cd}+\delta^{ac}\delta^{bd}+\delta^{ad}\delta^{bc}\right) = \quad (11.24)$$
$$= \frac{1}{2}f^{acc'}f^{c'bd} - \frac{3}{2}d^{acc'}d^{c'bd} + \frac{1}{2}\left(\delta^{ab}\delta^{cd}-\delta^{ac}\delta^{bd}+\delta^{ad}\delta^{bc}\right) + \frac{1}{4}\left(\delta^{ab}\delta^{cd}+\delta^{ac}\delta^{bd}+\delta^{ad}\delta^{bc}\right) =$$
$$= \frac{1}{2}f^{acc'}f^{c'bd} + 3d^{abcd}\,.$$

If we have a look at eqn. (11.12), we realize that there is a term proportional $R^{abcd}_{\mu\sigma\lambda\nu}$ in the first line. Due to (8.25) this yields in terms with color factors d^{abcd} and corresponding permutations of color indices. For the derivation of (11.23) one has to add and subtract terms which involve four A-operators in order to get covariant derivatives. Merging the subtracted expressions with those in the first line of eqn. (11.12) the resulting color factor is no longer proportional to d^{abcd}. Instead one gets the term in eqn. (11.24).

Again, with the help of (10.15) and (10.16) we can project out the twist-four contributions and with the help of the results in section 9 we can substitute the A-operators by F-operators:

$$H_3|_{\tau=4} = \int \mathrm{d}x_1\mathrm{d}x_2\mathrm{d}x_3 \left\{ d^{\mu\nu}d^{\sigma\lambda}R^1_{\mu\sigma\lambda\nu}(x_1p,x_2p,x_3p)\, d_{\mu'\nu'\sigma'\lambda'}\,{}_4G_1^{\mu'\sigma'\lambda'\nu'}(x_1,x_2,x_3) + \text{perm.}\right\}\,, \quad (11.25)$$

where

$${}_4G_1^{\mu\sigma\lambda\nu}(x_1,x_2,x_3) = \int \frac{\mathrm{d}\lambda}{2\pi}\frac{\mathrm{d}\eta}{2\pi}\frac{\mathrm{d}\tau}{2\pi} \mathrm{e}^{\mathrm{i}\lambda x_1}\mathrm{e}^{\mathrm{i}\eta(x_2-x_1)}\mathrm{e}^{\mathrm{i}\tau(x_3-x_2)} \times \quad (11.26)$$
$$\times \left[\frac{-1}{x_1x_3(x_2-x_1)(x_3-x_2)} n_\alpha n_\beta n_\gamma n_\delta \langle p|\mathrm{T}\left\{g^2 l_1^{abcd}F^{\nu\delta}_d(0)F^{\lambda\gamma}_c(\tau n)F^{\sigma\beta}_b(\eta n)F^{\mu\alpha}_a(\lambda n)\right\}|p\rangle \right.$$
$$\left. - \frac{1}{2}\frac{1}{x_1x_3} n_\alpha n_\beta \langle p|\mathrm{T}\left\{F^{\nu\beta}_d(0)\omega^{\lambda}_{\lambda'}\mathrm{D}^{\lambda'}_{ac}(\tau n)\omega^{\sigma}_{\sigma'}\mathrm{D}^{\sigma'}_{cd}(\eta n)F^{\mu\alpha}_a(\lambda n)\right\}|p\rangle\right]$$

and the permutations in (11.25) have to be understood in the same sense as in (11.10) (cf. (10.15), (10.16)). For H_3 we get contributions of the two-gluon operator as well as of the four-gluon operator.

The representation of H_3 in a gauge invariant form as in eqn. (11.25) is not unique. For example, we can derive expressions where the quark-loop is represented by functions R^2 or R^3. These expressions can be obtained in two ways. One can either start with eqn. (11.12), make use of the relations in table 2.1 and apply the same methods which led to (11.25). Or one starts with (11.25) and expresses R^1 in terms of functions R^2 or R^3 with the help of the expressions in table 2.1. The results can be summarized as follows. If we exchange $R^1_{\mu\sigma\lambda\nu}(x_1p,x_2p,x_3p)$ by $R^2_{\mu\sigma\lambda\nu}(x_1p,x_2p,x_3p)$

or $R^3_{\mu\sigma\lambda\nu}(x_1p, x_2p, x_3p)$ in (11.25) we also have to exchange ${}_4G_1^{\mu\sigma\lambda\nu}(x_1,x_2,x_3)$ by ${}_4G_2^{\mu\sigma\lambda\nu}(x_1,x_2,x_3)$ or ${}_4G_3^{\mu\sigma\lambda\nu}(x_1,x_2,x_3)$, resp. The latter functions can be written as

$$
\begin{aligned}
{}_4G_2^{\mu\sigma\lambda\nu}(x_1,x_2,x_3) &= \int \frac{\mathrm{d}\lambda}{2\pi}\frac{\mathrm{d}\eta}{2\pi}\frac{\mathrm{d}\tau}{2\pi} \mathrm{e}^{\mathrm{i}\lambda x_1}\mathrm{e}^{\mathrm{i}\eta(x_2-x_1)}\mathrm{e}^{\mathrm{i}\tau(x_3-x_2)} \times \qquad (11.27)\\
&\times \left[\frac{-1}{x_1x_3(x_2-x_1)(x_3-x_2)} n_\alpha n_\beta n_\gamma n_\delta \langle p|\mathrm{T}\left\{ g^2 l_2^{abcd} F_d^{\nu\delta}(0) F_c^{\lambda\gamma}(\tau n) F_b^{\sigma\beta}(\eta n) F_a^{\mu\alpha}(\lambda n)\right\}|p\rangle \right.\\
&\left. - \frac{1}{2}\frac{1}{(x_2-x_1)x_3} n_\alpha n_\beta \langle p|\mathrm{T}\left\{ F_d^{\nu\beta}(0)\omega^\lambda_{\lambda'}\mathrm{D}^{\lambda'}_{bc}(\tau n)\omega^\mu_{\mu'}\mathrm{D}^{\mu'}_{cd}(\lambda n) F_b^{\sigma\alpha}(\eta n)\right\}|p\rangle \right]
\end{aligned}
$$

and

$$
\begin{aligned}
{}_4G_3^{\mu\sigma\lambda\nu}(x_1,x_2,x_3) &= \int \frac{\mathrm{d}\lambda}{2\pi}\frac{\mathrm{d}\eta}{2\pi}\frac{\mathrm{d}\tau}{2\pi} \mathrm{e}^{\mathrm{i}\lambda x_1}\mathrm{e}^{\mathrm{i}\eta(x_2-x_1)}\mathrm{e}^{\mathrm{i}\tau(x_3-x_2)} \times \qquad (11.28)\\
&\times \left[\frac{-1}{x_1x_3(x_2-x_1)(x_3-x_2)} n_\alpha n_\beta n_\gamma n_\delta \langle p|\mathrm{T}\left\{ g^2 l_3^{abcd} F_d^{\nu\delta}(0) F_c^{\lambda\gamma}(\tau n) F_b^{\sigma\beta}(\eta n) F_a^{\mu\alpha}(\lambda n)\right\}|p\rangle \right.\\
&\left. - \frac{1}{2}\frac{1}{x_1x_3} n_\alpha n_\beta \langle p|\mathrm{T}\left\{ F_d^{\nu\beta}(0)\omega^\sigma_{\sigma'}\mathrm{D}^{\sigma'}_{ac}(\eta n)\omega^\lambda_{\lambda'}\mathrm{D}^{\lambda'}_{cd}(\tau n) F_a^{\mu\alpha}(\lambda n)\right\}|p\rangle \right],
\end{aligned}
$$

where

$$
\begin{aligned}
l_2^{abcd} &= f^{acc'}f^{c'bd} + \frac{1}{4}\left(\delta^{ab}\delta^{cd}+\delta^{ac}\delta^{bd}+\delta^{ad}\delta^{bc}\right) = \qquad (11.29)\\
&= \frac{1}{2}f^{adc'}f^{c'bc} - \frac{3}{2}d^{adc'}d^{c'bc} + \frac{1}{2}\left(\delta^{ab}\delta^{cd}+\delta^{ac}\delta^{bd}-\delta^{ad}\delta^{bc}\right) + \frac{1}{4}\left(\delta^{ab}\delta^{cd}+\delta^{ac}\delta^{bd}+\delta^{ad}\delta^{bc}\right)
\end{aligned}
$$

and

$$
\begin{aligned}
l_3^{abcd} &= -f^{adc'}f^{c'bc} + \frac{1}{4}\left(\delta^{ab}\delta^{cd}+\delta^{ac}\delta^{bd}+\delta^{ad}\delta^{bc}\right) = \qquad (11.30)\\
&= \frac{1}{2}f^{abc'}f^{c'cd} - \frac{3}{2}d^{abc'}d^{c'cd} + \frac{1}{2}\left(-\delta^{ab}\delta^{cd}+\delta^{ac}\delta^{bd}+\delta^{ad}\delta^{bc}\right) + \frac{1}{4}\left(\delta^{ab}\delta^{cd}+\delta^{ac}\delta^{bd}+\delta^{ad}\delta^{bc}\right).
\end{aligned}
$$

The color factors l_i^{abcd} are related by permutation of color indices:

$$
l_1^{abcd} = l_2^{abdc} = l_3^{acbd}. \qquad (11.31)
$$

Notice the different Lorentz- and color structure and the different dependence on integration variables of the two-gluon operators in (11.26), (11.27) and (11.28).

11.2.4 Color Structure

As we have seen, H_3 contains contributions of the two- and four-gluon operators. In this subsection we will explore the color factors l_i^{abcd}, which enter into the contribution of the four-gluon operator and are given by eqns. (11.24), (11.29) and (11.30) depending on which representation of H_3 we are considering. If we have a look at table 2.1, we realize that there are also relations which transform one of the functions R^i into the same function R^i and only the dependence on the momenta and

the Lorentz-indices changes. For example, if we start with the *four-gluon operator* part of (11.25), make use of the relation in line seven, row one of table 2.1, exchange the integration variables such that $x_3 \to x_1 - x_2$, $x_2 \to x_1 - x_3$, $\lambda \to \lambda - \eta$, $\eta \to -\eta$ and $\tau \to \tau - \eta$ and make use of Lorentz-invariance we get an expression which has exactly the same form for the *four-gluon operator* part as in eqn. (11.26) but the color factor has to be exchanged by l_1^{adcb}, i.e. indices b and d are exchanged. Now, the color factor l_1^{abcd} in (11.24) has been written in three ways. There is the compact representation in the first line of (11.24), and in the second line it has been split up into symmetrical and anti-symmetrical parts with respect of exchange of color indices a and c or b and d. The anti-symmetrical part is given by the expression proportional $f^{acc'}f^{c'bd}$. Since the expression we got after usage of the relation in table 2.1 must be the same as in (11.25), we conclude that the term proportional $f^{acc'}f^{c'bd}$ in (11.24) within (11.25) must give a vanishing contribution. In other words the color factor that survives has the form

$$\tilde{l}_1^{abcd} = 3d^{abcd}\,. \tag{11.32}$$

We can repeat this argument with those expressions in which H_3 is expressed with the help of functions R^2 or R^3, (11.27), (11.28). Again, the surviving color tensors have the form

$$\tilde{l}_2^{abcd} = 3d^{abdc} \tag{11.33}$$

$$\tilde{l}_3^{abcd} = 3d^{acbd}\,. \tag{11.34}$$

11.3 Discussion of the Results

In this section we have presented our main results on the gluonic twist-four contributions, viz. eqns. (11.5), (11.10) and (11.25). While the expressions for H_1 and H_2 are valid beyond the one-loop case,[5] we have some restrictions in the case of H_3. For the color structure of a four-gluon system in the color singlet, there are five linearly independent states in the case of even C-parity. For example, one can expand the color structure with the help of the five states 1, $8_{\rm A}$, $8_{\rm S}$, $10 + \overline{10}$ and 27 (cf. appendix A). If we, now, explore our ansatz for the color structure of the four-gluon quark-loop, eqn. (8.25), we realize that we have not taken all color states into account. For an analysis which is valid to all orders one, therefore, has to incorporate these missing color states.

Let us, now, compare our results with those obtained by EFP [19]. As mentioned in the introduction, the computations in [19] can coarsely be divided into two steps. In the first step the authors consider the relevant diagrams and perform the factorization of the coefficient functions and matrix elements of the relevant operators. This leads to the operators in eqns. (5.1)-(5.4). They can be compared with the two- and four-gluon operators in eqns. (11.6), (11.11) and (11.26), which involve the same number of covariant derivatives.

In the second step, EFP used equations of motion in order to write the contributions of the two-quark operators (5.1)-(5.3) with the help of quantities which are linearly independent. Within the transverse basis, the resulting twist-four contributions to $F_{\rm T}$ and $F_{\rm L}$ are given in eqns. (5.7) and (5.8) plus terms which involve the four-quark operator (5.4). In our case the second step has not

[5] The Ward identities derived in section 8 are valid only for 1PI vertex functions. Therefore, contributions of diagrams which involve three- and four-gluon vertices like those in fig. 2.2 have to be incorporated separately into the expressions for H_1 through H_3.

yet been performed. It necessitates, first, the computation of the expressions for the quark-loops R.

On the other hand, one can try to find the relation between our results and the OPE, i.e. try to recover operators (1.1) and (1.2). For this, one has to compute the expressions for the quark-loops R, as well, and to take moments of eqns. (11.5), (11.10) and (11.25). The latter task will involve the consideration of signature. Notice, that the Lorentz-indices of the operators in (11.11) and (11.26) are not symmetrized. Although there are permutations involved in eqns. (11.10) and (11.25) these permutations imply the simultaneous exchange of Lorentz-indices of the quark-loop expressions and of the operators (cf. (10.11) and (10.15)). When considering signature, the expressions for ${}_3G^{\mu\sigma\nu}$ and ${}_4G_i^{\mu\sigma\lambda\nu}$ will be split up into symmetrical and anti-symmetrical parts. Taking moments will then result in an expansion of the operators in (11.6), (11.11) and (11.26) about the origin, so that finally operators (1.1) and (1.2) will be recovered. In summary we can say that the approach used here is rather intuitive (diagrammatical), i.e. one starts with certain diagrams which yield properties of the coefficient functions and these properties imply restrictions on the contributing operators. Within the OPE, on the other hand, one starts with a certain class of operators and has to find the corresponding coefficient functions.

Finally, let us, again, discuss the problem of operator mixing. As mentioned before, the computation of the quark-loop expressions R will yield terms which are proportional to logarithms in Q^2 and terms which are just constants. The terms which are proportional to logarithms have, actually, to be interpreted as part of the evolution of the contributions in eqns. (5.5) and (5.6), i.e. a certain number of t-channel gluons splits up into a certain number of quarks and gluons and couples to the virtual photon afterwards. This splitting yields the logarithm. The terms which are just constants, on the other hand, correspond to the NLO twist-four gluon coefficient functions. For the computation of the quark-loop expressions R it will, therefore, be necessary to re-identify the diagrams considered by EFP.

12 Conclusions

As we have outlined already in the first part of this thesis, gluonic twist-four contributions are expected to be, at least, sizeable in the small x_{B}, low Q^2 kinematical regime of HERA. The results presented in this second part are a first step towards a systematic analysis of twist-four gluon operators. For the derivation of these results we have extended the method developed by EFP [19]. Based on the diagrams in fig. 2.1 – i.e. diagrams with up to four t-channel gluons – and working in the axial gauge we could perform the factorization of the upper quark-loop parts and the lower blobs. The latter are expressed as matrix-elements of gluonic operators between proton states. In order to perform the mentioned factorization procedure we needed some Ward identities, which have been derived in section 8. The axial gauge proved to be very convenient for some reasons. First, gluonic A-operators occurring between proton states can easily be exchanged by F-operators in order to get explicitly gauge invariant expressions (section 9). Secondly, diagrams with more than four t-channel gluons lead to contributions of, at least, twist-six. This statement is proved in section 10. The analysis presented here is, therefore, in this sense consistent. Working in a covariant gauge, one would have to take contributions of diagrams with arbitrarily many t-channel gluons into account.

After the factorization had been performed we ended up with three contributions, viz. H_1, H_2 and H_3. The two- and three-gluon quark-loops are convoluted with matrix elements of the two-gluon operator, eqns. (11.5) and (11.10), while the four-gluon quark-loop is convoluted with both, the two- and the four-gluon operator, eqn. (11.25). In order to derive the latter result, we had to make intensive use of symmetry relations for the expression of the four-gluon quark-loop. These symmetry relations also led to restrictions on the color structure of the four-gluon operator contribution. Although the derivation initially yielded the color factor in eqn. (11.24), we could show that in the convolution of the four-gluon operator with function R^1 (cf. (8.25)) in eqn. (11.25) color factors which are anti-symmetrical in indices a and c give vanishing contributions. Therefore, only the factor in eqn. (11.32) survives.

Let us, now, compare the results obtained in this part with the expressions for the multi-gluon amplitudes used in part one. As we have discussed in section 1, the two-gluon (BFKL) amplitude is related to the two-gluon operator [41]. The reggeization of the three-gluon amplitude (1.43), on the other hand, is interpreted as a NLO contribution of the two-gluon operator. This seems to correspond to the result for H_2, eqn. (11.10), in which the three-gluon quark-loop couples only to the two-gluon operator. Moreover, the splitting of the four-gluon amplitude into a *reggeizing* and an *irreducible* part, eqn. (1.16), seems to correspond to the fact that the four-gluon quark-loop couples to both, the two- and the four-gluon operator, (11.25). These comparisons have to be made with care. First, in the case of the four-gluon amplitude, the leading-order term enters completely into the *reggeizing* part, and the *irreducible* part is interpreted as the mixing of the two- and the four-gluon operator. For the results presented here, it seems, on the first view, that we got contributions of the two- and four-gluon operators already at leading-order. The results on the four-gluon amplitude, on the other hand, suggest that, when computing the quark-loop expressions, the four-gluon operator contributions are likely to cancel. Secondly, it is the *reggeizing* part, which contains color factors like d^{abcd}, while the *irreducible* part is symmetrical under simultaneous exchange of color and momentum. A clear assignment of the *reggeizing* and the *irreducible* parts to the two- and four-gluon operator expressions obtained here is, therefore, not possible, yet. Such an assignment depends also on the choice of the operator-basis. Moreover, the approach used in this second part is of a more general nature than the twist-four expressions based on the high-energy approximation. The results obtained here contain some, in the sense of the high-energy approximation, sub-leading terms. We, therefore, expect that these sub-leading terms provide, at least, part of the differences between the four-gluon amplitude and the contributions of H_3. In order to get more distinct statements it will be necessary to compute expressions for the quark-loops R.

The next steps which need to be done are the computation of the expressions for the quark-loops and the consideration of evolution. While the first task might be *straight-forward* – although one has to keep in mind that the expressions will contribute to next-to-leading order gluon coefficient functions and leading-order quark-coefficient functions convoluted by Altarelli-Parisi splitting functions (cf. the discussion in section 11.3) – the computation of the anomalous dimensions might provide some difficulties. Since there is a large number of operators, one will have to handle the problem of operator-mixing. Moreover, although we have argued that at small-x_{B} gluon-operators are expected to dominate, the rôle of quark-operators is not quite clear. For a consistent treatment of twist-four beyond the DLA one should also take contributions of quark-operators into account. Such an analysis will also involve the problem of operator-mixing.

Summary

In this thesis we have presented our results on gluonic twist-four contributions to inclusive DIS structure functions. Twist-four gluon-operators are expected to lead to the dominating twist-four contributions at small x_{B}. In the first part we have discussed results based on a numerical evaluation of expressions for multi-gluon amplitudes in the DLA. For this, we have, first, summarized the analytical results for two-, three-, and four-gluon amplitudes. The corresponding expressions are based on the high-energy approximation and we have extracted the twist-four parts in the DLA. In the DLA, these twist-four parts are expected to be equal to the DLA contributions of twist-four two- and four-gluon operators in the limit $Q^2 \to \infty$ and $x_{\mathrm{B}} \to 0$. One of the problems in the numerical analysis is the determination of the free parameters for the non-perturbative initial distributions. In order to minimize the number of free parameters, we have also analysed twist-four contributions to diffractive $q\bar{q}$-production. This process can be related to diffractive vector meson production if one sums over all possible vector mesons in the final state and uses a duality argument. Moreover, using the AGK cutting rules, the initial distribution that enters into the diffractive $q\bar{q}$-production amplitude can be related to the initial distribution that enters into the inclusive four-gluon amplitude. Now, with the help of experimental data on longitudinal diffractive vector meson production, we could estimate both initial distributions.

The numerical results obtained by this way seem to confirm that the flattening of F_2 – considered as a function of x_{B} – for decreasing Q^2 is due to an interplay of leading- and higher-twist. The twist-four contribution is (in the scenarios with constant initial distributions) dominated by the transverse photon which leads to a negative correction.

On the other hand the approximations are very coarse, since the DLA is not sufficient for a quantitative fit to DIS structure functions. In the second part we have, therefore, performed the first step towards a consistent treatment of gluonic twist-four contributions beyond the DLA. For this, we have extended the method developed by EFP [19]. We have started with Feynman diagrams in which the virtual photon couples via a quark-loop and up to four t-channel gluons to the proton. Treating the expressions for the quark-loops separately, expanding these quark-loops about the longitudinal components of the gluon-momenta they depend on and using some Ward identities for the derivatives occurring in these expansions, we could write the LO gluonic twist-four contributions in an explicitly gauge invariant form.

Although we could show that we have considered gluonic twist-four contributions consistently, numerical evaluations based on our results are not possible, yet. First, we have not computed explicit expressions for the quark-loops. Since these expressions will contain terms proportional to logarithms in Q^2 and terms which are just constants, they are actually a composition of LO quark coefficient functions convoluted by Altarelli-Parisi splitting functions and of NLO gluon coefficient functions. Secondly, we have neglected evolution. Especially the latter task will be complicated, since the operators mix under renormalization.

In summary we can say that, if our numerical results are a sufficient approximation, a fit of DIS structure functions in the small x_{B}, low Q^2 regime based on leading-twist contributions has to be considered as in-accurate. On the other hand, our theoretical analysis shows that for the description of inclusive DIS structure functions in the small x_{B}, low Q^2 regime, the quantitative determination of the higher-twist contributions remains a challenge for theoretical physicists.

Acknowledgements

This work would not have been possible without the permanent support, guidance and encouragement of my mentor Prof. Dr. J. Bartels.

I would like to thank Hubert Spiesberger for the excellent collaboration and for many helpful discussions.

Hans Lotter taught me the foundations of small x_{B} physics. I'm in his debt.

Thanks to Lev N. Lipatov for discussions on the subject of our theoretical analysis.

Many thanks to Mark Wüsthoff for several conversations.

Discussions with Carlo Ewerz and Hamid Kharraziha are gratefully acknowledged.

Stefan Gieseke, René Staritzbichler and `Ispell` read parts of the manuscript. Of course, none of them is by no means responsible for any of the remaining mistakes.

Last but not least, I would like to thank all those people how wrote computer programs (LaTeX, GNU C/C++, Linux, ...) and put them on the public domain. Without this software, science today would not be possible.

This work was supported by *Graduiertenkolleg Theoretische Elementarteilchenphysik.*

Appendix A

Some Useful Quantities for the Four-Gluon Amplitude

We, first, give expressions for the vectors in color space $|i\rangle_\chi$ in the coupling scheme $\chi = (1234)$:

$$|1\rangle_{1234} = \frac{1}{8}\delta^{ab}\delta^{cd} \tag{A.1}$$

$$|8_{\rm A}\rangle_{1234} = \frac{-1}{6\sqrt{2}} f^{abl} f^{lcd} \tag{A.2}$$

$$|8_{\rm S}\rangle_{1234} = \frac{3}{10\sqrt{2}} d^{abl} d^{lcd} \tag{A.3}$$

$$\left|10+\overline{10}\right\rangle_{1234} = \frac{1}{2\sqrt{5}}\left\{\frac{1}{2}[\delta^{ad}\delta^{bc}-\delta^{ac}\delta^{bd}] + \frac{1}{3} f^{abl} f^{lcd}\right\} \tag{A.4}$$

$$|27\rangle_{1234} = \frac{1}{3\sqrt{3}}\left\{\frac{1}{2}[\delta^{ad}\delta^{bc}+\delta^{ac}\delta^{bd}] - \frac{1}{8}\delta^{ab}\delta^{cd} - \frac{3}{5} d^{abl} d^{lcd}\right\} . \tag{A.5}$$

They are normalized to one

$${}_\chi\langle i|j\rangle_\chi = \delta^{ij} \tag{A.6}$$

and eigenstates of the BFKL color factor $t_{2\to 2}$:

$$(t_{2\to 2})_{\alpha\alpha'}\,|i\rangle_{\alpha\alpha'\beta\beta'} = \varepsilon_i\,|i\rangle_{\alpha\alpha'\beta\beta'} \qquad (t_{2\to 2})_{\beta\beta'}\,|i\rangle_{\alpha\alpha'\beta\beta'} = \varepsilon_i\,|i\rangle_{\alpha\alpha'\beta\beta'}\ , \tag{A.7}$$

where

$$(t_{2\to 2})_{12} = f^{aa'l} f^{lb'b} \qquad (t_{2\to 2})_{13} = f^{aa'l} f^{lc'c} \qquad \text{etc.} \tag{A.8}$$

and $\varepsilon_i = \{-3, -\frac{3}{2}, -\frac{3}{2}, 0, 1\}$ for $i = \{1, 8_{\rm A}, 8_{\rm S}, 10+\overline{10}, 27\}$. They are related to vectors in other coupling schemes via transitions with the matrices

$$\Lambda = \begin{pmatrix} \frac{1}{8} & -\frac{1}{2\sqrt{2}} & \frac{1}{2\sqrt{2}} & -\frac{\sqrt{5}}{4} & \frac{3\sqrt{3}}{8} \\ -\frac{1}{2\sqrt{2}} & \frac{1}{2} & -\frac{1}{2} & 0 & \frac{1}{2}\sqrt{\frac{3}{2}} \\ \frac{1}{2\sqrt{2}} & -\frac{1}{2} & -\frac{3}{10} & \sqrt{\frac{2}{5}} & \frac{3}{10}\sqrt{\frac{3}{2}} \\ -\frac{\sqrt{5}}{4} & 0 & \sqrt{\frac{2}{5}} & \frac{1}{2} & \frac{1}{4}\sqrt{\frac{3}{5}} \\ \frac{3\sqrt{3}}{8} & \frac{1}{2}\sqrt{\frac{3}{2}} & \frac{3}{10}\sqrt{\frac{3}{2}} & \frac{1}{4}\sqrt{\frac{3}{5}} & \frac{7}{40} \end{pmatrix} \qquad \text{and} \qquad P = \mathrm{diag}(1,-1,1,-1,1) \tag{A.9}$$

in the following way:

$$\begin{aligned} |i\rangle_{1234} &= \sum_j \Lambda_{ij}\,|j\rangle_{1324} & |i\rangle_{1324} &= \sum_j \Lambda_{ij}\,|j\rangle_{1234} \\ |i\rangle_{1234} &= \sum_j (P\Lambda P)_{ij}\,|j\rangle_{1423} & |i\rangle_{1423} &= \sum_j (P\Lambda P)_{ij}\,|j\rangle_{1234} \\ |i\rangle_{1324} &= \sum_j (P\Lambda)_{ij}\,|j\rangle_{1423} & |i\rangle_{1423} &= \sum_j (\Lambda P)_{ij}\,|j\rangle_{1324}\,. \end{aligned} \tag{A.10}$$

Next, we give explicit expressions for the components of vector

$$\boldsymbol{\chi}(\omega\tilde{\nu}) \equiv \Sigma(\omega\tilde{\nu})\,\boldsymbol{V} \tag{A.11}$$

in eqns. (1.30) and (1.38). The results are the same for the three coupling schemes. Therefore, we list the components of $\boldsymbol{\chi}$ for the three contributing color states and write them as functionals of the auxiliary quantities $f_i(\omega\tilde{\nu})$, $i = 1\ldots 6$, and $g_j(\omega\tilde{\nu})$, $j = 1\ldots 7$. They are defined as follows:

$$\begin{aligned} f_1 &= -\frac{1}{32}\gamma_1 + \frac{3}{40}\gamma_8 - \frac{27}{160}\gamma_{27} - \frac{1}{4} & f_4 &= \frac{1}{\gamma_1} - \frac{1}{128}\gamma_1 - \frac{1}{16}\gamma_8 - \frac{27}{128}\gamma_{27} - \frac{1}{16} \\ f_2 &= -\frac{1}{128}\gamma_1 - \frac{1}{80}\gamma_8 - \frac{7}{640}\gamma_{27} - \frac{1}{16} & f_5 &= \frac{1}{\gamma_8} - \frac{1}{16}\gamma_1 - \frac{9}{200}\gamma_8 - \frac{27}{400}\gamma_{27} + \frac{3}{20} \\ f_3 &= -\frac{3}{32}\gamma_1 + \frac{9}{200}\gamma_8 - \frac{21}{800}\gamma_{27} - \frac{3}{20} & f_6 &= \frac{1}{\gamma_{27}} - \frac{27}{128}\gamma_1 - \frac{27}{400}\gamma_8 - \frac{49}{3200}\gamma_{27} - \frac{7}{80} \end{aligned} \tag{A.12}$$

and

$$\begin{aligned} g_1 &= \frac{\sqrt{3}}{2} f_1\cdot f_3 - 3\sqrt{3} f_2\cdot f_5 & g_4 &= f_5\cdot f_6 - \frac{3}{2} f_3^2 \\ g_2 &= \frac{9\sqrt{2}}{2} f_2\cdot f_3 - \frac{\sqrt{2}}{2} f_1\cdot f_6 & g_5 &= f_4\cdot f_6 - 27 f_2^2 \\ g_3 &= \frac{3\sqrt{6}}{2} f_1\cdot f_2 - \frac{\sqrt{6}}{2} f_3\cdot f_4 & g_6 &= f_4\cdot f_5 - \frac{1}{2} f_1^2 \end{aligned} \tag{A.13}$$

$$g_7 = 9 f_1\cdot f_2\cdot f_3 + f_4\cdot f_5\cdot f_6 - \frac{1}{2} f_1^2\cdot f_6 - 27 f_2^2\cdot f_5 - \frac{3}{2} f_3^2\cdot f_4\,, \tag{A.14}$$

where the functions $\gamma_i(\omega\tilde{\nu})$ are the diagonal elements of matrix $\gamma(\omega\tilde{\nu})$ in eqn. (1.28), and we have used γ_8 instead of $\gamma_{8_{\rm S}}$. With these functions the elements of the vector $\boldsymbol{\chi}$ are given by the following

expression:

$$g_7 \cdot \chi_j = v_j g_7 \gamma_j + \sum_{i=1}^{6} g_i \left(\kappa_{1i}^{(j)} \gamma_j \gamma_1 + \kappa_{2i}^{(j)} \gamma_j \gamma_8 + \kappa_{3i}^{(j)} \gamma_j \gamma_{27} + \kappa_{4i}^{(j)} \gamma_1 + \kappa_{5i}^{(j)} \gamma_8 + \kappa_{6i}^{(j)} \gamma_{27} \right) , \qquad \text{(A.15)}$$

where $j \in \{1, 8_S, 27\}$, $v_1 = 2$, $v_8 = 4\sqrt{2}$, $v_{27} = 6\sqrt{3}$ (cf. (1.29)) and the coefficients $\kappa_{li}^{(j)}$ are listed in table A.1. The pole at $\omega\tilde{\nu} = 4(1+\delta)N_c\alpha_s/\pi$ (eqn. (1.39)) is due to a zero of function g_7, eqn. (A.14).

Finally, the color tensor d^{abcd} in (1.41) has the form [30]:

$$\begin{aligned} d^{abcd} &= \mathrm{tr}\{t^a t^b t^c t^d\} + \mathrm{tr}\{t^d t^c t^b t^a\} = \\ &= \frac{1}{6}\delta^{ab}\delta^{cd} + \frac{1}{4} d^{abl} d^{lcd} - \frac{1}{4} f^{abl} f^{lcd} \\ &= \frac{1}{6}\delta^{ad}\delta^{bc} + \frac{1}{4} d^{adl} d^{lbc} + \frac{1}{4} f^{adl} f^{lbc} , \end{aligned} \qquad \text{(A.16)}$$

where the Gell-Mann matrices t^a are normalized to

$$\mathrm{tr}\{t^a t^b\} = \frac{1}{2}\delta^{ab} . \qquad \text{(A.17)}$$

i	1	2	3	4	5	6
$\kappa_{1i}^{(1)}$	$\frac{3\sqrt{3}}{32}$	$\frac{\sqrt{2}}{16}$	$\frac{3\sqrt{6}}{16}$	$\frac{1}{64}$	$\frac{1}{8}$	$\frac{27}{64}$
$\kappa_{2i}^{(1)}$	$\frac{9\sqrt{3}}{20}$	$\frac{7\sqrt{2}}{40}$	$-\frac{3\sqrt{6}}{40}$	$\frac{1}{8}$	$-\frac{3}{10}$	$\frac{27}{40}$
$\kappa_{3i}^{(1)}$	$\frac{213\sqrt{3}}{160}$	$\frac{81\sqrt{2}}{80}$	$\frac{51\sqrt{6}}{80}$	$\frac{27}{64}$	$\frac{27}{40}$	$\frac{189}{320}$
$\kappa_{4i}^{(1)}$	$\frac{3\sqrt{3}}{4}$	$\frac{\sqrt{2}}{2}$		$\frac{1}{4}$		
$\kappa_{5i}^{(1)}$	$\frac{6\sqrt{3}}{5}$	$-\frac{6\sqrt{2}}{5}$		2		
$\kappa_{6i}^{(1)}$	$\frac{21\sqrt{3}}{20}$	$\frac{27\sqrt{2}}{10}$		$\frac{27}{4}$		
$\kappa_{1i}^{(8)}$	$\frac{9\sqrt{6}}{80}$	$\frac{7}{80}$	$-\frac{3\sqrt{3}}{80}$	$\frac{\sqrt{2}}{32}$	$-\frac{3\sqrt{2}}{40}$	$\frac{27\sqrt{2}}{160}$
$\kappa_{2i}^{(8)}$	$\frac{3\sqrt{6}}{10}$	$-\frac{3}{5}$	$-\frac{9\sqrt{3}}{25}$	$\frac{\sqrt{2}}{4}$	$\frac{9\sqrt{2}}{50}$	$\frac{27\sqrt{2}}{100}$
$\kappa_{3i}^{(8)}$	$\frac{51\sqrt{6}}{80}$	$-\frac{27}{80}$	$\frac{99\sqrt{3}}{400}$	$\frac{27\sqrt{2}}{32}$	$-\frac{81\sqrt{2}}{200}$	$\frac{189\sqrt{2}}{800}$
$\kappa_{4i}^{(8)}$		$\frac{1}{4}$	$\frac{3\sqrt{3}}{4}$		$\frac{\sqrt{2}}{2}$	
$\kappa_{5i}^{(8)}$		2	$\frac{6\sqrt{3}}{5}$		$-\frac{6\sqrt{2}}{5}$	
$\kappa_{6i}^{(8)}$		$\frac{27}{4}$	$\frac{21\sqrt{3}}{20}$		$\frac{27\sqrt{2}}{10}$	
$\kappa_{1i}^{(27)}$	$\frac{71}{160}$	$\frac{9\sqrt{6}}{80}$	$\frac{17\sqrt{2}}{80}$	$\frac{3\sqrt{3}}{64}$	$\frac{3\sqrt{3}}{40}$	$\frac{21\sqrt{3}}{320}$
$\kappa_{2i}^{(27)}$	$\frac{17}{20}$	$-\frac{3\sqrt{6}}{40}$	$\frac{33\sqrt{2}}{200}$	$\frac{3\sqrt{3}}{8}$	$-\frac{9\sqrt{3}}{50}$	$\frac{21\sqrt{3}}{200}$
$\kappa_{3i}^{(27)}$	$\frac{189}{160}$	$\frac{81\sqrt{6}}{80}$	$\frac{189\sqrt{2}}{400}$	$\frac{81\sqrt{3}}{64}$	$\frac{81\sqrt{3}}{200}$	$\frac{147\sqrt{3}}{1600}$
$\kappa_{4i}^{(27)}$	$\frac{1}{4}$		$\frac{\sqrt{2}}{2}$			$\frac{3\sqrt{3}}{4}$
$\kappa_{5i}^{(27)}$	2		$-\frac{6\sqrt{2}}{5}$			$\frac{6\sqrt{3}}{5}$
$\kappa_{6i}^{(27)}$	$\frac{27}{4}$		$\frac{27\sqrt{2}}{10}$			$\frac{21\sqrt{3}}{20}$

TABLE A.1: Expansion coefficients for the three different color states in eqn. (A.15).

Appendix B

Numerical Inverse Mellin Transforms

For the evaluation of the expressions for the multi-gluon amplitudes it is necessary to perform numerical inverse Mellin transforms in one and two dimensions. In order to get fast and accurate results we have developed an algorithm, which is based on a method of J.N. Lyness et.al. [62]. We review this algorithm in this appendix. Lyness et.al. have developed their method in order to compute fast Fourier transforms of long-tailed functions. We, first, summarize their results and show how the method can be applied to inverse Mellin transforms, afterwards.

Splitting up a Fourier transform into real and imaginary components one ends up with a cosine and a sine transform:

$$g_c(v) = \int_{-\infty}^{\infty} \mathrm{d}u\, f(u) \cos uv \tag{B.1}$$

$$g_s(v) = \int_{-\infty}^{\infty} \mathrm{d}u\, f(u) \sin uv\,. \tag{B.2}$$

Now, Lyness et.al. show that these transforms can be computed efficiently for long-tailed functions $f(u)$ with the help of the following formulae:

$$g_c(v) = \frac{1}{2} \sum_{\substack{k=1 \\ k \text{ odd}}}^{\infty} \mu_k \frac{\pi}{vk} \sum_{j=-\infty}^{j=\infty} (-)^j f\left(\frac{j\pi}{vk}\right) \tag{B.3}$$

$$g_s(v) = \frac{1}{2} \sum_{\substack{k=1 \\ k \text{ odd}}}^{\infty} \mu_k \frac{\pi}{vk} \sum_{j=-\infty}^{j=\infty} (-)^j f\left(\frac{(2j+1)\pi}{2vk}\right)\,. \tag{B.4}$$

For the sum over j it is necessary to use some convergence accelerating algorithm, like the epsilon algorithm [63–65], since, otherwise, the computation takes too much time. Notice also that, for certain combinations of j and k, the function $f(u)$ gets evaluated more than ones at the same point. It is, therefore, possible to save evaluation time by storing these values into memory. The constants μ_k are the Möbius numbers, which are defined as follows:

$$\mu_k = \begin{cases} 0 & \text{when } k \text{ has a square factor other than 1} \\ (-)^j & \text{where } j \text{ is the number of distinct prime factors of } k. \end{cases} \tag{B.5}$$

The first twelve Möbius numbers are 1, −1, −1, 0, −1, 1, −1, 0, 0, 1, −1, 0, starting with $k = 1$.

For our purposes we have to perform inverse Mellin transforms of the kind

$$F(x) = \int_{c-\mathrm{i}\infty}^{c+\mathrm{i}\infty} \frac{\mathrm{d}\omega}{2\pi\mathrm{i}}\, \mathrm{e}^{-\omega \ln x}\, f(\omega) \tag{B.6}$$

which, after transformation of variables, $\omega = c + \mathrm{i}\lambda$, can be written as a Fourier transform,

$$F(x) = \mathrm{e}^{-c \ln x} \int_{-\infty}^{\infty} \frac{\mathrm{d}\lambda}{2\pi}\, \mathrm{e}^{-\mathrm{i}\lambda \ln x} f(c + \mathrm{i}\lambda)\,, \tag{B.7}$$

of a complex valued function $f(c+\mathrm{i}\lambda)$. Splitting up the function f and the exponential in eqn. (B.7) into real and imaginary parts, we end up with cosine and sine transforms as in eqns. (B.1) and (B.2). Now, since the algorithm summarized in eqns. (B.3) and (B.4) has been developed in order to transform long-tailed functions, it has to be used with care when applied to (B.7). The key element is the choice of the real part c. It turns out that the accuracy of the algorithm depends crucially on the choice of this real part. If the singularities of the function f are sufficiently known, one can vary c and compare the results the algorithm returns for different values of c. As it turns out the return values usually vary rapidly with the real part. Only in certain intervals the algorithm yields approximately the same return values for different c. It is these return values which approximate the *true* values of $F(x)$ best.

For two-dimensional Mellin transforms we are going to illustrate our method with the help of the following *test-function*, which can also be transformed analytically [66]:

$$\begin{aligned} F(x, Q^2) &= \int \frac{\mathrm{d}\omega}{2\pi\mathrm{i}}\, x^{-\omega} \int \frac{\mathrm{d}\nu}{2\pi\mathrm{i}} \left(\frac{Q_0^2}{Q^2}\right)^{-\nu} \frac{1}{\omega(\nu - \alpha/\omega)} = \\ &= \int \frac{\mathrm{d}\omega}{2\pi\mathrm{i}}\, x^{-\omega} \frac{1}{\omega} \left(\frac{Q_0^2}{Q^2}\right)^{-\alpha/\omega} = \\ &= \mathrm{I}_0 \left(\sqrt{4\alpha \ln\frac{Q^2}{Q_0^2} \ln\frac{1}{x}}\right)\,, \end{aligned} \tag{B.8}$$

where I_0 is a Modified Bessel Function. While for the inner integration, in the example the ν-integration, the method described above might be the most efficient one, we can lower the evaluation time for the outer integration. For this we are using the saddle point approximation, which tells us to evaluate the function depending on ω in the second line of (B.8) at

$$\omega_0 = \sqrt{\frac{\alpha \ln \frac{Q^2}{Q_0^2}}{\ln \frac{1}{x}}}\,. \tag{B.9}$$

Using the numerical method described above, one has to vary the real part of ω. As it turns out, the best choice for this real part is just ω_0, so that the time consuming variation can be dropped.

On the other hand, we could also have chosen the ν-integration to be the outer one. This means that one has to apply the real part variation to the, now, inner ω-integration, while the saddle

point approximation yields the value

$$\nu_0 = \sqrt{\frac{\alpha \ln \frac{1}{x}}{\ln \frac{Q^2}{Q_0^2}}} \tag{B.10}$$

for the real part of the ν-integration. When it comes to deciding if one should use the ω- or the ν-integration as the outer one, it turns out that one should choose ω to be the outer integration variable if $\omega_0 > \nu_0$ and ν to be the outer integration variable, otherwise.

In the case of ΔF^{I}, eqn. (1.38), the methods outlined here can be easily applied. The four-gluon Greens-function has the leading-pole (1.39). For the determination of the best choice for the real part of the outer integration in (1.38) we can, therefore, use the second line of (B.8) as an approximation to the result of the inner integration in (1.38). The numerical integration of (1.38), now, consists of two steps. For the inner integration use the *variation of the real part* method, and for the outer integration choose the real part we have just determined. This turns out to be a convenient way.

Bibliography

[1] V.N.Gribov, L.N.Lipatov, *Sov.J.Nucl.Phys.* **15** (1972) 78.

[2] G.Altarelli, G.Parisi, *Nucl.Phys.* **B 126** (1977) 298.

[3] Yu.L.Dokshitzer, *Sov.Phys.JETP* **73** (1977) 1216.

[4] M.Glück, E.Reya, A.Vogt, *Eur.Phys.J.* **C 5** (1998) 461.

[5] A.D.Martin, R.G.Roberts, W.J.Stirling, *Phys.Lett.* **B 387** (1996) 419.

[6] R.Ball, S.Forte, *Nucl.Phys.Proceedings Suppl.* **54 A** (1997) 163.

[7] M.G.Ryskin, *Z.Phys.* **C 57** (1993) 89.

[8] S.J.Brodsky, L.Frankfurt, J.F.Gunion, A.H.Mueller, M.Strikman, *Phys.Rev.* **D 50** (1994) 3134.

[9] J.C.Collins, L.Frankfurt, M.Strikman, *Phys.Rev.* **D 56** (1997) 2982.

[10] A.D.Martin, M.G.Ryskin, T.Teubner, *Phys.Rev.* **D 55** (1997) 4329, ibid. **D 56** (1997) 3007.

[11] A.D.Martin, M.G.Ryskin, *Phys.Lett.* **B 431** (1998) 395.

[12] ZEUS Collaboration, J.Breitweg et. al., *Eur.Phys.J.* **C 7** (1999) 609.

[13] S.Gottlieb, *Nucl.Phys.* **B 139** (1978) 125.

[14] M.Okawa, *Nucl.Phys.* **B 172** (1980) 481, ibid. **B 187** (1981) 71.

[15] S.P.Luttrell, S.Wada, B.R.Webber, *Nucl.Phys.* **B 188** (1981) 219.

[16] M.Kleine, Diplomarbeit, University of Hamburg 1995.

[17] R.L.Jaffe, M.Soldate, *Phys.Rev.* **D 26** (1982) 49.

[18] R.L.Jaffe, *Nucl.Phys.* **B 229** (1983) 205.

[19] R.K.Ellis, W.Furmanski, R.Petronzio, *Nucl.Phys.* **B 212** (1983) 29, ibid. **B 207** (1982) 1.

[20] J.Qiu, *Phys.Rev.* **D 42** (1990) 30.

[21] A.P.Bukhvostov, G.V.Frolov, L.N.Lipatov, E.A.Kuraev, *Nucl.Phys.* **B 258** (1985) 601.

[22] J.R.Forshaw, D.A.Ross, *Quantum Chromodynamics and the Pomeron*, Cambridge University Press, 1997.

[23] E.A.Kuraev, L.N.Lipatov, V.S.Fadin, *Sov.Phys.JETP* **44** (1976) 443, ibid. **45** (1977) 199, Ya.Ya.Balitskii, L.N.Lipatov, *Sov.J.Nucl.Phys.* **28** (1978) 822.

[24] M.Froissart, *Phys.Rev.* **123** (1961) 1053.

[25] A.Martin, *Phys.Rev.* **129** (1963) 1432.

[26] V.S.Fadin, L.N.Lipatov, *Phys.Lett.* **B 429** (1998) 127.

[27] J.Bartels, *Nucl.Phys.* **B 151** (1979) 293, ibid. **B 175** (1980) 365, DESY-91-074.

[28] L.V.Gribov, E.M.Levin, M.G.Ryskin, *Phys.Rep.* **100** (1983) 1.

[29] J.Bartels, *Phys.Lett.* **B 298** (1993) 204, *Z.Phys.* **C 60** (1993) 471.

[30] J.Bartels, M.Wüsthoff, *Z.Phys.* **C 66** (1995) 157.

[31] L.N.Lipatov, *Phys.Lett.* **B 251** (1990) 284.

[32] L.N.Lipatov, *JETP Lett.* **59** (1994) 596.

[33] L.D.Faddeev, G.P.Korchemsky, *Phys.Lett.* **B 342** (1995) 311.

[34] J.Bartels, L.N.Lipatov, M.Wüsthoff, *Nucl.Phys.* **B 464** (1996) 298.

[35] H.Lotter, PhD Thesis, University of Hamburg 1996, DESY-96-262.

[36] G.P.Korchemsky, hep-ph/9711277.

[37] N.Mahnke, Diplomarbeit, University of Hamburg 1998.

[38] Ch.Klinger, Diplomarbeit, University of Hamburg 1996.

[39] C.Ewerz, PhD Thesis, University of Hamburg 1998, DESY-THESIS-1998-025.

[40] J.Bartels, H.Lotter, M.Wüsthoff, *Z.Phys.* **C 68** (1995) 121.

[41] L.N.Lipatov, *Sov.Phys.JETP* **63** (1986) 904.

[42] V.A.Abramovsky, V.N.Gribov, O.V.Kancheli, *Sov.J.Nucl.Physics* **18** (1974) 308.

[43] J.Bartels, M.G.Ryskin, *Z.Phys.* **C 76** (1997) 241.

[44] R.K.Ellis, F.Hautmann, B.R.Webber, *Phys.Lett.* **B 48** (1995) 582; R.K.Ellis, Z.Kunszt, E.M.Levin, *Nucl.Phys.* **B 420** (1994) 517; ERRATUM-ibid. **B 433** (1995) 498.

[45] M.Wüsthoff, PhD Thesis, University of Hamburg 1995, DESY 95-166.

[46] L.D.Faddeev, *Sov.Phys.JETP* **12** (1961) 1014.

[47] E.M.Levin, M.G.Ryskin, A.G.Shuvaev, *Nucl.Phys.* **B 387** (1992) 589.

[48] J.Bartels, M.G.Ryskin, *Z.Phys.* **C 62** (1994) 425.

[49] G.P.Salam, *J.High Energy Phys.*, 07(1998)019.

[50] A.De Rujula, S.L.Glashow, H.D.Politzer, S.B.Treiman, F.Wilczek, A.Zee, *Phys.Rev.* **D 10** (1974) 1649.

[51] R.Ball, S.Forte, *Phys.Lett.* **B 335** (1994) 77, ibid. **B 336** (1994) 77.

[52] J.Bartels, H.Lotter, M.Wüsthoff, *Phys.Lett.* **B 379** (1996) 239; ERRATUM-ibid. **B 382** (1996) 449.

[53] N.N.Nikolaev, B.G.Zakharov, *Phys.Lett.* **B 332** (1994) 177.

[54] J.Bartels, M.Wüsthoff, *Proc. DIS97*, Chicago 1997.

[55] J.Bartels, M.Strikman, in preparation.

[56] J.Bartels, H.Jung, M.Wüsthoff, DESY-99-027, hep-ph/99 03 265.

[57] M.G.Ryskin, M.Besancon, *Proc. Physics at HERA*, Hamburg, Oct.1991 (eds. W.Buchmüller and G.Ingelman) **Vol. 1**, p. 215.

[58] E.Levin, M.Wüsthoff, *Phys.Rev.* **D50** (1994) 4306.

[59] K.Charchula, E.M.Levin, *Proc. Physics at HERA*, Hamburg, Oct.1991 (eds. W.Buchmüller and G.Ingelman) **Vol. 1**, p. 223.

[60] W.Kummer, *Acta Phys.Austr.* **41** (1975) 315.

[61] A.Bassetto, G.Nardelli, R.Soldati, *Yang-Mills Theories in Algebraic Non-Covariant Gauges: Canonical Quantization and Renormalization*, World Scientific, 1991.

[62] J.N.Lyness, T.J.Kaper, *SIAM J.Sci.Stat.Comput.* **8** (1987) 1005.

[63] P.Wynn, *Math.Tables Aids Comp.* **10** (1956) 91.

[64] D.A.Smith, W.F.Ford, *SIAM J.Numer.Anal.* **16** (1979) 223, *Math.Comp.* **38** (1982) 481.

[65] Manual of *NAG Fortran Library*, Mark 16, Function C06BAF.

[66] F.Oberhettinger, *Tables of Mellin Transforms*, Springer, Berlin, Heidelberg, New York 1974.